Vision modulates with the progression of step: Peak of performance changes with eccentricity and task but not ground slope

Cameron Kyle Phan

School of Psychology

The University of Sydney

A thesis submitted to fulfil the requirements of the degree of

Doctor of Philosophy (PhD)

2025

Statement of Originality

This is to certify that the content of this thesis is my own work. This thesis has not been submitted for any other degree or purpose.

I certify that the intellectual content of this thesis is the product of my own work, and that all assistance received in preparing this thesis and all sources have been acknowledged.

Cameron Kyle Phan

November 1, 2025

Abstract

Majority of the research into the perception of individuals has been conducted in static, limited, and controlled environments. With the advent of new technologies, mobile and wearable virtual reality in particular, it is now possible to expand our understanding of perceptual phenomena to moving individuals. In this thesis, three studies are presented that leverage the consistency in walking patterns to contribute to the recent research into the changes individuals' visual perception undergo over the course of a step. The first study expanded on a novel finding of a sinusoidal modulation in visual detection performance across a stride cycle by testing whether the modulation differs between central and peripheral vision. The results unveiled a larger modulation that peaked later in the stride cycle for the detection of peripherally presented targets as opposed to centrally presented targets. In the second study, the difference between the performance in two visual tasks, orientation and motion identification, was investigated. Results showed a phasic difference between the modulations in visual orientation identification and motion identification performance. The third study changed the walking conditions instead of the visual task to probe whether the motor demands of walking was the primary driver of the modulations in visual perception. The results were unexpected in that sloped walking did not shift the peak of performance along the course of the step but instead a second peak was found for inclined walking. Overall, these findings highlight the need to investigate the influence of walking, and more broadly, the influence of active movements on individuals' perceptual experiences.

Dedication

This thesis is dedicated to those who made me who I am today. To Yuki, I miss you every single day. To my grandpa, who told me that it was okay to fail and that there is never just a single path to take. To my aunt, who helped raise me like a second mother. Most importantly, to my mother, the woman who made sure I would have the opportunities she never had, taught me never to take things for granted, and showed me that knowing when to fight or when not to fight is far more important to succeeding than knowing how to fight.

Acknowledgements

First and foremost, I would like to express my deepest gratitude to Professor David Alais, whose guidance and insight were pivotal to the completion of this thesis. I would not have as many opportunities as I have had in these years without his trust and support. I would like to thank Matthew Davidson, who began this line of research and provided me with support when I felt most isolated during my time abroad. Thank you to Professor Frans Verstraten for fostering my social network in the field and for the care he showed for my development as an academic and as a person. I must give big thanks to my procrastination buddies throughout these years, one Ms. Kate Pickard, who I think of as a sister, and a Dr. Alessia Tonelli, a human encyclopedia of psychophysics and pop culture. An honourable mention to the friends I have gained over the course of this thesis, in particular; Guandong, Gabe, and Jacob.

Statement of Authorship Attribution

The research presented in this thesis was conducted by the candidate, Cameron K. Phan, at the School of Psychology, The University of Sydney. Chapters 2 to 4 were prepared as manuscripts intended for publication. Chapter 2 is currently published, and an earlier version has been hosted as a preprint article. Chapter 3 is currently under submission.

Chapter 2 of this thesis is currently published at PNAS Nexus as:

> Phan, C. K., Davidson, M. J., & Alais, D. (2025). Optimal phase for central and peripheral visual detection differs within the stride cycle. *PNAS Nexus*, *4*(9), pgaf270. https://doi.org/10.1093/pnasnexus/pgaf270

Chapter 2 of this thesis is currently hosted as a preprint article on bioRxiv as:

> Phan, C. K., Davidson, M. J., Alais, D. (2024) Walking entrains unique oscillations for central and peripheral visual detection. *bioRxiv*.
> https://doi.org/10.1101/2024.07.04.602020

Chapter 3 of this thesis is currently submitted for publication at Proceedings of the Royal Society B as:

> Phan, C. K., Rideaux, R., Alais, D. (2025) Walking Produces Oscillations of Orientation and Direction Perception at the Step Rate. *Proceedings of the Royal Society B.*

In addition to the authorship attribution statements above, in cases where I am not the corresponding author of a published item, permission to include the published material has been granted by the corresponding author.

Cameron Kyle Phan

November 1, 2025

As supervisor for the candidature upon which this thesis is based, I can confirm that the authorship attribution statements above are correct.

Professor David Alais

November 1, 2025

Artificial Intelligence Statement

No content produced by generative AI tools has been used in the preparation of this thesis.

Australian Government Support Acknowledgement

This research was supported by an Australian Government Research Training Program (RTP) Scholarship (SC3227) awarded to Cameron Kyle Phan.

Contents

Statement of Originality **2**

Abstract **3**

Dedication **4**

Acknowledgements **5**

Statement of Authorship Attribution **6**

Artificial Intelligence Statement **8**

Australian Government Support Acknowledgement **9**

Chapter 1 ..... **17**

1.1 Walking 18

1.2 Gait Cycle 19

1.2.1 Measurement 20

1.3 Active Vision 21

1.3.1 Active Perception 21

1.3.2 Visual Perception 22

1.4 Technology 23

1.4.1 Virtual Reality 23

1.5 Research Aims 24

1.5.1 Stride-based modulation in central and peripheral visual detection 24

1.5.2 Stride-based modulation difference between visual hierarchy levels 24

1.5.3 Effect of different walking requirements on stride-based modulations of visual detection 25

2..... 26

Chapter 2 26

2.1 Materials and Methods..... 30

2.1.1 Participants..... 30

2.1.2 Apparatus and Materials 30

2.1.3 Procedure..... 32

2.1.4 Data Analyses..... 36

2.1.5 Eye Movement Data..... 37

2.1.6 Gait Extraction 37

2.1.7 Performance Relative to Stride 38

2.1.8 Super-subject Analysis 39

2.1.9 Exclusion Criteria..... 40

2.2 Results..... 40

2.2.1 Visual detection psychometric functions interact with motion type and target location..... 41

2.2.2 Stride-cycle phase modulates performance for targets at central and peripheral locations..... 42

2.2.3 Participant level analysis of modulations at central and peripheral locations 45

2.2.4 Within-participants comparison of modulations at central and peripheral locations 48

2.3 Discussion 52

2.3.1 Performance modulations at central and peripheral locations are modulated by the phases of the stride-cycle 52

2.3.2 Participant level modulations cluster in phase 53

2.3.3 Performance modulations differ in amplitude and phase based on visual field location 55

2.3.4 Conclusion 57

2.4 Acknowledgements 57

3 58

Chapter 3 58

3.1 Chapter 3 Experiment 1 62

3.2 Methods 62

3.2.1 Design 62

3.2.2 Participants 63

3.2.3 Apparatus and Materials 64

3.2.4 Stimuli 64

3.2.5 Procedure 65

3.2.6 Data Analyses 69

3.2.7 Eye Movement Data 69

3.2.8 Gait Extraction 70

3.2.9 Performance Relative to Stride 70

3.2.10 Exclusion Criteria 72

3.3 Results 72

3.4 Discussion 78

3.5 Chapter 3 Experiment 2 81

3.6 Methods 81

3.6.1 Design 81

3.6.2 Participants 81

3.6.3 Materials 81

3.6.4 Procedure 82

3.6.5 Exclusion Criteria 82

3.7 Results 82

3.8 Discussion 90

3.9 General Discussion 92

3.10 Acknowledgements 95

4 96

Chapter 4 96

4.1 Methods 99

4.2 Design 99

4.2.1 Participants 100

4.2.2 Apparatus and Materials 100

4.2.3 Procedure 103

4.2.4 Data Analyses 104

4.2.5 Gait Extraction 105

4.2.6 Performance Relative to Stride 105

4.2.7 Alternative Modulation Shape 106

4.3 Results 109

4.4 Discussion 116

4.5 Acknowledgements 119

5 120

Chapter 5 120

5.1 General Discussion 121

5.1.1 Summary of findings 121

5.1.2 Limitations and future directions 126

References 129

Appendix 147

Supplementary Figures 147

List of Figures

Figure 2.1 Example of Procedure 35

Figure 2.2 Modulations in Performance at Central and Peripheral Target Locations Within the Stride-Cycle 43

Figure 2.3 Significant Modulations at the Participant Level are Clustered in Phase 46

Figure 2.4 Modulations of Super Subject 50

Figure 3.1 Stimulus Orientation Alignment with Head Roll Experienced During Walking 61

Figure 3.2 Schematic of Target Stimuli and Responses 68

Figure 3.3 Accuracy for Orientation Identification Across Stride Cycle 75

Figure 3.4 Response Rate for Orientation Identification Across Stride Cycle 76

Figure 3.5 Response Time for Orientation Identification Across Stride Cycle 78

Figure 3.6 Accuracy for Motion Direction Identification Across Stride Cycle 86

Figure 3.7 Response Rate for Motion Direction Identification Across Stride Cycle 87

Figure 3.8 Response Time for Motion Direction Identification Across Stride Cycle 89

Figure 4.1 Apparatus and Procedure 102

Figure 4.2 Sinusoidal Functions Fitted for Performance 108

Figure 4.3 Modulations in Performance Across Step Progression 111

Figure 4.4 Piecewise Sinusoidal Fits on Hit Rate Across Step Progression 114

Figure 4.5 Four Cycles per Stride Fourier Fits for Group-Level Hit Rate 115

List of Tables

Table 2.1 Mean Hit Rate and Response Times by Experimental Condition 42

Table 3.1 Mean Response Rate, Accuracy, Correct and Overall Response Times by Experimental Condition 73

Table 3.2 Mean Response Rate, Accuracy, Correct and Overall Response Times by Experimental Condition 85

1

Chapter 1

Vision modulates with the progression of step: Peak of performance changes with eccentricity and task but not ground slope

Vision modulates with the progression of step: Peak of performance changes with eccentricity and task but not ground slope

Individuals are not static by nature, nor are the environments they perceive. The source of the dynamism in perceptual experience is composed of external environmental changes, internal neurological modulators, and the interactions between both. Despite the multifaceted nature of perception, the vast majority of the existing research on perception has involved individuals in passive, static scenarios with highly controlled perceptual targets. Whether our perception differs when we are engaged in movement remains relatively unexplored.

The potential influence of action on perception and the involvement of perception on action planning and execution is not a novel concept (Gibson, 1955, 1962). Action, or more generally movement, has been recognised as a factor that produces changes in a percept (Bardy et al., 1996; Chapman et al., 1987; Gibson, 1955, 1962; Warren & Hannon, 1988). As an observer moves through a scene, the relevant features, such as visual location, visual and auditory intensity, and more, change in a manner consistent with the movement. These changes have been speculated to produce a perceptual experience equivalent to changing the features of the objects themselves in the same static and passive scenarios in which such effects have been studied, without accounting for potential modulatory effects of movement (Bardy et al., 1996; Warren & Hannon, 1988). With the advancement of technology, we can now control the external features of the perceptual environment whilst an individual moves, allowing us to investigate the modulation of perceptual phenomena that may occur during movement.

1.1 Walking

Locomotion is essential to the lives of most, if not all, animals, including humans (Burr & Robinson, 2004; Drew & Marigold, 2015; Eilam, 1995; Rakovac, 2021; Thomson & Simanek,

1977; Webb, 1984). It is the process of moving from one place to another. An active movement is one where the performer plans and voluntarily executes the movement, often to achieve a goal (Cullen, 2004). Therefore, forms of biomechanical locomotion, such as swimming, running, or walking, are essential active movements individuals may engage in. In particular, walking is an active movement that is regularly performed as a component of daily living for those who are able-bodied. Furthermore, as walking has a cyclic pattern, any modulations in perceptual experience during walking would most likely manifest in a similarly consistent repetitive pattern.

1.2 Gait Cycle

The physical manifestation of walking has been reliably observed and thoroughly described in kinematic literature (Gard et al., 2004; Kharb et al., 2011; Selinger et al., 2015; Winter, 1983). The gait cycle it produces is composed of two steps (i.e., stride) and can be demarcated into eight stages, which begins with the heel of one foot contacting the ground surface (i.e., heel strike) and ends with the heel strike of the same foot. Each step, the heel strike of one foot to the heel strike of the other foot, can be more simply divided into two phases. The swing phase, when one foot is not in contact with the ground surface, and the stance phase, when both feet are in contact with the ground surface. The step begins and ends with the stance phase with the swing phase in between. As such, a stride or gait cycle involves three stance phases and two swing phases with the middle stance phase taking a larger portion of the cycle.

During the gait cycle, the ground reaction forces and muscular activity change during the transition between stages (Gard et al., 2004; Riley et al., 2007). Ground reaction forces experienced peak at heel strike, reaching approximately 120% body weight, and peak once again at toe-off (Richards et al., 2013). For the remainder of the gait cycle, the ground reaction forces are negligible. Similarly, muscular engagement during the gait cycle shows the greatest change

as an individual enters and leaves the stance phase (Gard et al., 2004; Riley et al., 2007). As a consequence of these forces and action, head stability is greatest during the swing phase, when individuals are in what can be described as a planned free-fall. The bipedal nature of human gait creates a lateral difference in centre of mass dependent on the initiating foot and hence, a lateral roll oscillation during the gait cycle. These consistencies in pattern make walking an active movement that is more constrained in possibilities than other less stereotyped movements and the cyclic nature of such pattern should produce a repeated observable modulation of phenomena, providing a form of control of possible confounds.

1.2.1 Measurement

Due to the gait cycle being so highly consistent within individuals walking patterns and across individuals, measurement of step has been thoroughly described, documented and implemented (Lacquaniti et al., 1999; Winter, 1983). For simple step counting, accelerometers in the form of Inertial Measurement Units (IMUs) have been used, these are commonly found in consumer mobile and wearable devices due to their small size and availability (Ferrete Ribeiro & Santos, 2017). As changes in ground reaction forces and the interactions between the shifts in centre-of-mass and gravity produce patterned changes in acceleration, particularly in the vertical dimension, IMUs have also been used to measure the progression of the gait-cycle (Hwang & Effenberg, 2021; Windau & Itti, 2016). On the same principle, velocity has been used as a measurement variable in determination of gait-cycle with changes in the coronal dimension used to determine difficulty and specific progression in step. Use of positional tracking allows for measurement of shifts in centre-of-mass and the difference in gait-cycle patterns along the body, mostly focused on the head, torso, waist, knees, and ankles.

1.3 Active Vision

1.3.1 Active Perception

Until recently, research into perceptual phenomena has involved stationary observers experiencing highly controlled perceptual environments, often deprived of any perceptual objects apart from the target of interest. In rare cases where observers were not stationary, they were passively moved by external apparatuses, such as a motion platform. When perceptual research has entertained active movements, it has focused on the actions afforded by the perceived environment (Gibson, 1955, 1962) or has used movements as an explanatory factor in the development of perceptual phenomena found in passive, static experiments (Hogendoorn et al., 2017; Warren & Hannon, 1988). This limited scope into perception during active movement can be attributed to the limited opportunities to present controlled stimuli without the consequences of the active movement themselves changing the perceptual input, such as the intensity and acoustic quality of an auditory object changing as the observer moves closer or further away, or the light reflected off an object changing as an individual moves relative to the light source and object due to angle.

Under the broader scope of cognition, active perception falls within a somewhat controversial and renewed school of thought, embodied cognition (Barsalou, 2010; Clark, 1999; Pecher & Zwaan, 2005; Wilson, 2002). Where traditionally, cognition has focused on the mind separate from the body and its movements (Foglia & Wilson, 2013), embodied cognition posits the importance of the mind in serving the body and its interactions with the world (Clark, 1999; Engel et al., 2013; Wilson, 2002). Within this framework, both sensory and motor systems play integral roles in cognition (Barsalou, 2010; Pecher & Zwaan, 2005), such it has been proposed that the primary role of the brain is not to perform computations to reflect the environment

internally but to produce actions to interact with said environment (Engel et al., 2013). A requirement for optimal, or more appropriately efficient, embodied cognition is the mastery and coordination of sensorimotor contingencies (O'Regan & Noë, 2001). Much like the affordances mentioned earlier, having the ability to account for action and the consequences it has for sensory input provides a more accurate representation of the environment and the potential actions that can be taken (Clark, 1999; O'Regan & Noë, 2001). In observing the effects of active movements on perception, one can speculate on the changes in internal representations that undergo cognitive processes and the resultant actions or adjustments in movement of the observing individual (Clark, 1999; Engel et al., 2013).

1.3.2 Visual Perception

The recent forays into active perception have been into the phenomenology of the visual experience of the observer (Cao & Händel, 2019; Davidson et al., 2023, 2024; Matthis et al., 2017, 2018; Szekely et al., 2024), this thesis will continue this trend. The rationale for this approach is two-pronged; first, the human sensory experience is vision-dominated and thus, daily living is much more reliant on vision, and second, technology has been faster in advancing visual display and communication than the next contender, audition. Some might argue that the latter reason is a consequence of the first, but it cannot be denied that both factors exist. As for the chemoreceptor-reliant sensory modalities, gustation and olfaction, the non-transient nature of their stimuli introduces the need to rid of any previous stimuli to accurately investigate their phenomena. As research into active perception is in its infancy, the studies in this thesis and its focus are on active visual perception.

1.4 Technology

1.4.1 Virtual Reality

Virtual Reality (VR) provides researchers with the ability to produce visual stimuli and visual environments that are both highly controlled, like classic visual perception research, and dynamic, not unlike most visual environments outside of a lab (Wilson & Soranzo, 2015). With advancement in graphical hardware and software, commercial VR has completely transitioned to head-mounted displays (HMDs) and wireless controllers, away from projected environments in an enclosed space (Lum et al., 2020). These HMDs have either one or two screens, which are situated like glasses lenses, displaying the simulated visual environment. Two screens, currently the most common design, provide binocular disparity and produce an experience of depth with greater fidelity.

In most cases, all components of the VR device (i.e., HMD, controllers, trackers) include an IMU that interacts with light-based tracking to output positional and rotational data that can be accessed. Some HMDs have eye tracking technology installed and provide accurate readings of gaze, pupil size and dilation, and eye openness. The versatility of VR software allows the use of nearly any peripheral input device and entertains a myriad of different controllers that include a variety of response making interactions, such as trigger pulls, grip actuators, trackpads and many more. Furthermore, recent developments in VR technology have made wireless VR a viable option for mobile interactions with greater range of motion than the existing seated or limited space standing VR environments. VR technology has advanced to a stage of development that makes it a viable option for perceptual research and more importantly, the most suitable option for active visual perception research (Malpica et al., 2020; Witte et al., 2025).

1.5 Research Aims

1.5.1 Stride-based modulation in central and peripheral visual detection

In the first empirical chapter, the possibility that stride-based modulations in visual detection differ by visual eccentricity is explored. Davidson et al. (2024) found that individuals' visual detection ability modulates two cycles per stride for hit rate, response time, and response making. Addition to replicating these findings, the difference in this modulatory phenomenon between central and peripheral vision was investigated. As each visual eccentricity has been proposed to serve different purposes, mainly purporting to central vision being for more static, high acuity looking tasks and peripheral vision being for more dynamic, pre-emptive seeing tasks, it would be understandable for each eccentricity to demonstrate different phenomena during walking. Any difference in modulatory nature of stride will provide a better understanding as to its underlying mechanisms.

1.5.2 Stride-based modulation difference between visual hierarchy levels

The second empirical chapter continues the investigation of potential sources for different stride-based modulations in visual abilities. Moving beyond the basic contrast sensitivity detection tasks used in previous paper (Davidson, et al., 2024), two-alternative forced-choice tasks were used in the second chapter, one task was for visual orientation identification and the other for visual motion direction identification. These visual abilities have been found to rely on different cortical areas along the visual hierarchy. Therefore, any difference in modulation of these abilities alongside the previous findings may uncover a pathway of propagation similar to travelling cortical waves. However, if modulations do not exist for these abilities, the explanation for the visual detection performance modulations may be rooted in an inherent susceptibility of the transduction and subcortical early stages of vision.

1.5.3 Effect of different walking requirements on stride-based modulations of visual detection

The third and final empirical chapter of this thesis returns to the original visual detection task discarding any stimulus manipulations beyond contrast. Instead, the study conducted in this chapter investigates the effect of surface slope on stride-based performance modulations. In daily life, individuals can rarely avoid walking on terrain more complex than a standard flat regular surface (Matthis et al., 2017, 2018; Matthis & Fajen, 2014). With the implementation of a motion platform and large mounted treadmill, the visual detection performance of individuals was recorded whilst they were walking up an incline, down a decline, or on flat surface. If the modulation pattern changes between the flat and the inclination conditions, it would suggest that stride-based modulations are not simply event- triggered modulations but dependent on the involvement of the particulars of motor system engagement.

2

Chapter 2

Stride-based modulation in central and peripheral visual detection

The following chapter is currently published in PNAS Nexus as:

Phan, C. K., Davidson, M. J., & Alais, D. (2025). Optimal phase for central and peripheral visual detection differs within the stride cycle. *PNAS Nexus*, *4*(9), pgaf270. https://doi.org/10.1093/pnasnexus/pgaf270

The study presented in this chapter was designed by C.P. and M.D., the data was collected by C.P., data was analysed by C.P. with contributions from M.D. and D.A., writing and editing was by C.P., M.D., and D.A.

Stride-based modulation in central and peripheral visual detection

Perceptual research has traditionally required participants to complete tasks in highly controlled and stimulus-limited environments with restricted physical autonomy (e.g., with seated observers, and head stabilised on a chin rest). However, perception in daily life is typically far more dynamic with observers voluntarily self-generating actions (e.g., saccades, reaching, locomotion) which in turn alter the sensory inputs driving perceptual experience. This difference between experimental and real-life conditions reduces the ecological validity of previous work and has left the field of active perception in the context of everyday actions relatively unexplored.

The importance of everyday actions in perception has been appreciated for many years (Bardy et al., 1996; Chapman et al., 1987; Gibson, 1955, 1962; Warren & Hannon, 1988) but technical challenges have been an impediment to empirically investigating natural behaviour. Recent advances in portable, wearable devices and virtual reality technology have removed many of these barriers, and active perception research can now be more easily conducted. For example, a number of recent studies involving observers performing perceptual tasks during walking have provided insight into the interaction between everyday actions and perception (Davidson et al., 2023, 2024; Matthis et al., 2017, 2018; Matthis & Fajen, 2014; Selinger et al., 2015).

Walking is a movement generated by most able-bodied individuals on a daily basis, facilitating locomotion through the environment to intended destinations (Winter, 1983). Walking is a very cyclic behaviour with well-established phases that are consistently observed and easily modelled across multiple performers (MacDougall & Moore, 2005). The consistency of gait during walking has been widely studied and step rates across the population on smooth, level

ground are clustered around 2 Hz (Gard et al., 2004; Hausdorff et al., 1996; Hirasaki et al., 1999; Moore et al., 2001; Pozzo et al., 1990). Within individuals, step rates are also highly consistent and rhythmic (MacNeilage, 2020; MacNeilage & Glasauer, 2017). Because walking is such a common daily action, is well studied biomechanically and involves consistent repetitions of a cyclical voluntary action, it is one of the most suitable movements for investigating the effects of action on perception.

When walking through an environment, an individual must remain alert for potential obstacles lying on the path ahead as well as monitor for risks and collisions peripheral to the intended course (Drew & Marigold, 2015; Matthis et al., 2017). With that in mind, the present study examines detection of visual targets in the central versus peripheral field in walking observers. Previous work by Cao and Händel (2019) found neurophysiological and behavioural results suggesting enhanced processing of peripheral visual input while walking (relative to stationary) using a contrast sensitivity task. Enhanced peripheral processing was implied by greater suppression of central visual targets from competing peripheral targets. This interesting work prompted our current study design which involves simple detection of brief targets in either a central or peripheral location which is more akin to detecting targets that may appear suddenly on a path or adjacent to it. We also introduce a new analysis in which detection performance is binned relative to the phases of the stride-cycle, so that any modulations of visual detection during walking can be revealed.

Previous experiments from our group found modulations of visual detection performance when binning performance relative to the phases of the stride-cycle. These modulations primarily occurred at low frequencies, such as 2 or 4 cycles per stride (cps; Davidson et al., 2024), that were entrained to the rhythm of individual footfall. Notably, these modulations were recorded

during a visual detection task that required fixating on a slowly drifting target region, precluding an analysis of stride-cycle effects based on target eccentricity. Previous work has also shown that rhythms in perception can propagate across retinotopic visual space (Fakche & Dugué, 2024; Sokoliuk & VanRullen, 2016), possibly supported by the spatial propagation of neural oscillations across the cortex (Lozano-Soldevilla & VanRullen, 2019; Prechtl et al., 2000). Here we investigated whether locomotion induced modulations of perception also differ across retinotopic space, by comparing performance at central and peripheral target locations when binned according to the phases of an individual's stride-cycle.

The current study employed a simple visual detection task during free walking using a wireless virtual reality (VR) headset. By using VR, we were able to simulate an outdoor setting that could be replicated across participants (Fink et al., 2007), resulting in a naturalistic optic flow that was absent when treadmills (e.g., Benjamin et al., 2018; Gramann et al., 2010) or stationary bicycles (e.g., Bullock et al., 2017) have been used in past research. The use of wireless VR also enabled the tight experimental control of visual stimuli, simultaneous recording of eye-movements, and the capture of changes in head height from which the phases of the stride-cycle were extracted (Davidson et al., 2024). Observers thus experienced both natural unencumbered walking and the natural circular relationship between sensory input and motor output that is inherent to our everyday experience.

We hypothesised that visual detection performance would be enhanced in the visual periphery while walking, in accordance with previous research (Cao & Händel, 2019). We additionally hypothesised that the modulations in central visual detection performance entrained by the stride-cycle would differ when compared to targets at peripheral locations, given recent evidence that the optimal phase for perceptual oscillations shifts across retinotopic space (Fakche

& Dugué, 2024; Sokoliuk & VanRullen, 2016). To preview our results, we found average visual performance was poorer for peripheral targets, and that stride-cycle based modulations were reduced in amplitude and phase-leading for targets at the periphery relative to parafoveal locations.

2.1 Materials and Methods

2.1.1 Participants

Participants were 40 undergraduate psychology students from the University of Sydney who participated in exchange for course credit. Six participants were excluded, as per criteria below, leaving a final sample of N = 34. The large sample size was selected due to the lack of prior studies examining modulations within the gait cycle, difficulties in determining an appropriate sample size for power, and to ensure that potential effects would be detected. Each participant provided informed consent before commencing and had normal or corrected-to-normal vision (not verified). The study protocol was approved by the University of Sydney Human Research Ethics Committee (HREC 2021/048). Participants' experiences with virtual reality were not collected nor was it a requirement for participation, however, previous participation in other virtual reality experiments from our laboratory was possible. No participants withdrew due to discomfort.

2.1.2 Apparatus and Materials

An HTC Vive Pro Eye head-mounted display (HMD) was used to display the virtual environment and two wireless HTC Vive Controllers (2018) were used for collecting responses. The HMD contained dual 3.5-inch high-resolution OLED displays (1440 x 1600 pixel resolution, 90 Hz refresh rate) with 110-degree field of view. Positions of the HMD and controllers were tracked in three-dimensional space at 90 Hz resolution, using five HTC Vive Base Station 2.0's

enclosing an open 4.5 m x 12 m rectangular space. To allow the utilization of such a large space and unencumbered walking conditions, the virtual reality environment was transmitted to the HMD using the HTC Vive Wireless Adapter for Vive Pro. The SRanipal Runtime (Version 1.3.2.0; SDK 1.3.6.8) was used to handle eye tracking data collection by the integrated Tobii eye-tracker within the HMD, sampled at 90 Hz.

The virtual reality (VR) environment and experimental procedure were designed and presented within Unity (Version 2020.3.14f1), using the SteamVR Plugin (Version 2.7.3; SDK 1.14.15) on a Windows 11 PC (2 × 16 GB, DDR5 4400 MHz) with a 12th Gen Intel Core i7-12700K processor (3.60 GHz), and an NVIDIA GeForce RTX 3070 (8 GB, GDDR6) graphics card. The VR environment consisted of a clear space that matched the dimensions of the tracked physical space, set in an open outdoor scene sparsely populated with trees with a singular simulated natural light source. The trees, ground texture, and skybox used to create the outdoor environment were all free assets available on the Unity Asset store.

All task-relevant visual stimuli were presented on a grey (RGBA 102, 102, 102, 255; 0.4, 0.4, 0.4, 1.0) rectangular screen with simulated dimensions of 13.1° × 50.9° based on a 1 metre viewing distance (see Figure 2.1b). The target stimulus was an ellipsoid shape randomly orientated 45° clockwise or anticlockwise from vertical subtending 1.2° along its major axis. The QUEST (Watson & Pelli, 1983) adaptive staircase algorithm was implemented to adjust the target contrast (between 0.4, matching the background, and 1.0) that produced an overall hit rate of 75% for each stimulus condition. There were four independent staircases for left central, right central, left peripheral and right peripheral targets; Figure 2.1c displays an example change in contrast at central and peripheral locations. The initial slope (β) was set to 3.5, chance rate (γ) to .5, and lapse rate (δ) to .01 for each staircase, which had resolutions of .004 for the range 0.4

to 1. As the QUEST procedure settled at 75% hit rate after ~40 targets (after walking ~5-6 lengths of our 9.5 m path), a jitter was added to each trial's contrast to prevent the staircases from stagnating and not adjusting for changes in performance.

2.1.3 Procedure

Participants were provided with a participant information statement, followed by an opportunity to ask any questions before they completed the consent form. They were then introduced to the wireless VR apparatus, hand-controllers, power bank, the tracked physical space, and the initial eye tracking calibration procedure before being fitted with the apparatus and given the hand-controllers.

Once the VR program was initiated, participants completed a 4-point calibration process for the HMD's in-built eye trackers, handled by the eye tracking software. Additional calibration was performed after any potential events that may have affected the accuracy of the tracking (e.g., signal drop-outs, breaks). Participants were then told to situate themselves in front of the virtual display screen, standing on a virtual red cross placed 1 m away from the screen in the centre of the virtual environment, and to read the task instructions. The instructions outlined the flash detection task and the requirements to maintain gaze on the fixation cross. Participants were instructed to make speeded responses via trigger pull on the right-hand controller whenever they detected the target. Participants were also informed that to initiate each 9 second trial sequence, indicated by a green target on the fixation cross, a left-hand trigger pull was required (Figure 2.1a). They were given the opportunity to ask questions to better their understanding. They were then asked to describe the task they were to complete to verify their understanding. If correct in understanding, the participant was instructed to begin the first of three 9 sec trial sequences while standing still. Otherwise, the participant was assisted in their understanding by

alternate verbal instructions until they understood the task correctly and were given the opportunity to repeat the practice trial sequence. During this practice the targets presented were easy to detect, with a fixed supra-threshold contrast (adaptive staircases were not updated). Before beginning their first block of walking trials, participants were instructed to stand on a red cross repositioned to indicate the starting location of the walking sequence. The task was identical whilst walking, maintaining central fixation and with the additional instruction to maintain approximately 1 m between themselves and the display as it moved along a straight line at constant speed set by the walking guide.

Walking speed was set by the virtual walking guide, an animated 3D object in the virtual environment positioned in front of the observer which traversed a 9.5 m distance in 9 seconds and served as a pacesetter for the participant. Following the walking guide resulted in a walking speed of 1.06 m/s. Although slightly slower than typical human walking speed of approximately 1.4 m/s over long distances in natural environments (Hausdorff et al., 1996; Matthis et al., 2018), this reduced speed was found to be appropriate and comfortable based on the unfamiliarity some participants had with walking freely in a VR environment (Davidson et al., 2024). During each 9 second walking trial, targets were displayed to the left or right of fixation by 3.7° in the central condition (with no vertical offset) and by 12° in the peripheral condition (see Figure 2.1b). All locations were jittered by 0.5° horizontally. Crucially, simultaneous eye-movement recordings enabled the eccentricity of each target relative to fixation to be calculated, with subsequent exclusion from analysis when targets were not presented within our predefined central and peripheral regions of interest.

During trial sequences in walking blocks, the virtual display screen would smoothly traverse linearly along the walking path at a constant velocity and height, beginning motion

when the participant started the trial sequence (i.e., left-hand trigger pull). For the first two trial sequences of the block, the participant was accompanied to ensure their safety, and to verify this approximate distance was maintained comfortably whilst walking. Upon traversing the walking path, the participant was required to turn 180° before starting the following trial sequence, such that they returned on the path they had walked. Once comfortable with the procedure while walking, the participant was allowed to complete the remainder of the experiment independently, initiating the sequences themselves with left-hand trigger pulls.

Participants completed 10 blocks, five stationary blocks and five walking blocks, with the order of the blocks randomised except the first block. Each block had twenty 9-s trial sequences, each of which had a maximum of 9 targets presented. Targets were presented in one of four possible locations as per the factorial design, either left or right of fixation and either centrally (± 3.7°) or peripherally (± 12°), with the inclusion of a ± 0.5° horizontal jitter. Targets were presented for 20 ms, with the inter-trial timing of visual stimuli determined pseudo-randomly: no targets were shown in the first and last 500 ms of each trial sequence, with the first target in each sequence occurring at an average sequence time of 943 ms (SD = 381 ms). Subsequent targets were shown with a minimum ITI of 620 ms + 10-20 ms jitter, and to decrease predictability, each target had a 10% chance of being withheld (min and maximum targets shown per 9s sequence = 6-9; ITI M = 681 ms, SD = 139 ms, max ITI = 2600 ms).

Participants were instructed to respond as quickly and accurately as possible, using a single response option. Overall, participants followed task instructions, as a very low number of trigger-presses were recorded outside of target response windows (Mean per 9 s trial sequence = 0.24, SD = 0.16). Successful target detection (a Hit) occurred when a response was recorded within 800 ms of the stimulus onset, and a Miss was recorded otherwise. Responses within the

first 200 ms after target onset were discarded from analysis, owing to them being implausibly fast, and ambiguous as to their origin (either a delayed response to a previous miss, rapid detection, or false alarm).

Figure 2.1

Example of Procedure

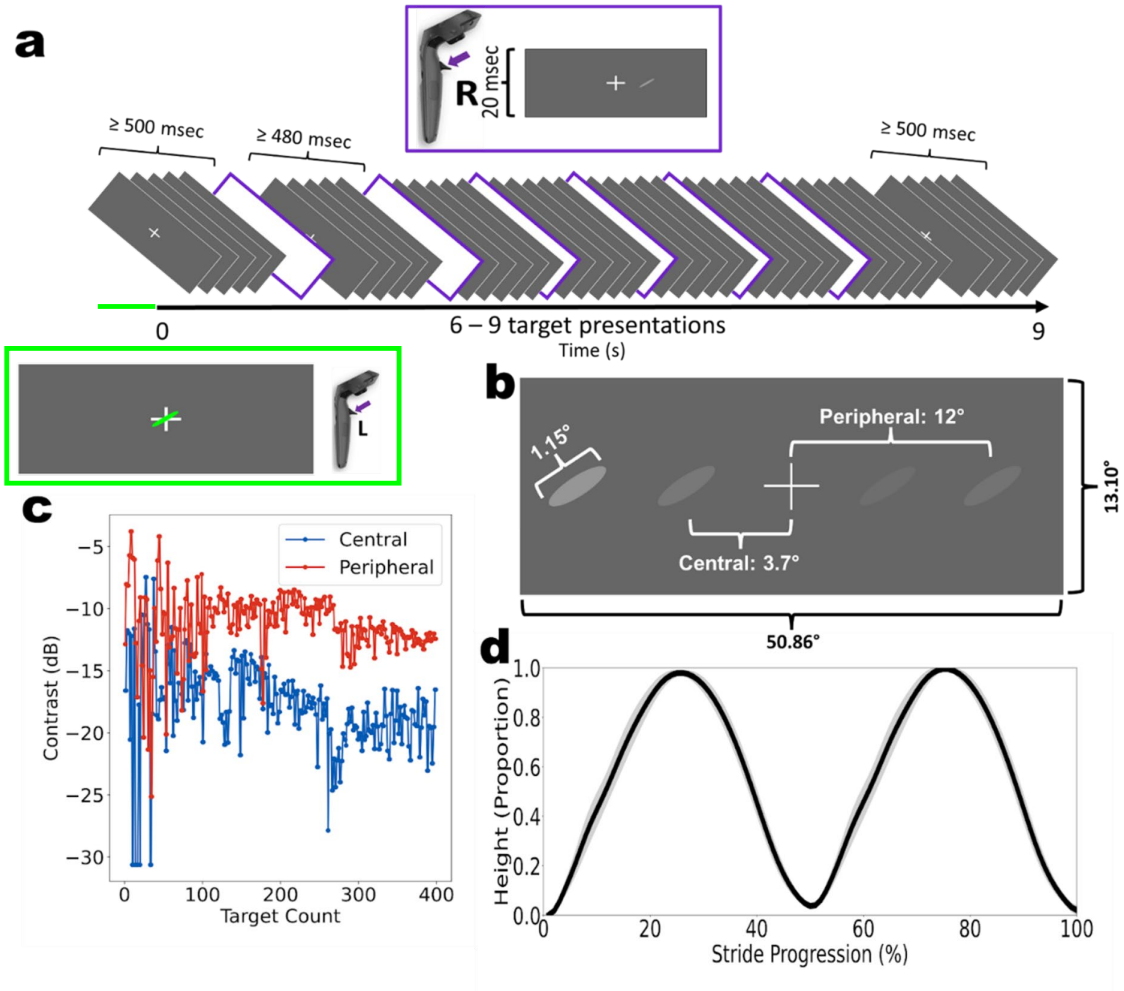

a Example trial sequence while completing a 9 second walking trial. The presentation of a target and response window is outlined in purple. The example sequence has six of these target presentations, indicated by a purple outlined box. Each walking trial had between 6 and 9 targets

presented. The pre-sequence display and initiating trigger pull, corresponding to the < 0 time is indicated in green below the timeline.

b Schematic of display parameters with the possible target presentation locations (not to scale). Four possible contrasts examples are provided (one per location, yet during the experiment only one target appeared at a time.

c Example data demonstrating the change in contrast for presentation of central and peripheral targets, in blue and red respectively.

d Grand mean change in head height during a stride (two sequential steps). Each stride was resampled to a normalised range of 1-100% for each participant ($N = 34$).

2.1.4 Data Analyses

Each sequence provided 3D time-series data (x, y, z coordinates) for head position, target position, gaze origin, and gaze direction. Individual steps were extracted based on head height, which follows a roughly sinusoidal pattern during walking. Peaks and troughs in vertical head position correspond to the approximate swing and stance phases of the stride-cycle (Hirasaki et al., 1999; MacNeilage & Glasauer, 2017; Mulavara & Bloomberg, 2002) which we identified using a peak detection algorithm. Changes in head height during all strides (two sequential steps) were averaged for all participants, as displayed in Figure 2.1d, and then normalised between the lowest and highest value to a range of 0-1. Target performance data (i.e., hits, misses, and response times) were mapped according to target onset relative to the nearest percentile of the stride-cycle. All analyses were performed using custom Python (version 3.11.1) code, and ANOVAs were performed in JASP (version 0.18.0.0).

2.1.5 Eye Movement Data

At each time point gaze coordinates were calculated using gaze origin and direction values, facilitating the calculation of target eccentricity. Individuals' eye gaze data were projected onto the simulated display screen as polar coordinates and used to verify correct fixation. Specifically, the proportion of frames where an individual deviated from the fixation cross (exceeding 1° eccentricity) during each 9 second sequence was used to quantify overall fixation. One participant was removed for recording a 75% proportion of deviation from fixation. Using the same projection procedure, the eccentricity of the targets relative to fixation at the moment of stimulus onset was also calculated. We retained central targets for analysis when they were presented within 7° of eccentricity from gaze fixation, and peripheral targets for analysis when presented between 7° and 20° of eccentricity from fixation. Any targets that were presented within 0.5° or beyond 20° of eccentricity from the locus of fixation were excluded as potential blinks or extraneous eye-movements.

2.1.6 Gait Extraction

Stride-onsets were extracted based on the time-series of the vertical head position as described in (Davidson et al., 2024). As walking shifts the centre of mass sinusoidally (Hirasaki et al., 1999; MacNeilage & Glasauer, 2017), troughs on the vertical axis of motion correspond to the double support stance phase of the gait cycle. Stride-lengths were normalised for analysis by resampling the time-series data to 100 points (taken as percentage of stride-cycle progression; see Figure 2.1d). Our categorisation of stance and swing phases was approximated as per the findings of MacNeilage and Glasauer (2017), attributing the ~1-10%, ~40-60%, and ~90-100% of the gait progression to the stance phase. These swing and stance phases are displayed with grey shading in our visualization of stride-cycle based effects (see Figure 2.2 and Figure 2.4). We

note our analyses focus on changes in performance between these approximations of swing and stance phases - and future work will be necessary to more precisely probe the stride-cycle with greater temporal resolution.

2.1.7 Performance Relative to Stride

All target onsets were allocated to the percentile (from 1-100%) of the stride they occurred in. For stride analyses, performance was averaged for targets occurring within 40 linearly spaced bins of 2.5% width, with zero overlap. We analysed hit rate, taken as the proportion of responses to presented targets out of total presented targets, and response times relative to target onset within each stride-cycle. Responses within 200 ms and beyond 800 ms of target presentation were excluded from all analyses to remove responses made in anticipation and lapses in attention. We additionally analysed the likelihood of committing a response (trigger pull) as a function of stride-cycle phase by an identically binned average of response counts.

We tested for significant sinusoidal modulation in each measure at both the participant and group level. For each measure, a Fourier series model was fitted using the equation:

$$f(t) = a_0 + a_1 \cos(\varphi t) + b_1 \sin(\varphi t) = a_0 + A \cos(\varphi t + \phi) \quad (2.1)$$

where $\boldsymbol{\varphi}$ is the periodicity (cycles per stride), $\boldsymbol{t}$ is the progression of the stride (as a percentage), $\boldsymbol{a_1}$ and $\boldsymbol{b_1}$ are the coefficients of the cosine and sine components and $\boldsymbol{a_0}$ is a constant, the central value of the modulation. The resulting fits had amplitudes of $\boldsymbol{A}$ and shifts in phase of $\boldsymbol{\phi}$. At the group level, we retained the Fourier model with maximum goodness of fit when stepping from .1 to 10 cps, in increments of .1 cps (displayed as an overlay in Figure 2.2). For tests of statistical significance, the goodness of fit (R^2) at each frequency (cps) was used as an indication of sinusoidal modulation strength. For statistical purposes, a null distribution of R^2 values was

calculated by first shuffling the labels for each percentile bin (from 1-100% with replacement), before repeating our main analysis. Specifically, on each permutation (N = 1000), we repeated our binning procedure and refit the Fourier series model over the entire frequency range of interest (.1 to 10 cps, in 1 steps). The 95th percentile of R^2 values at each frequency (see Figure 2.3, dotted lines) was used to test for significance by comparing the R^2 of the original data to the 95th percentile of the permuted data, with significant modulations at a given frequency indicated when the original R^2 exceeds the 95th percentile of the permuted data.

We also repeated our main analysis when aligning to clock-time (seconds) as opposed to the phases of the stride-cycle. As in our previous work (Davidson et al., 2024), this analysis allows us to also test for oscillations in standing data, and to compare the goodness-of-fit statistics when using cycles-per-stride compared to cycles-per-second (Hz). The results of this analysis are shown in Figure A1 and demonstrate that stride-cycle alignment is the superior frame-of-reference for capturing behavioural modulations in visual performance.

2.1.8 Super-subject Analysis

To test whether there were differences between the amplitudes and phases (ϕ) of central and peripheral performance modulation models, a super subject dataset was made for each performance measure composed of participants who showed significant modulations at ~2.0 cps (1.5-2.5 cps) at both eccentricities. For example, the super subject datasets contained all target presentations for the nine participants with modulations at central (n = 5311 targets), and peripheral locations (n = 6703 targets). The super subject performance was fitted for modulations at the mean of the best fitting frequencies for both eccentricities of the respective group-level performance modulations (hit rate = 2.05, response time = 2.05, response making = 1.95; see Figure 2.4). The super subject datasets were then resampled via bootstrap (with replacement)

1000 times, excluding a portion equivalent to a single participant on each iteration (hit rate prop. = 1/9, n = 1335 trials; response time prop. = 1/13, n = 1282 targets; response making prop. = 1/18, n = 1317 targets). Each bootstrapped dataset was fitted at the same frequency as their respective super subject dataset and the distribution of their phases (see Figure 2.4) compared to test for phase differences between modulations at the two eccentricities. Two-sample Kolmogorov-Smirnov tests were performed on the distribution functions.

2.1.9 Exclusion Criteria

Participants with data from less than four walking or stationary blocks were excluded for insufficient data collection (n = 1). Head position data was visually inspected for aberrant sequences and abnormal strides that may have occurred due to hardware malfunction, signal drop-out, or abnormal walking patterns (e.g., limping). Across all participants, an average of 0.57 sequences (SD = 0.85, range 0 – 4) and an average of 0.43 steps (SD = 1.88, range 0 – 11) were excluded using this procedure. No participants were excluded based on this procedure. Participants determined not to have fixated (i.e., kept gaze within 1°), according to the data analysis process, for at least 75% of their collective data points were excluded (n = 1). Additionally, those with overall hit rate for each adaptive staircase less than 65% (n = 3) or greater than 85% (n = 1) were excluded for possible floor and ceiling effects, respectively. Specific targets were excluded from analyses if they were closer than 0.5° (M = 5.58 targets, SD = 5.17, range 0 – 23) or exceeded 20° in visual eccentricity (M = 120 targets, SD = 217, range 0 – 982).

2.2 Results

A two-way 2 (Motion: Stationary vs Walking) x 2 (Visual Eccentricity: Central vs Peripheral) repeated-measures ANOVA was performed on the 75% contrast thresholds, provided

by fitting participants' psychometric functions. There was a main effect of eccentricity, such that participants' detection thresholds were lower for centrally presented targets than for peripherally presented targets ($F(1, 33) = 53.96$, $p < .001$, $\eta^2 = .280$). The main effect of motion and the interaction between motion and eccentricity was not significant (*p's* > .05).

2.2.1 Visual detection psychometric functions interact with motion type and target location

A three-way 2 (Visual Eccentricity: Central vs Peripheral) x 2 (Visual Field: Left vs Right) x 2 (Step Foot: Left vs Right) repeated-measures ANOVA was performed on the hit rate and response times from target presentations during walking. There were no significant main effects nor any significant interactions for either hit rate or response times (see Table 2.1), (*p's* > .05).

Together, these results demonstrate overall that thresholds, hit rate and reaction times were matched in our conditions, owing to the successful application of our QUEST staircase to equate performance. Notably however, there was an effect of target location on the contrast thresholds reached to match performance. Contrast thresholds decreased in the centre relative to the periphery to maintain 75% detection.

Table 2.1

Mean Hit Rate and Response Times by Experimental Condition

Visual Eccentricity	Visual Field	Step Foot	Hit Rate		Response Time	
			M	*SD*	*M*	*SD*
Central	Left	Left	.77	.08	355	27
		Right	.76	.10	358	37
	Right	Left	.77	.06	354	26
		Right	.77	.06	357	23
Peripheral	Left	Left	.76	.07	362	22
		Right	.76	.06	362	22
	Right	Left	.75	.04	355	25
		Right	.75	.05	356	25

Note. The proportion of correct responses to target presentations was taken as a measure of hit rate. The response time is presented in milliseconds (ms).

2.2.2 Stride-cycle phase modulates performance for targets at central and peripheral locations

In addition to comparing average performance between central and peripheral target locations while walking, our wireless VR environment enabled an analysis of changes in performance relative to the phases of the stride-cycle. When binning target-onsets to their relative stride-cycle phase (see Methods), hit rate and reaction times at both central and peripheral locations showed significant modulations at ~2 cps at the group-level (see Figure 2.2). Response likelihood was also modulated at ~2 cps. Modulations in hit rate occurred such that participants had improved detection for targets presented whilst they were in the approximate swing phase of their steps (see Figure 2.2a, d). Similarly, targets presented during the swing phase were also responded to faster than those in the approximate stance phase (see Figure 2.2b, e). When aligning response onsets to stride-cycle phase, response likelihood was greatest in the early stance phase, and lowest in the swing phase (see Figure 2.2c, f).

Figure 2.2

Modulations in Performance at Central and Peripheral Target Locations Within the Stride-Cycle

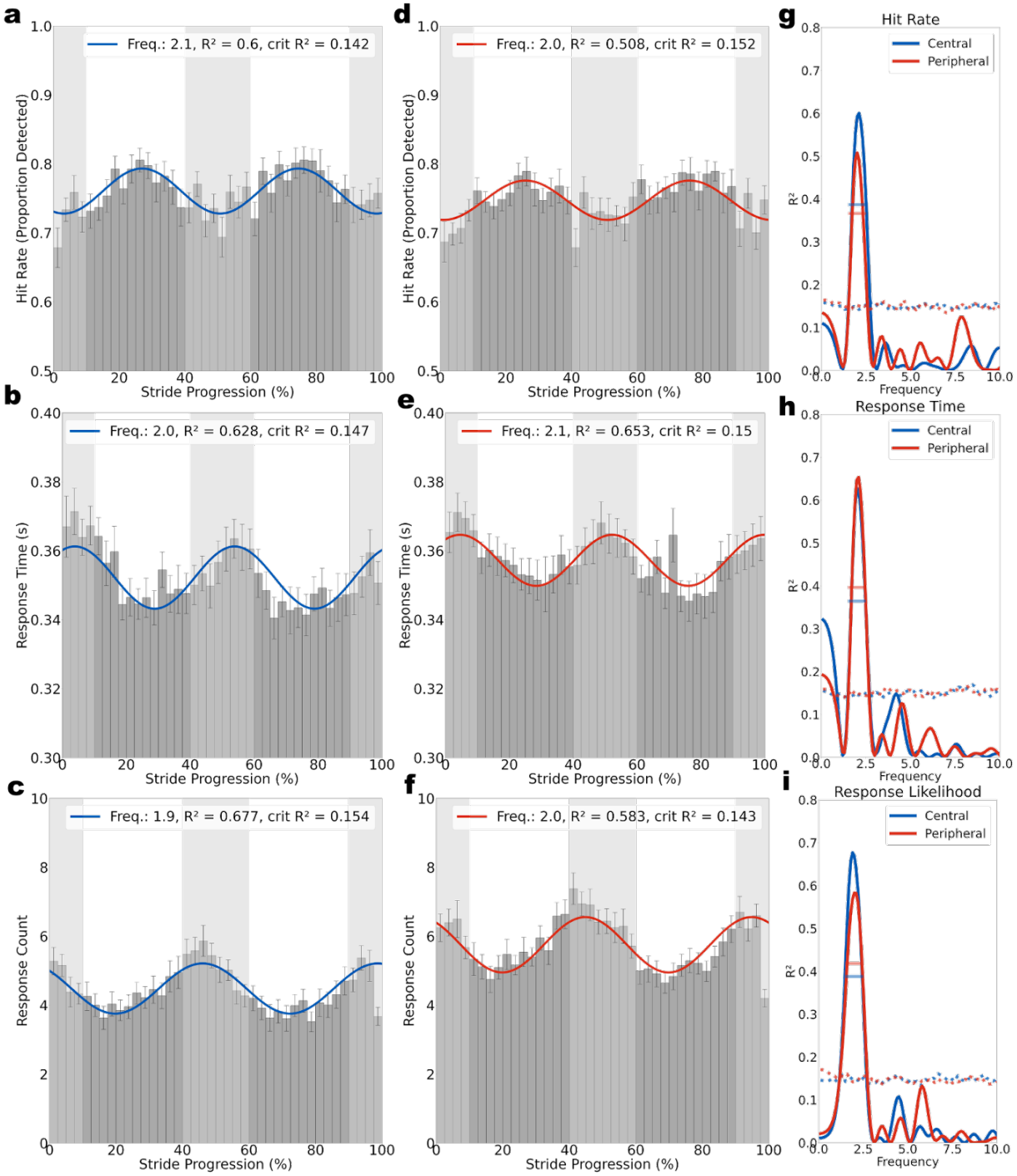

Note. Best-fitting Fourier models to group-level data ($N = 34$) are displayed for central (blue) and peripheral (red) targets. Light and dark grey regions indicate the estimated stance and swing phases of the stride-cycle, respectively.

a, d Group-level hit rate modulates at 2.1 cps and 2.0 cps for centrally and peripherally presented targets, respectively.

b, e Group-level reaction time data modulates at 2.0 cps and 2.1 cps for centrally and peripherally presented targets, respectively.

c, f Group-level response likelihood modulates at 1.9 cps and 2.0 cps for centrally and peripherally presented targets, respectively.

g-i Group-level Fourier models were fit at a fixed frequency between 0.1-10 cps (in steps of 0.1). The solid blue and red lines display the goodness-of-fit (R^2) calculated for each performance measure at central and peripheral target locations, respectively. Dotted lines show the upper 95th percentile of R^2 values at each fitted frequency obtained from a null distribution of group-level data shuffled in time (n = 1000 permutations). Solid horizontal lines show the upper 95th percentile when retaining the maximum R^2 value across all frequencies in the range 1.5- 2.5 cps per permutation (a more conservative test, guided by the results and frequency range of interest in Davidson et al., 2024)

We tested the statistical significance of these group level modulations using a two-step permutation procedure (see Methods). In brief, the observed fit-strength at a given modulation (e.g., R^2 value at 2 cps) was compared to the upper 95th percentile of R^2 values obtained from fitting the same Fourier model to permuted data (n = 1000 permutations). As shown in Figures 2.2 g-i, the R^2 values from the Fourier models fit to observed data at ~2 cps far exceeded the

upper 95th percentile of R^2 values expected by chance. This indicates the highly oscillatory nature of the participants' performance over the gait cycle.

2.2.3 Participant level analysis of modulations at central and peripheral locations

We next performed participant-level analyses of modulations according to stride-cycle phase to determine the prevalence and phase-consistency of modulations at central and peripheral target locations. For this, only participants with significant modulations in the range 1.5–2.5 cps were included. To estimate the phase-clustering, each participant was fitted with a Fourier model with a fixed frequency set to the mode of significant modulations within each subset of significant participants. For modulations in hit rate (see Figure 2.3a), to central (n = 18) and peripheral targets (n = 18) the mode was 1.9 cps. The distribution of phase angles at both locations was significantly non-uniform (Rayleigh's test of non-uniformity; central Z = 4.64, p = .008; peripheral Z = 7.80, $p < .001$).

The phase distributions for modulations in response time (central n = 19 participants, peripheral n = 15 participants) were also significantly non-uniform (central: $Z = 10.34$, $p < .001$, modal frequency 2.1 cps; peripheral: $Z = 4.93$, p = .006, modal frequency 2.0 cps; see Figure 2.3b). A large portion of our sample demonstrated significant modulations in response likelihood (central n = 21, peripheral n = 26) that were also significantly non-uniform (central, $Z = 9.07$, $p < .001$, modal frequency 1.6 cps; peripheral, $Z = 6.19$, $p = .002$, modal frequency 1.9 cps; see Figure 2.3c).

Figure 2.3

Significant Modulations at the Participant Level are Clustered in Phase

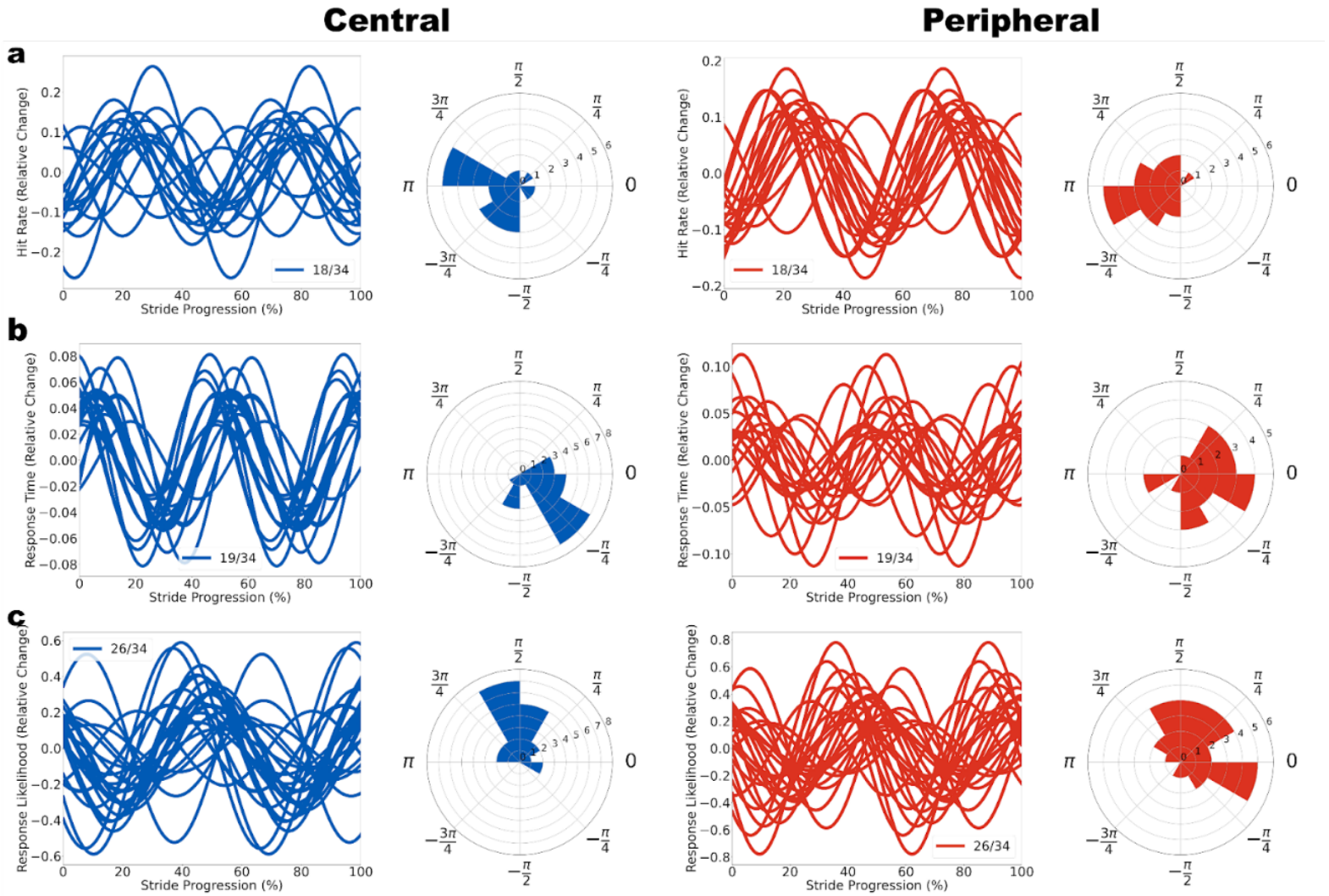

Note. Modulations for centrally presented targets are presented in blue (left panels) and modulations for peripherally presented targets are presented in red (right panels). Black radial lines on polar plots represent the mean phase for the subset of participants with significant modulations. For each performance measure, the modal frequency was fitted for all participants.

a n = 18 participants displayed significant modulations in hit rate (1.5–2.5 cps) for centrally presented targets. Right column shows hit rate modulations following peripheral targets (n = 18). The fit at modal 1.9 cps is displayed for both eccentricities, with phase clustering shown in the polar plots.

b Displays the subset of participants with significant modulations at 2.1 cps in response time for central (n = 19) and peripheral targets (n = 19) fit at 2.0 cps.

c Displays participant modulations in response likelihood at 1.6 cps following central (n = 26) and at 1.9 cps for peripheral (n = 26) targets.

2.2.4 Within-participants comparison of modulations at central and peripheral locations

We additionally performed a complementary super subject analysis to confirm differences in oscillatory features between central and peripheral locations. This analysis focused only on the subset of participants which had significant modulations at both central and peripheral locations (hit rate $n = 9$, response time $n = 13$, response making $n = 18$). Importantly, by including only those participants, this analysis mitigates the risk that the differences we report at each eccentricity may be driven by comparisons between unique subsets of participants (such as those with significant modulations at only one eccentricity).

On the aggregated super-subject data, we repeated our group-level Fourier fit analysis using a bootstrapped resampling procedure, excluding a portion of trials equivalent to a single participant on each iteration ($n = 1000$). For each resampled dataset, the amplitudes and the phases for each Fourier model were retained for statistical comparisons (see Methods). The phases for the central hit rate modulations (mode = 3.09 radians) were distributed significantly later than those for the peripheral hit rate modulations (mode = 2.90 radians), such that hit rate peaked 1.48% earlier in the gait cycle for central targets, $D = .945$, $p < .001$ (see Figure 2.4a). A difference in the phases of the central (mode = 5.58 radians) and peripheral (mode = 5.70 rad) response time modulations was found, where response times peaked 0.93% earlier in the gait cycle for central targets, $D = .990$, $p < .001$ (see Figure 2.4b). Similarly, the distribution of phases for peripheral response likelihood modulations (mode = 4.23 radians) were instead significantly higher than those for the central response likelihood modulations (mode = 4.40 radians), such that the likelihood of a response being made peaked 3.85% earlier in the gait cycle for peripheral targets, $D = 1.000$, $p < .001$ (see Figure 2.4c).

The amplitudes of central and peripheral modulations also differed significantly. The amplitude of central modulations in hit rate (mode = .055) were distributed lower than those for peripheral modulations (mode = .061), $D = .966$, $p < .001$ (see Figure 2.4a). For response time, central modulation amplitudes (mode = 182 ms) were distributed higher than peripheral modulation amplitudes (mode = 162 ms), $D = .986$, $p < .001$ (see Figure 2.4b). Similarly, amplitudes for response likelihood modulations for central targets (mode = 18.36) were distributed higher than for peripheral targets (mode = 16.37), $D = .999$, $p < .001$ (see Figure 2.4c).

Figure 2.4

Modulations of Super Subject

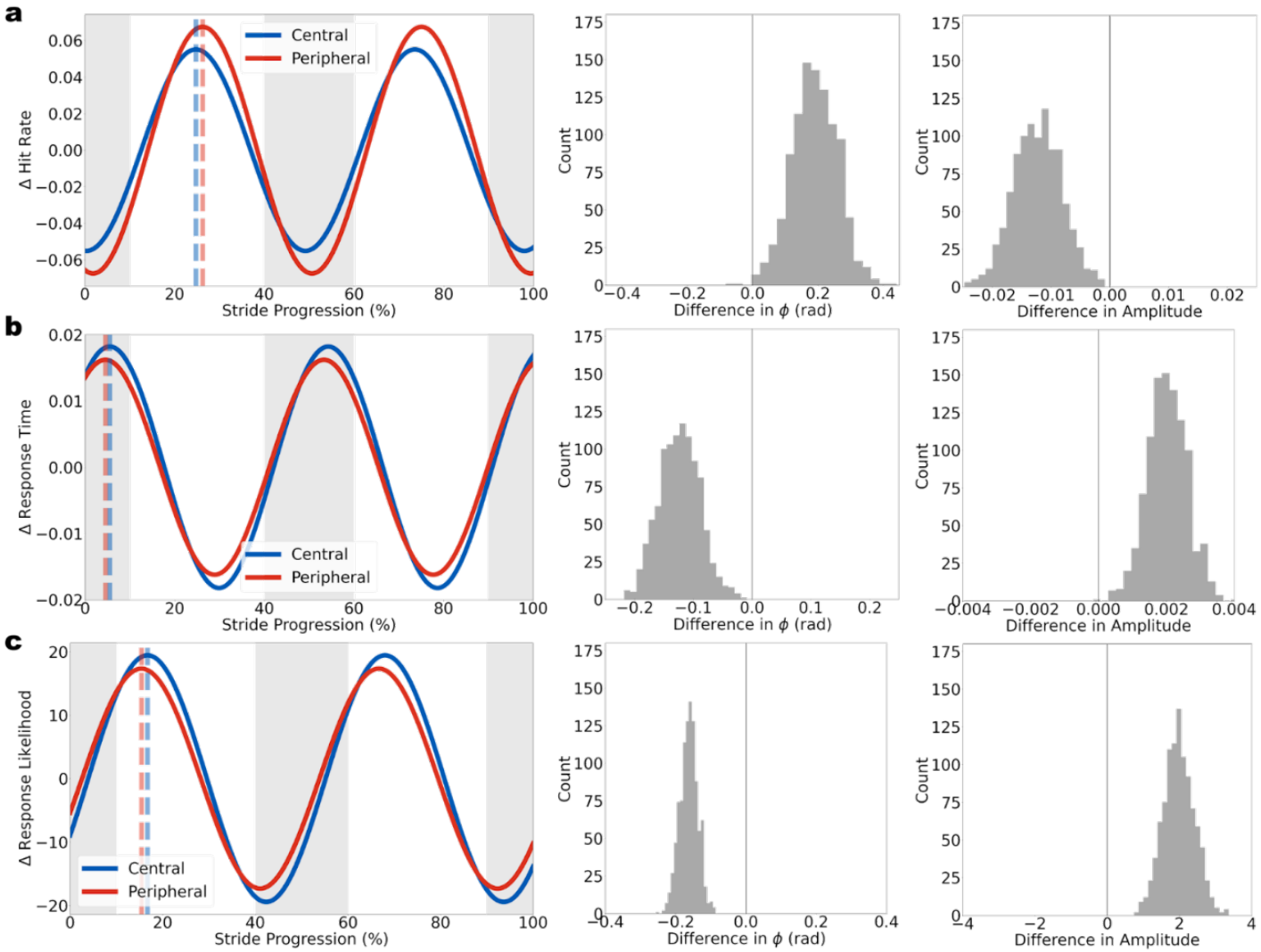

Note. Plot of normalised modulations of a super subject comprised of all participants with significant modulations for both centrally and peripherally presented targets for each performance measure. Dashed lines indicate the peak of modulations. Frequency distributions of the phase difference (ϕ) and the amplitude difference between the central and peripheral targets for 1000 bootstrapped resamples of the super subject dataset are displayed. Difference values were calculated by subtracting the parameter for the peripheral location from the corresponding central location parameter. Vertical lines on difference distribution plots represent the equivalence point.

a Modulations in hit rate of super subject, fitted at 2.05 cps.

b Modulations in response time of super subject, fitted at 2.05 cps.

c Modulations in response likelihood of super subject, fitted at 1.95 cps.

Overall, these analyses demonstrate that modulations in visual detection hit rate and reaction time differ significantly in amplitude and phase for targets presented at central compared to peripheral target locations.

2.3 Discussion

The current study examined the effects of walking on visual detection performance, with a specific focus on changes in performance at central and peripheral visual field locations within the stride-cycle. Participants made speeded trigger-pull responses with their right hand to indicate their detection of a presented target. Pronounced modulations in task performance were entrained to the rhythm of the stride-cycle, with a significant difference in the amplitude and phase lag of modulations at central compared to peripheral target locations.

2.3.1 Performance modulations at central and peripheral locations are modulated by the phases of the stride-cycle

When examining changes in performance relative to stride-cycle phase, strong modulations were present in hit rate and reaction time for both central and peripheral targets. These results confirm the modulatory effects of walking on visual perception observed in other studies (Cao & Händel, 2019; Chen et al., 2022a, 2022b) and adds to recent work showing more specifically that perceptual modulations are linked to the stride-cycle (Davidson et al., 2023, 2024). Consistent with Davidson et al. (2024), within-stride modulations were found for all three performance measures: hit rate, response time, and response likelihood. These group-level modulations were all at a frequency of ~2 cps with improved hit rate and reaction times in the approximate swing phase of the stride-cycle, and responses most likely around the time of heel-strike.

2.3.2 Participant level modulations cluster in phase

At the participant-level, we observed significant phase clustering of these modulations, such that hit rate in most observers improved during the swing-phase of each stride and reaction times were faster. Here, as in Davidson et al. (2024), we note that individual participants who exhibited significant modulations showed some variability in the precise location of their performance peak. Peaks tended to cluster around the middle of the swing-phase but a small group of outliers showed a counter-phase relationship to the average group-level result and thus showed a performance decrease in the swing-phase. While the group level result is clear, here and in our other study of gait-related perceptual modulations (Davidson et al., 2024), the reason behind the outlying participants is not clear. Two possible reasons are that those participants who showed clear anti-phase results adopted a different response strategy, or they may have had unusual or idiosyncratic gait patterns. A simple visual inspection of gait patterns (based on head position data) indicated that participants showing anti-phase performance did not differ markedly from other participants. A full gait analysis quantifying spatiotemporal factors and kinematics would provide more insight into this possibility. More studies will be needed to understand the anti-phase performance shown by a minority of observers.

One potential explanation of anti-phase performance that can be excluded is an account based on eye movements towards the targets. In the present study there were only occasional instances of large eye-movements. These will inevitably occur in designs involving peripherally presented targets as participants are sometimes tempted to break central fixation and look directly at the peripheral target. Our participants were instructed not to break fixation (trials were excluded when it did occur; see Methods) and told that the strategy cannot be effective as target duration was just 20 ms and saccades take far longer than this to program and execute (saccadic

latencies range from 150 to 200 ms; Smit et al., 1987). We can be confident, therefore, that all data included in our analyses involved central fixation and that artefacts such as blur when the eyes move across an HMD display did not confound our results. As a result, we can rule out an explanation of these phase differences across participants in terms of differences in large eye-movement activity, but other options remain, and future studies will be needed to explore them. For example, future studies may wish to replicate our results using real-world objects in the centre and periphery, and if possible, record eye-movements with higher resolution to account for microsaccades.

Another alternative explanatory mechanism for the variability in participant-level modulations relates to the demands of locomotion itself. At the beginning (i.e., toe off) and end of a step (i.e., heel strike), the requirement for motor planning and execution shifts sensory focus from the visual modality to comparing motor efference copies with afferent proprioception (Chagnaud et al., 2012; Cullen, 2004; Wolpert & Flanagan, 2001). At these critical stages of the stride-cycle, the unpredictability of head movements is also greatest (MacNeilage & Glasauer, 2017), potentially shifting requirements toward the vestibular modality for increased proprioception, balance and stability (Bent et al., 2005). It is currently unclear whether differences in baseline balance, proprioception, or dual-task abilities may account for some of the differences in participant level-effects we have observed. A potential manipulation that could serve to investigate this effect would be to heighten the motor requirements of specific portions of the stride-cycle, for example by having participants walk up an inclined path or on an unstable surface. The use of a passive control condition – such as by replaying the locomotion induced optic flow in a motion simulator, could also serve to decouple the motor and proprioceptive

demands experienced while walking, to test their respective influence on the modulations we have observed.

2.3.3 Performance modulations differ in amplitude and phase based on visual field location

Both central and peripheral vision exhibited modulations for each performance measure (hit rate, reaction time and response likelihood), however, there were differences between the amplitudes and phases of the modulations across the eccentricities. Specifically, we revealed that the modulation in hit rate was significantly smaller in amplitude, and later in phase, for central compared to peripheral targets. This pattern of differences was reversed when comparing the modulations in response time between the target locations. What might drive these modulation differences between visual eccentricities? Prior research has indicated that differences in visual ability across different visual locations are fundamentally tied to the non-uniform distribution of receptors on the retina and primary visual areas (Curcio & Allen, 1990; Rovamo & Virsu, 1979; Virsu & Rovamo, 1979; see Himmelberg et al., 2023 for review). At present however, it is unknown how these asymmetries may map from the tradition of seated experimental settings to the active observer, or whether different regions may be activated asymmetrically during the stride-cycle (Parker et al., 2020).

One possibility advocated by Cao and Händel (2019) is that a trade-off may occur between central and peripheral locations during walking, with the periphery prioritised for safe navigation because potential moving hazards are most likely to enter from the periphery. Detecting these efficiently would avoid potential collisions and keep the individual reactive to the inevitable changes occurring during locomotion in a dynamic perceptual environment. In our data set, central and peripheral targets were never presented simultaneously, which precludes a

direct test of this proposed trade-off, but it remains a tantalising proposition to test in future research. Notably however, the modulation in detection performance was higher in amplitude for targets at peripheral locations during walking, potentially indicating a minor disadvantage with respect to variation within the stride-cycle. Future research could test whether these amplitude differences scale with increasing eccentricity, and at other polar angles from fixation (i.e. off the horizontal axis), to confirm whether increase in modulation depth varies with eccentricity. For example, future work could investigate whether this difference applies to different visual location comparisons, such as vertical (as opposed to lateral) eccentricity (Abrams et al., 2012; Corbett & Carrasco, 2011), perceived depth (Nasr & Tootell, 2018), and between nasal and temporal fields (Paradiso & Carney, 1988; Rafal et al., 1991).

Similarly, recent work has identified that induced perceptual oscillations propagate across the visual field, potentially supported by travelling waves across the cortex (Fakche & Dugué, 2024; Sokoliuk & VanRullen, 2016). Both theta (3-7 Hz) and alpha (8-12 Hz) oscillations have been implicated as modulators of visual and auditory sensitivity (Di Gregorio et al., 2022; Ergenoglu et al., 2004; Fuentemilla et al., 2008; Köhler et al., 2021; Sakowitz et al., 2000; Weisz et al., 2011; Zoefel & VanRullen, 2017) and in divided and focused visual attention (Fiebelkorn et al., 2018; Re et al., 2019). While we did not explicitly manipulate attention, previous manipulations, such as via a valid or invalid cue, have successfully altered the phase of oscillatory performance on visual detection tasks (Busch & VanRullen, 2010; Fiebelkorn et al., 2018; Ho et al., 2017; Landau & Fries, 2012; Zhang et al., 2012). To understand the extent to which the phase differences we have observed also rely on attentional processes, the incorporation of a cue to central and peripheral locations could be an informative condition to include. Similarly, whether the phase shifts we have observed continue to scale with increasing

eccentricity will be an exciting prospect for future research. Additionally, due to the expansion and contraction effects of optic flow and similar vector motion, it would be interesting to see whether there is an interaction between these eccentricity effects and manipulations of walking speed, heading direction, and cue position.

2.3.4 Conclusion

The current study has confirmed the modulatory effect of locomotion upon visual detection, measuring modulations in visual detection performance at both central and peripheral target locations when controlling for eye-movements. Modulation in central vision detection was significantly smaller in amplitude, and modulation in peripheral vision was slightly phase-leading, suggesting an interaction between the entrainment of performance and visual field locations. Future research may focus on the inclusion of increased target locations in order to characterise the potential relationship modulation phase has with visual eccentricity. In addition, as modern locomotion regularly incorporates dual-task requirements that may divide attention (such as while holding a phone), an important step will be to determine whether performance modulations while walking can be biased by an attentional cue.

2.4 Acknowledgements

Research was supported by an Australian Government Research Training Program (RTP) Scholarship (SC3227) to Cameron K. Phan and an Australian Research Council grant (DP210101691) to Professor David Alais and Professor Frans Verstraten.

3

Chapter 3

Stride-based modulation difference between visual hierarchy levels

The following chapter is currently in submission at the Proceedings of the Royal Society B as:

Phan, C. K., Rideaux, R., Alais, D. (2025) Walking Produces Oscillations of Orientation and Direction Perception at the Step Rate. *Proceedings of the Royal Society B.*

The study presented in this chapter was designed by C.P., the data was collected by C.P., data was analysed by C.P., writing was completed by C.P., editing was completed by C.P., R.R. and D.A., and funding was acquired by C.P., R.R. and D.A..

Stride-based modulation difference between visual hierarchy levels

With the advent of new technologies, such as virtual reality and wireless devices, a more action-oriented approach to perceptual research has become possible (Davidson et al., 2023, 2024; Matthis et al., 2017, 2018; Matthis & Fajen, 2014; Phan et al., 2025). Despite this advancement in empirical research, there remains a plethora of perceptual phenomena to investigate in the context of action and self-generated voluntary movement, including simple detection of basic sensory features. In many daily activities, the perceptual features of an object determine the interactions one has with it. An object's orientation may dictate the specifics of how an individual physically interacts with it through reaching and grasping, while an object generating sound may facilitate estimations of its location and motion. Basic features are therefore pivotal in decisions to interact with an object, and yet even the most basic visual tasks have recently been shown to be modulated by action (Davidson et al., 2023, 2024; Phan et al., 2025; Szekely et al., 2024).

Walking is the most consistently observed and patterned active movement engaged by most people, demonstrating easily recognized and demarcated phases from physical indicators such as the walking individual's head height and centre-of-mass location (Hwang & Effenberg, 2021; Kharb et al., 2011; Rakovac, 2021). Head height displays an approximately sinusoidal modulation, with peaks occurring in the swing phase of the gait cycle and troughs occurring in the stance phase (Hwang & Effenberg, 2021; Rakovac, 2021). Perceptual abilities when measured during walking have now been shown to exhibit similar sinusoidal modulations (Davidson et al., 2023, 2024; Phan et al., 2025). Detection of visual targets increases during the swing phase of walking (Davidson et al., 2024; Phan et al., 2025). These modulations are not restricted to the perceptual domain: motor actions, such as the trigger pulls made to respond to

the visual stimulus, are entrained to the footfall of the gait cycle and tracking an object's path over space by moving the hand is more precise during the swing phase (Davidson et al., 2023, 2024; Phan et al., 2025). The existence of gait-related modulations in the motor and perceptual domains suggests that action-related modulation may be prevalent feature of many perceptual abilities.

The current study employed a free-walking paradigm by utilizing wireless virtual reality (VR) technology and tested for gait-linked modulations of an orientation identification task and a motion identification task. The procedure is adapted from the flash detection task employed in Chapter 2 which compared central and peripheral locations. Here we retain the visual location manipulation from Chapter 2 to verify their finding of a bias for dynamic, moving objects in peripheral vision and one for static objects in central vision. The other gait effects noted above (perceptual sensitivity peaking in swing phase, and motor responses more likely in stance phase) did not depend on eccentricity (Chapter 2). Investigating orientation over the gait cycle is of interest because primary visual cortex shows a bias towards horizontal and vertical orientations (Appelle, 1972; Campbell et al., 1966; Furmanski & Engel, 2000; Heeley & Timney, 1988; Paradiso & Carney, 1988) and therefore orientation identification should vary as the head rolls from side to side during location towards the supporting foot. Orientations that match or are orthogonal to the observer's head should be better perceived than objectively vertical or horizontal orientation, and this will vary cyclically over the gait cycle with a peak at greatest angular head tilt (Figure 3.1).

Figure 3.1

Stimulus Orientation Alignment with Head Roll Experienced During Walking

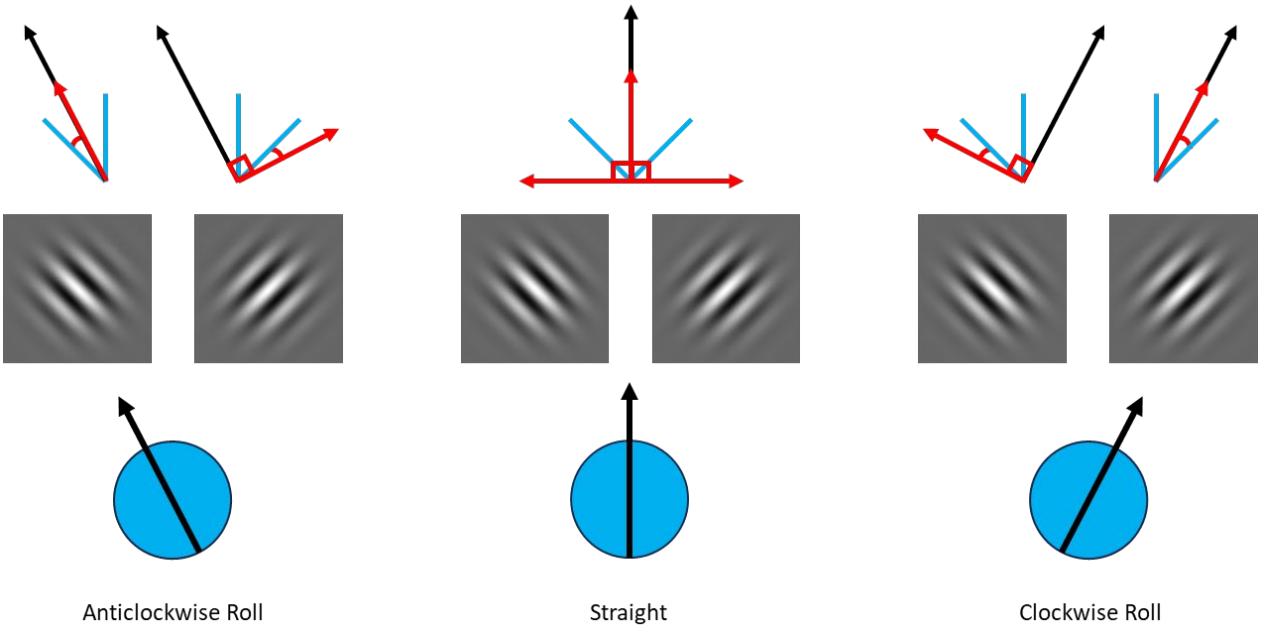

Note. Schema of head rolls that would occur during walking and examples of alignment of potential orientated stimuli. Black arrows indicate head roll rotation, red arrows indicate relative orthogonal and vertical directions, and blue rays indicate stimulus orientation in world space. Red angle markings illustrate the closest orthogonal or vertical angle. As made evident, when head roll is at vertical (straight), the stimulus orientation is maximally oblique (45°).

In contrast to the expected head-related orientation bias in perception, the bias found in motion perception appears to be dependent on observer-relative motion. When the observer's self-motion is opposite a visual object's motion, the object appears to move faster and be more salient (Fetsch et al., 2013; Hogendoorn et al., 2017). During the gait cycle, the walking individuals head shifts up and down when entering and exiting the swing phase, respectively. Therefore, it would be expected that there would be a greater likelihood of a correct perception of motion direction when the individual enters a phase in which their head moves opposite to the

motion. In addition, any differences in the observed perceptual modulations as a function of visual eccentricity would provide insight into the prioritization of visual feature processing across the retina whilst walking (Lewis et al., 2011). Irrespective of the visual feature being investigated and in line with prior studies (Davidson et al., 2023, 2024; Phan et al., 2025), the modulations across the gait-cycle are expected to manifest in the two cycles per stride region (1.5 to 2.5 cps) and thus serves as our frequency of interest.

3.1 Chapter 3 Experiment 1

3.2 Methods

3.2.1 Design

The study employed a four-way 2 (Motion: Stationary vs Walking) × 2 (Visual Eccentricity: Central vs Peripheral) × 2 (Visual Field: Left vs Right) × 2 (Orientation: Left vs Right) repeated-measures factorial design. A factorial design was employed to account for any potential confounds between the independent variables. The comparisons of interest were between the levels of each of these independent variables.

Walking speed was set by the virtual walking guide, an animated 3D object in the virtual environment position in front of the observer which traversed a 9.5 m distance in 9 secs. Following the walking guide resulted in a walking speed of 1.06 m/s, slightly slower than typical human walking speed of approximately 1.4 m/s over long distances in natural environments (Hausdorff et al., 1996; Matthis et al., 2018). The slower walking speed was found to be a comfortable pace in our previous work, and appropriate given the uncertainty and unfamiliarity some participants may have experienced when walking freely in a VR environment (Davidson et al., 2024). The target's eccentricity was calculated for each presentation in real-time, based on the viewing distance of the head-mounted display to the simulated experimental screen. Central

targets were displayed 3.7° (± 0.5°) to the left or right of fixation with no vertical offset, and peripheral targets were displayed 12° (± 0.5°) from fixation. The eccentricity was calculated with the assumptions that participant gaze was perpendicular to the virtual display screen and that fixation was maintained on the fixation cross.

The responses were no longer simple yes-no responses seen in prior studies (Davidson et al., 2024; Phan et al., 2025) and now were a two-alternative quadrant mapped response. This change in response options provided not only a measure of individuals' perceptions of a visual object's orientation, but also an opportunity for replication of the phenomena seen in the yes-no response tasks. Lack of a response will still indicate a target that has not been detected whilst an incorrect response indicates detection, albeit an incorrect percept of the visual feature of interest. Thus, in addition to analysing participants' performance for overall accuracy (i.e., number of correct responses out of total target presentations), response rate (number of targets responded to out of total target presentations) and response accuracy (number of correct responses out of total responses made) were analysed. Participants' response times were analysed both in an overall manner and exclusively for correct responses.

3.2.2 Participants

Participants were 41 undergraduate psychology students from the University of Sydney who participated in exchange for course credit. The participation consisted of a single session that lasted approximately one hour. 13 participants were excluded, as per criteria below, leaving a final sample of N = 28 (M_{Age} = 20.3 years, SD_{Age} = 1.6, range = 18 – 23; 27 right hand dominant). Each participant provided informed consent before commencing and had normal or corrected-to-normal vision (not verified). The study protocol was approved by the University of Sydney Human Research Ethics Committee (HREC 2021/048).

3.2.3 Apparatus and Materials

An HTC Vive Pro Eye head-mounted display (HMD) was used to display the virtual environment and two wireless HTC Vive Controllers (2018) were used for collecting responses. The HMD contained dual 3.5-inch high-resolution OLED displays (1440 x 1600 pixel resolution, 90 Hz refresh rate) with 110-degree field of view. Positions of the HMD and controllers were tracked in three-dimensional space at 90 Hz resolution, using five HTC Vive Base Station 2.0's enclosing an open 4.5 m x 12 m rectangular space. To allow the utilization of such a large space and unencumbered walking conditions, the virtual reality environment was transmitted to the HMD using the HTC Vive Wireless Adapter for Vive Pro. The SRanipal Runtime (Version 1.3.2.0; SDK 1.3.6.8) was used to handle eye tracking data collection by the integrated Tobii eye-tracker within the HMD, sampled at 90 Hz.

The virtual reality (VR) environment and experimental procedure were designed and presented within Unity (Version 2020.3.14f1), using the SteamVR Plugin (Version 2.7.3; SDK 1.14.15) on a Windows 11 PC (2 × 16 GB, DDR5 4400 MHz) with a 12th Gen Intel Core i7-12700K processor (3.60 GHz), and an NVIDIA GeForce RTX 3070 (8 GB, GDDR6) graphics card. The VR environment consisted of a clear space, that matched the dimensions of the tracked physical space, set in an open outdoor scene sparsely populated with trees with a singular simulated natural light source. The trees, ground texture, and skybox used to create the outdoor environment were all free assets available on the Unity Asset store.

3.2.4 Stimuli

All task-relevant visual stimuli were presented on a grey (RGBA 102, 102, 102, 255; 0.4, 0.4, 0.4, 1.0) rectangular screen with simulated dimensions of 20 cm × 82.8 cm (45° visual angle at 1 m horizontally). The target stimulus was a circular Gabor pattern ($frequency_{grating}$ = 1.92

cycles/deg, $SD_{gaussian}$ = 0.52°), simulated to be 1.75 cm (2.78° at 1 m), orientated 45° (± 5°) clockwise (right orientation) or anticlockwise from vertical (left orientation). The QUEST (Watson & Pelli, 1983) adaptive staircase algorithm was implemented to adjust the overall contrast of the Gabor patterns to produce an overall accuracy rate of 75% for each combination of motion and target eccentricity condition (i.e.: unique staircases for central targets whilst stationary, central targets whilst walking, peripheral targets whilst stationary, and peripheral targets whilst walking). The initial slope (β) was set to 3.5, chance rate (γ) to .5, and lapse rate (δ) to .01 for each staircase, which had resolutions of .01 (i.e. 1%) for the range .01 to 1. As the QUEST procedure stabilised at 75% accuracy after ~40 targets (~ 8-10 walking sequences), a small jitter was added to each trial's target contrast to prevent the staircases from stagnating and not adjusting for changes in performance.

The virtual display screen would smoothly traverse linearly along the walking path at a constant velocity and constant height. This linear movement was independent of the participants' head positions and was mapped as a straight path in world space coordinates.

3.2.5 Procedure

Participants were provided with a participant information statement, followed by an opportunity to ask any questions before they completed the consent form. All participants were informed that they could revoke their consent and participation at any time during the procedure if they wished not to provide their data or did not wish to complete their participation without the need to provide a reason. They were then introduced to the wireless VR apparatus, hand-controllers, power bank, the tracked physical space, and the initial eye tracking calibration procedure before being fitted with the apparatus and given the hand-controllers.

Once the VR program was initiated, participants completed a 4-point calibration process for the in-built eye tracking component of the HMD, handled by the eye tracking software. Additional calibration was performed after any potential events that may have affected the accuracy of the tracking (e.g., signal drop-outs, breaks). Participants were then told to situate themselves in front of the virtual display screen, standing on a virtual red cross 1 m away from the screen in the centre of the virtual environment, and to read the task instructions. The instructions outlined the orientation identification task and the requirement to always fixate on the fixation cross and requirement to make speeded responses, pressing the quadrants on either hand controllers' trackpad corresponding to either end of the Gabor grating bands (see Figure 3.2). Participants were also informed that to initiate each sequence, indicated by an example of the target at 100% contrast directly below the fixation cross, simultaneous trigger pulls on both hand controllers were required. They were then asked to describe the task they were to complete to verify their understanding. If correct in understanding, the participant was instructed to begin the first of three 9 s sequences while standing still. Otherwise, the participant was assisted in their understanding by alternate verbal instructions until they understood the task correctly and were given the opportunity to repeat the practice trial sequence. During this practice the targets presented were easy to detect, with a fixed supra-threshold constant in overall contrast (100%) and were not used to update any of the adaptive staircases. In addition to general understanding of the task, the practice allowed for the correction of thumbpad responses to maximise response detection by the controllers and for the participant to become comfortable with making such responses.

Before beginning their first block of walking sequences, participants were instructed to stand on a red cross that had repositioned to indicate the starting location of the walking

sequence. The task was identical whilst walking, maintaining fixation with the additional instruction to maintain approximately 1 m between themselves and the display. For the first two sequences of the block, the participant was accompanied to ensure their safety, and to verify this approximate distance was maintained comfortably whilst walking. Upon traversing the walking path, the participant was required to turn 180° before starting the following sequence, such that they return on the path they had walked to reach the end point to reach the previous start point. Once comfortable with the procedure of walking blocks, the participant was allowed to complete the remainder of the block independently, initiating the sequences themselves with dual-hand trigger pulls. Approximately, every five sequences, participants were prompted to check their response making alignment on the thumbpads before initiating the next sequence to avoid potential issues in their thumb position drifting.

Participants completed 10 blocks, five stationary blocks and five walking blocks, with the order of the blocks randomized except for the first block. Each block had twenty 9-sec sequences, each of which had 5 or 6 targets presented relative to predefined anchor points, with each target having a 10% chance of being withheld from presentation. Targets were presented in one of four possible locations as per the factorial design, either left or right of fixation and either centrally or peripherally, restricted to the area spanned by the virtual display screen. Targets were presented for 40 ms and were spaced by variable intertrial intervals with a minimum of 1200 ms. Targets were never presented during the first 250 ms of sequences. During sequences in walking blocks, the virtual display screen would smoothly traverse linearly along the walking path at a constant velocity and constant height, beginning motion when the participant started the sequence (i.e., left-hand trigger pull).

Figure 3.2

Schematic of Target Stimuli and Responses

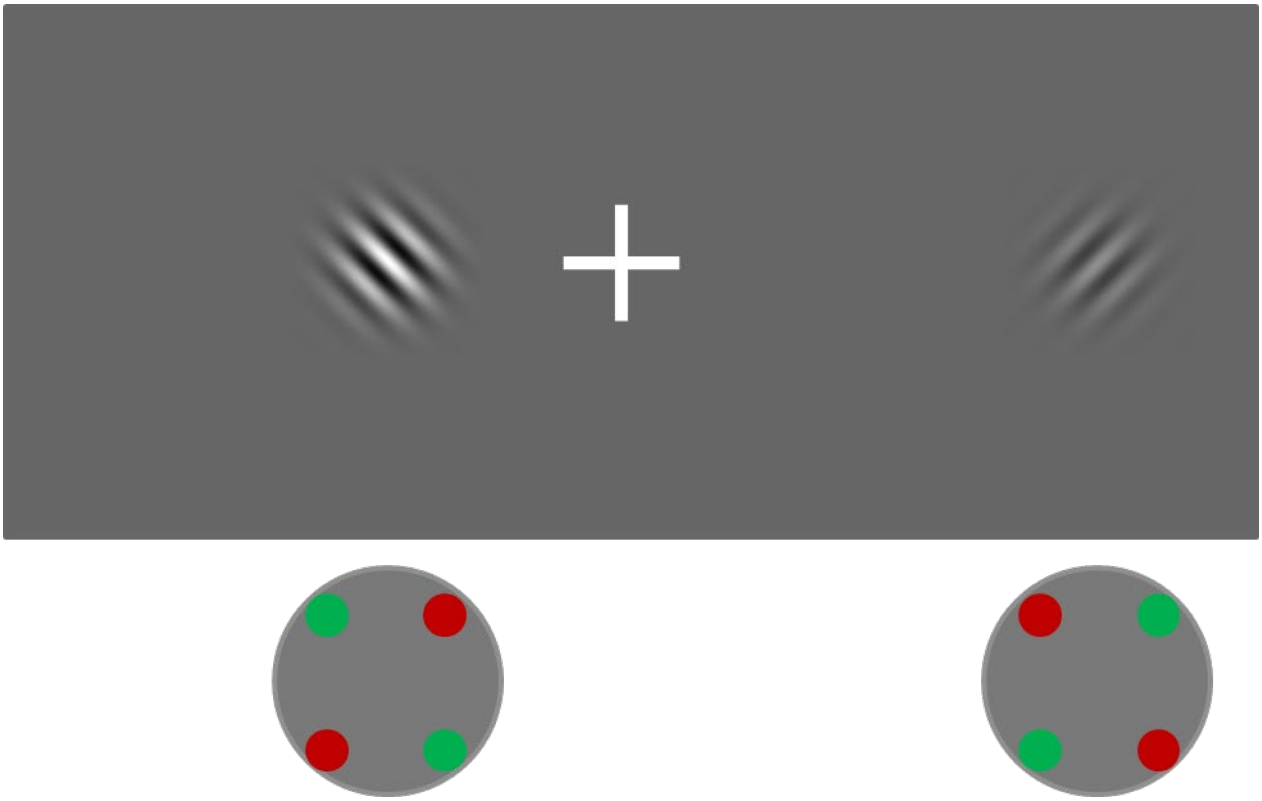

Note. Example of two targets, one in the central left position and the other in the peripheral right position. Central targets were presented 3.7° (± 0.5°) visual angle away from the fixation cross at the centre of the simulated screen and peripheral targets were presented 12° (± 0.5°) visual angle away. Targets were either presented to the left or right of the fixation cross. Only one target was ever presented at a time. Grey circles below the grey screen represent the thumbpads of the controllers, green circles indicate the correct responses, and red circles indicate incorrect responses to the respective example target above. Thumbpads were not visible to participants during the tasks. Not to scale.

3.2.6 Data Analyses

Each sequence provided 3D time-series data (x, y, z, coordinates) for head position, target position, gaze origin, and gaze direction. Individual steps were extracted based on head height, which follows a roughly sinusoidal pattern during walking. Peaks and troughs in vertical head position correspond to the approximate swing and stance phases of the stride cycle, which we identified using a peak detection algorithm. Target performance data (i.e., hits, misses, false alarms and response times) were mapped according to target onset relative to the nearest percentile of the stride cycle. All analyses were performed using custom Python (version 3.11.1) code, and ANOVAs were performed in JASP (version 0.18.0.0).

The ANOVAs performed on the overall walking performance did not include the Motion factor that was included in the experimental design. Instead, a Step Foot (Left vs Right) factor was added to compare average performance between the foot used to initiate the step during which the target was presented. In the case that performance was significantly different between initiating foot, the stride-based analyses would need to separate the target and responses into left and right foot-initiated strides (i.e., left-right-left and right-left-right supporting foot progression). This is particularly the case for comparisons that are in reference to the initiating foot, such as the relative lateral visual field and the relative orientation congruency. In such cases, instead of the binary separation of the targets and responses, they would be further divided by the initiating foot. This would provide an insight into how difficulty plays a role in the parameters of stride-based modulations.

3.2.7 Eye Movement Data

At each time point gaze coordinates were calculated using gaze origin and direction values, facilitating the calculation of target eccentricity. Individuals' eye gaze data were projected

onto the simulated display screen as polar coordinates and used to verify correct fixation. Specifically, the proportion of frames where an individual deviated from the fixation cross (exceeding 1° eccentricity) during each 9 s sequence was used to quantify overall fixation. One participant was removed for recording a 75% proportion of deviation from fixation. Using the same projection procedure, the eccentricity of the targets relative to fixation at the moment of stimulus onset was also calculated. We retained central targets for analysis when they were presented within 7° of eccentricity from gaze fixation, and peripheral targets for analysis when presented between 7° and 20° of eccentricity from fixation. Any targets that were presented within 0.5° or beyond 20° of eccentricity from the locus of fixation were excluded as potential blinks or extraneous eye-movements.

3.2.8 Gait Extraction

Stride-onsets were extracted based on the time-series of the vertical position of head-movement data as described in Davidson et al. (2024) and Phan et al. (2025). As walking shifts the centre of mass sinusoidally, troughs on the vertical axis of motion correspond to the double support stance phase of the gait cycle. Stride lengths were normalised for analysis by resampling the time-series data to 100 points (taken as percentage of progression). Strides had no defined reference order, resulting in a majority of presentation and response events being included twice in the analysis due to the overlap between the second step of one stride cycle and the first step of the next.

3.2.9 Performance Relative to Stride

All target onsets were allocated to the percentile (from 1-100%) of the stride they occurred in. For stride analyses, performance was averaged within 20 linearly spaced bins, with zero overlap. Performance metrics analysed were response rate, taken as the proportion of

responses made to presented targets, accuracy, taken as the proportion of correct orientation identifications out of total responses to presented targets, response time relative to target onset within progression (i.e., percentage), and response likelihood within progression, which was a binned average of percentile response counts.

Significant modulations were tested for each dependent variable for stride at the group level. Stepping from .1 to 10 cycles per stride (cycles per stride), in increments of .1, single component Fourier series (n = 1) were fitted with the equation:

$$f(t) = a_0 + a_1 \cos(\varphi t) + b_1 \sin(\varphi t) = a_0 + A \cos(\varphi t + \phi) \quad (1)$$

where $\boldsymbol{\varphi}$ is the periodicity (cycles per stride), $\boldsymbol{t}$ is the progression of the stride (as a percentage), $\boldsymbol{a_1}$ and $\boldsymbol{b_1}$ are the coefficients of the cosine and sine components and $\boldsymbol{a_0}$ is a constant, the central value of the modulation. The resulting fits had amplitudes of $\boldsymbol{A}$ and shifts in phase of $\boldsymbol{\phi}$. For each forced fit at each frequency, the goodness of fit (R^2) was used as an indication of strength. A resampling procedure was performed, where each of the 100 percentile bins were reallocated the measure of another bin, with replacement. These were then binned into their larger width bins and fits were performed as it was for the original data. This resampling was performed 1000 times with each resample having been fitted for the same frequencies as the original dataset. The R^2 values for the 1000 resamples at each fitted frequency were taken to represent the null distribution for strength of the modulations detected in the original data at the specific frequency, as the temporal intercorrelation of bins was effectively destroyed. The R^2 values for each frequency retained earlier were compared to the 95th percentile of their respective null distributions, with those greater than this critical value taken to indicate a significant modulation.

3.2.10 Exclusion Criteria

Participants with data from less than four walking and less than four stationary blocks were excluded for insufficient data collection (n = 3). Head position data was visually inspected for aberrant sequences and abnormal gaits that may have occurred due to hardware malfunction, signal drop-out, or aberrant walking patterns (e.g., limping). Across all participants, an average of 0.37 sequences (*SD* = 0.66, range 0 - 3) and an average of 9.79 steps (*SD* = 11.46, range 0 – 28) were excluded using this procedure. Those with excluded data points that no longer met sufficient data collection were excluded (n = 1). Participants determined to not have fixated (i.e., kept gaze within 1°), according to the data analysis process, for at least 75% of their collective data points (n = 3), were excluded. Additionally, those with overall accuracy for each adaptive staircase less than 60% (n = 6) or greater 90% (n = 0) were excluded for possible flooring and ceiling effects, respectively (n = 6). Specific targets were excluded from analyses if they were closer than 0.5° (*M* = 5.29 targets, *SD* = 6.32, range 0 – 17) or exceeded 20° in visual eccentricity (*M* = 31.21 targets, *SD* = 27.88, range 0 – 88), most being too slow in walking or not fixating properly, respectively.

3.3 Results

A two-way 2 (Motion: Stationary vs Walking) x 2 (Visual Eccentricity: Central vs Peripheral) repeated-measures ANOVA was performed on the 75% contrast thresholds, provided by fitting participants' psychometric functions. No main or interaction effects were found, *p*'s > .05.

A four-way 2 (Visual Eccentricity: Central vs Peripheral) x 2 (Visual Field: Left vs Right) x 2 (Step Foot: Left vs Right) x 2 (Gabor Orientation: Left vs Right) repeated-measures ANOVA was performed on four dependent variables: response rate, accuracy, correct response time, and

overall response time from target presentations during walking. The results are shown in Table 3.1.

Table 3.1

Mean Response Rate, Accuracy, Correct and Overall Response Times by Experimental Condition

Visual Eccentricity	Visual Field	Step Foot	Gabor Orientation	Response Rate		Accuracy		Overall Response Time		Correct Response Time	
				M	*SD*	*M*	*SD*	*M*	*SD*	*M*	*SD*
Central	Left	Left	Left	.88	.14	.82	.14	.65	.11	.65	.11
			Right	.85	.16	.77	.13	.64	.10	.65	.11
		Right	Left	.87	.14	.76	.20	.64	.11	.65	.11
			Right	.84	.17	.77	.16	.63	.08	.64	.09
	Right	Left	Left	.85	.15	.79	.14	.63	.11	.63	.11
			Right	.87	.17	.80	.17	.62	.10	.62	.11
		Right	Left	.87	.17	.79	.17	.64	.02	.65	.10
			Right	.87	.17	.78	.16	.62	.10	.62	.10
Peripheral	Left	Left	Left	.84	.15	.79	.15	.66	.09	.66	.10
			Right	.83	.16	.76	.15	.67	.08	.67	.09
		Right	Left	.85	.15	.80	.16	.66	.10	.67	.10
			Right	.81	.21	.75	.19	.67	.08	.67	.09
	Right	Left	Left	.84	.17	.77	.16	.67	.10	.68	.11
			Right	.85	.16	.77	.16	.65	.10	.65	.11
		Right	Left	.82	.17	.76	.15	.67	.09	.67	.09
			Right	.85	.16	.78	.14	.64	.10	.64	.10

Note. Response rate refers to the proportion of responses to target presentations. Accuracy is the proportion of correct responses to target presentations. Response times are presented in seconds (s). Gabor orientation was relative to vertical, with ‘right’ being 45° clockwise and ‘left’ 45° anticlockwise.

For response rate, there was only a significant main effect of eccentricity such that participants were more likely to respond to targets presented centrally than peripherally, $F(1, 27) = 10.315$, $\eta^2 = .009$, $p = .003$. For accuracy, there were no significant main effects nor any significant interactions (see Table 1), $p > .05$. For overall response time, there was a significant main effect of eccentricity with participants responding faster to central than peripheral targets,

$F(1, 27) = 23.500$, $\eta^2 = .095$, $p < .001$. Participants were also significantly faster to respond to targets presented in their right visual fields, $F(1, 27) = 7.103$, $\eta^2 = .021$, $p = .013$. These main effects of eccentricity, $F(1, 27) = 20.125$, $\eta^2 = .081$, $p < .001$, and visual field target location, $F(1, 27) = 7.533$, $\eta^2 = .022$, $p = .011$, were significant for correct response times. There were no significant pairwise interactions for response times, p's > .05. Additional interactions (three-way or four-way) were not significant or were not directly interpretable (e.g., driven by a single condition), p's > .05.

Our wireless VR environment enabled an analysis of changes in performance relative to the phases of the stride cycle by binning target onsets relative to their stride-cycle phase (see Methods). This enabled the fitting of Fourier models and comparison to permuted data (see plots on right side of Figures 3.3-3.5). We tested the statistical significance of the group-level modulations using a two-step permutation procedure, which allowed the estimation of fit strength (R^2) at chance level (see Methods). All modulations mentioned in the following had Fourier model fits with R^2 values exceeding the upper 95th percentile of R^2 values expected by chance and thus were deemed statistically significant using this method, consistent with previously published studies (Ho et al., 2017; H. Zhang et al., 2019).

Results for accuracy (i.e., proportion of correct responses to all target presentations) for the orientation identification task are plotted in Figure 3.3. For five out of six target stimulus conditions, there is a modulation at ~2 cps at the group-level. The exception was for gratings tilted congruently with the head tilt appropriate for the initiating step (i.e., counterclockwise grating for left-foot step, clockwise for right foot). These ~2 cps modulations show similar phasic shifts, with accuracy peaking at the end of the swing phase of the stride cycle and

dropping as the swing phase began. These modulations did not show any meaningful changes in phase when excluding non-responses (Figure A2).

Figure 3.3

Accuracy for Orientation Identification Across Stride Cycle

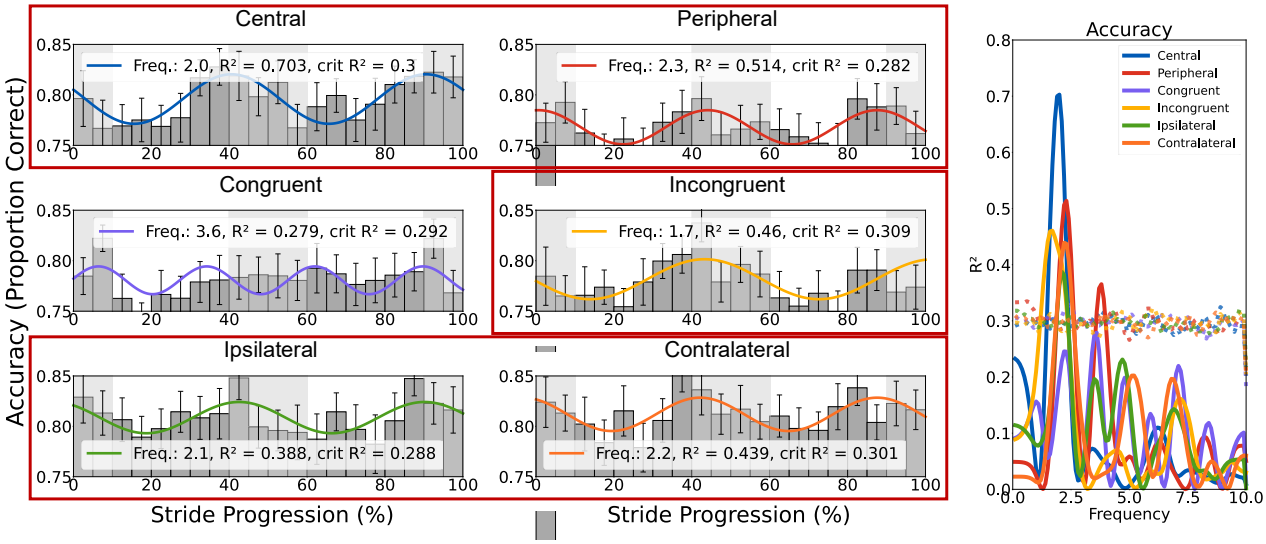

Note. Fourier fits on group-level ($N = 28$) accuracy (proportion of correct responses out of total target presentations) data for the orientation identification task broken down by six target conditions. Plots with significant Fourier fits in the frequency range of interest (1.5 – 2.5 cps) are outlined in red. Error bars indicate ±1 SEM. Light and dark grey columns indicate the estimated stance and swing phases of the stride cycle, respectively. Fourier models, as shown to the right, were fit at a fixed frequency for all values between 0.1-10 cps (in steps of 0.1) on the group-level data ($N = 28$). The coloured solid lines display the goodness-of-fit (R^2) for each frequency for each target condition. Dotted lines show the upper 95th percentile of R^2 values at each fitted frequency obtained from a null distribution of group-level data shuffled in time (n = 1000 permutations).

Figure 3.4 shows response rates (i.e., the proportion of targets responded to) for the orientation identification task over the gait cycle. Response rates for the 6 target conditions

oscillate idiosyncratically. The only ~2 cps modulation arises for targets presented in the periphery (with participants more likely to respond to a peripheral target at the end of the swing phase). Importantly, the response rate oscillations do not appear to be systematically related to the accuracy modulations in Figure 3.3. This discounts the possibility that the modulations of accuracy in Figure 3.3 were driven by a modulation in basic visibility.

Figure 3.4

Response Rate for Orientation Identification Across Stride Cycle

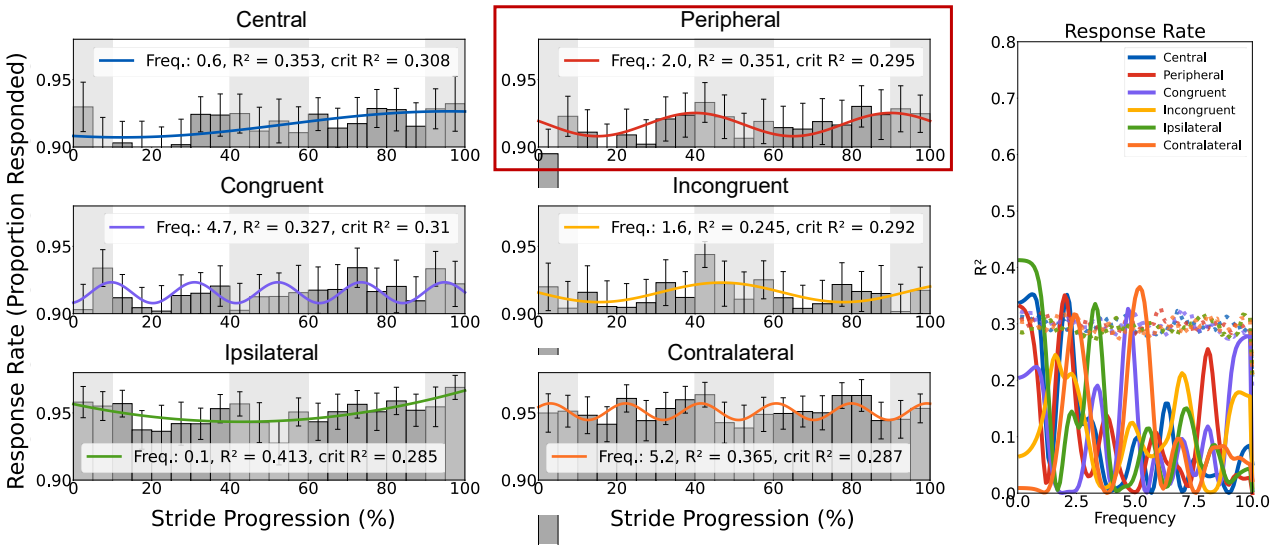

Note. Fourier fits on group-level ($N = 28$) response rate data (i.e., proportion of target presentations responded to) for the orientation identification task broken down by the six target conditions. The only significant Fourier fit in the frequency range of interest (1.5 – 2.5 cps) was in the peripheral condition (outlined in red). Error bars indicate ±1 SEM. Light and dark grey columns indicate the estimated stance and swing phases of the stride cycle, respectively. Fourier models, as shown to the right, were fit at a fixed frequency between 0.1-10 cps (in steps of 0.1) on the group-level data ($N = 28$). The coloured solid lines display the goodness-of-fit (R^2) for each frequency for each target condition. Dotted lines show the upper 95th percentile of R^2 values

at each fitted frequency obtained from a null distribution of group-level data shuffled in time (n = 1000 permutations).

Response times for the orientation identification task are shown in Figure 3.5. Congruently orientated targets and incongruently orientated targets, and those in the visual field contralateral to the initially supporting foot, modulated at ~3 cps and ~1.5 cps, respectively, and did so even when excluding incorrect responses (Figure A3). The peaks in ~3 cps response-time modulation occurred for congruently orientated targets peaked as the initiating stance phase ended, when entering the stance phase of the proceeding foot (incongruent foot), and during the swing phase of the incongruent foot. A counter-phase modulation is seen in incongruently orientated targets, such that responses to these targets were slowest in the swing phase of the initiating step, when exiting the proceeding stance phase and when entering the ending stance phase. For contralateral targets, response times were slowest in the stance phase and fastest in the swing phase. These response time oscillations do not appear to be the result of a modulation in response making preference as response likelihood modulated at ~2 cps, being greatest in the swing phase, and lowest in the stance phase, irrespective of condition (Figure A4 and A5).

Figure 3.5

Response Time for Orientation Identification Across Stride Cycle

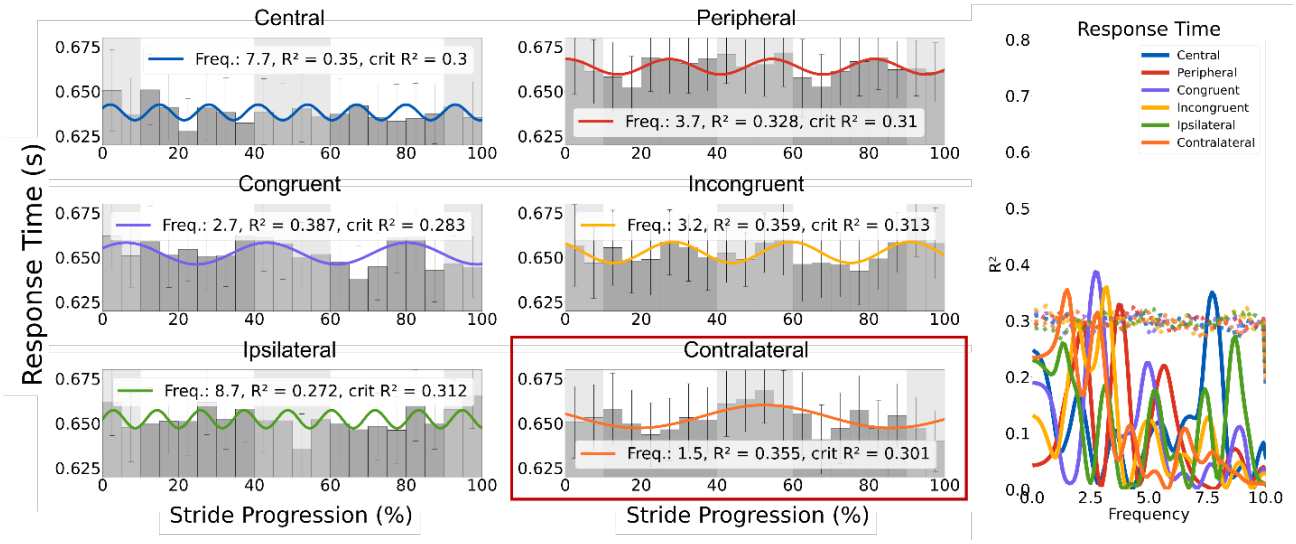

Note. Fourier fits on group-level ($N = 28$) response time (s) data for the orientation identification task broken down by six target conditions. Significant Fourier fits in the frequency range of interest (1.5 – 2.5 cps) are outlined in red. Error bars indicate ±1 SEM. Light and dark grey columns indicate the estimated stance and swing phases of the stride cycle, respectively. Fourier models, as shown to the right, were fit at a fixed frequency between 0.1-10 cps (in steps of 0.1) on the group-level data ($N = 28$). The coloured solid lines display the goodness-of-fit (R^2) for each frequencies calculated for each target condition. Dotted lines show the upper 95th percentile of R^2 values at each fitted frequency obtained from a null distribution of group-level data shuffled in time (n = 1000 permutations).

3.4 Discussion

Chapter 3 Experiment 1 examined the effects of walking on visual orientation identification, investigating the changes in performance within the stride-cycle and the differences in these changes between different visual location and feature pairings. Participants

made speeded button press responses on a thumbpad to indicate the orientation of the stimulus grating, effectively reducing the task to a two-alternative forced-choice.

Modulations in orientation identification accuracy were entrained to the rhythm of the stride-cycle for every condition of visual location and relative feature except when the stimulus orientation was aligned to the roll of the head appropriate for the initiating foot. Interestingly, a modulation for stimuli that were tilted in the opposite direction to the initial head roll of stride was observed. Perception of visual orientation is dependent on the orientation selectivity of simple and complex cells present in the primary visual cortex (V1), which demonstrate a tuning of cortical activity in response to observing different orientations (Appelle, 1972; Ben-Yishai et al., 1995; Harrison et al., 2023; Hubel & Wiesel, 1962). This neural population tuning across V1 is characterised by greater activity in response to the cardinal directions (i.e., vertical and horizontal), which decreases as the orientations experienced are more oblique (i.e., towards 45°) (Harrison et al., 2023). Therefore, the selectivity of the modulation to stimuli opposing head roll could be indicative of a difference in susceptibility to the modulatory role of walking across the orientation domain, which could be measured by a modulation of the population tuning of the neurons in V1. However, as the phase alignment of all significant modulations was consistent across conditions, with accuracy peaking as individuals entered each support phase of the stride, it might simply be an overall visual performance modulation and not selective for stimulus conditions at all. If this were the case, the lacking modulation for congruently aligned stimuli may be explained by a reduction of power as the data density is halved when the targets are divided for congruency comparison. Regardless, for the ~2 cps modulation seen in the remaining conditions, it is important to note that the phase alignment is shifted in comparison to previous findings of stride-based modulations in visual detection hit rate (Davidson et al., 2024; Phan et

al., 2025). The two tasks differ in that the visual detection task in those two papers relied on simple contrast sensitivity whilst the orientation identification used here in Chapter 3 Experiment 1 retains the contrast sensitivity manipulation with the addition of orientation selectivity. The phasic shift seen in the modulations between tasks may suggest that the stride-based modulations of visual perception depend on task complexity. Therefore, it would be interesting to investigate whether added complexity shifts the stride-based modulations. Complexity could be added through additional stimulus feature combinations or the involvement of later visual cortices, such as making the task a global motion identification which requires the involvement of V5 (Albright & Stoner, 1995; Anstis et al., 1998; Newsome & Pare, 1988; Zeki, 2015).

Similarly, there appears to be a shift in the response-making modulations observed in Chapter 3 Experiment 1 in comparison with previous walking studies (Davidson et al., 2024; Phan et al., 2025). Instead of the responses being more likely during the stance phase, the response likelihood peaks during the swing phase. The source of this shift is most likely the greater decision making and motor production requirements that a mapped multiple-choice decision has as opposed to a simple button press. Another difference is the selectivity of response-time modulation patterns. The congruency conditions appear to have anti-phase modulations, demonstrating a change in processing prioritisation between orientations that are more horizontal and those that are closer to verticality, in the egocentric head-centred perspective, along the progression of the stride cycle. Overall, due to the greater response times in general for the orientation identification task, the previous-response time modulations found for contrast sensitivity in (Davidson et al., 2024; Phan et al., 2025) may not have occurred.

3.5 Chapter 3 Experiment 2

3.6 Methods

3.6.1 Design

The second experiment implemented a motion direction variable for the internal drift of the Gabor patterned target, resulting in a 2 (Motion: Stationary vs Walking) × 2 (Visual Eccentricity: Central vs Peripheral) × 2 (Visual Field: Left vs Right) × 2 (Orientation: Left vs Right) × 2 (Drift Direction: Up vs Down) factorial design. As with Chapter 3 Experiment 1, a factorial design was employed to account for any potential confounds between the independent variables. The comparisons of interest were between the levels of each of these independent variables.

3.6.2 Participants

Participants were 33 undergraduate psychology students from the University of Sydney who participated in exchange for course credit. The participation consisted of a single session that lasted approximately one hour. 16 participants were excluded, as per the exclusion criteria for Chapter 3 Experiment 1, leaving a final sample of N = 17 (M_{Age} = 19.8 years, SD_{Age} = 2.8, range = 18 – 30; 15 right hand dominant). Each participant provided informed consent before commencing and had normal or corrected-to-normal vision (not verified). The study protocol was approved by the University of Sydney Human Research Ethics Committee (HREC 2021/048).

3.6.3 Materials

The visual target was the same as in Chapter 3 Experiment 1 (i.e., oriented at ±45°), however, the grating drifted at 3 cycles per second, either (obliquely) upwards or downwards.

3.6.4 Procedure

The procedure was identical to Chapter 3 Experiment 1, except that participants were tasked with identifying the vertical movement (i.e., up or down) of the internal drift of the target pattern by pressing the corresponding vertical hemifield of the trackpad on either hand controller. The stimuli were presented for 200 ms and were spaced by variable intertrial intervals with a minimum of 1200 ms.

3.6.5 Exclusion Criteria

Average of 0.37 sequences (*SD* = 0.66, range 0 - 3) and an average of 9.79 steps (*SD* = 11.46, range 0 – 28) were excluded. One participant no longer met sufficient data collection. Three participants were excluded for not having fixated for at least 75% of their collective data points. Those with overall accuracy for each adaptive staircase less than 60% (n = 12) were excluded for possible flooring. Specific targets were excluded from analyses if they were closer than 0.5° (*M* = 5.29 targets, *SD* = 6.32, range 0 – 17) or exceeded 20° in visual eccentricity (*M* = 31.21 targets, *SD* = 27.88, range 0 – 88), most being too slow in walking or not fixating properly, respectively.

3.7 Results

A two-way 2 (Motion: Stationary vs Walking) x 2 (Visual Eccentricity: Central vs Peripheral) repeated-measures ANOVA was performed on the 75% contrast thresholds for correct responses, provided by fitting participants' psychometric functions. Contrast required for motion identification responses were significantly higher during walking than when stationary, $F(1, 16) = 11.20$, $\eta^2 = .136$, $p = .004$. Centrally presented targets required lower contrasts to be correctly responded to than peripherally presented targets, $F(1, 16) = 6.24$, $\eta^2 = .092$, $p = .024$. There was a significant interaction between target eccentricity and motion, such that it the difference

between motion was larger for peripherally presented targets than for centrally presented targets, $F(1, 16) = 6.86$, $\eta^2 = .102$, $p = .019$. This interaction appears to have been due to a significant increase in contrast required for peripheral targets during walking, $t(16) = 3.51$, $d = 1.449$, $p_{holm} = .017$. Similarly, both main effects appear to be driven by the higher contrast required for correct responses to peripherally presented targets during walking than any other stimulus condition, as all other post-hoc pairwise comparisons were not significant, $p_{holm} = .05$.

A five-way 2 (Visual Eccentricity: Central vs Peripheral) x 2 (Visual Field: Left vs Right) x 2 (Step Foot: Left vs Right) x 2 (Gabor Orientation: Left vs Right) x 2 (Drift Direction: Up vs Down) repeated-measures ANOVA was performed on the same four dependent variables as Chapter 3 Experiment 1: response rate, accuracy, correct response time, and overall response time from target presentations during walking. The results are shown in Table 3.2.

Participants were responded to a greater proportion of targets presented centrally than those presented peripherally, $F(1, 16) = 4.80$, $\eta^2 = .037$, $p = .044$. There were no other significant main effects on response rate nor any significant interactions of interest. Participants responded with greater accuracy when targets were presented centrally than when presented peripherally, $F(1, 16) = 49.56$, $\eta^2 = .062$, $p < .001$. There were no other significant main effects on accuracy nor any significant interactions of interest. For overall response times, individuals were significantly faster to respond to targets presented centrally than those presented peripherally, $F(1, 16) = 74.54$, $\eta^2 = .153$, $p < .001$. There was a significant interaction between the orientation of the target and the foot that initiated the step it was presented during, such that when the target was tilted to the same side as the foot response times were greater, $F(1, 16) = 5.89$, $\eta^2 = .005$, $p = .027$. There were no other significant main effects on overall response times nor any significant interactions of interest. When excluding incorrect responses, response times retained the main

effect of eccentricity, $F(1, 16) = 79.05$, $\eta^2 = .148$, $p < .001$, and Step Foot x Gabor Orientation interaction, $F(1, 16) = 10.03$, $\eta^2 = .008$, $p = .006$. There were no other significant main effects on the correct response times nor any additional significant interactions of interest.

Table 3.2

Mean Response Rate, Accuracy, Correct and Overall Response Times by Experimental Condition

Visual Eccentricity	Visual Field	Step Foot	Gabor Orientation	Drift Direction	Response Rate		Accuracy		Overall Response Time		Correct Response Time	
					M	*SD*	*M*	*SD*	*M*	*SD*	*M*	*SD*
Central	Left	Left	Left	Up	.73	.09	.86	.12	.73	.09	.73	.09
				Down	.78	.11	.81	.15	.77	.10	.78	.11
			Right	Up	.73	.10	.82	.11	.75	.10	.73	.10
				Down	.74	.10	.84	.10	.74	.10	.74	.10
		Right	Left	Up	.71	.09	.85	.14	.71	.10	.71	.09
				Down	.73	.12	.75	.18	.75	.11	.73	.12
			Right	Up	.72	.12	.74	.25	.73	.12	.72	.12
				Down	.75	.13	.83	.19	.75	.13	.75	.13
	Right	Left	Left	Up	.74	.10	.85	.08	.74	.10	.74	.10
				Down	.72	.09	.79	.15	.73	.10	.72	.09
			Right	Up	.73	.10	.79	.18	.73	.09	.73	.10
				Down	.73	.09	.85	.13	.73	.09	.73	.09
		Right	Left	Up	.72	.09	.83	.17	.72	.09	.72	.09
				Down	.73	.12	.77	.16	.73	.12	.73	.12
			Right	Up	.76	.10	.75	.19	.76	.09	.76	.10
				Down	.73	.13	.85	.15	.73	.14	.73	.13
Peripheral	Left	Left	Left	Up	.77	.10	.80	.16	.77	.09	.77	.10
				Down	.82	.09	.61	.18	.80	.09	.82	.09
			Right	Up	.76	.12	.67	.17	.78	.11	.76	.12
				Down	.79	.09	.70	.20	.78	.09	.79	.09
		Right	Left	Up	.75	.09	.89	.10	.75	.10	.75	.09
				Down	.81	.12	.66	.22	.81	.11	.81	.12
			Right	Up	.79	.10	.72	.18	.79	.10	.79	.10
				Down	.81	.10	.74	.15	.81	.09	.81	.10
	Right	Left	Left	Up	.78	.11	.72	.20	.78	.10	.78	.11
				Down	.76	.10	.72	.14	.77	.09	.76	.10
			Right	Up	.81	.11	.67	.18	.79	.09	.81	.11
				Down	.75	.11	.83	.09	.76	.11	.75	.11
		Right	Left	Up	.81	.11	.71	.21	.78	.10	.81	.11
				Down	.75	.11	.76	.12	.76	.11	.75	.11
			Right	Up	.82	.09	.60	.22	.80	.09	.82	.09
				Down	.75	.11	.83	.17	.75	.10	.75	.11

Note. The proportion of responses to target presentations was taken as a measure of response rate. The proportion of correct responses to target presentations was taken as a measure of accuracy. Response times are presented in seconds (s). Gabor orientation was relative to vertical, with ‘right’ being 45° clockwise and ‘left’ 45° anticlockwise and the gratings drifted (obliquely) ‘upwards’ or ‘downwards’.

As shown in Figure 3.6, overall accuracy appears to modulate at ~2 cps at the group-level for all target stimulus conditions, except when the target was presented centrally or was drifting upwards, both of which do not appear to have any modulations in the frequency range of interest. These ~2 cps modulations show similar phasic shifts, such that accuracy peaked at the start of the swing phase of the stride cycle and dropped as the stance phase began. Similar accuracy modulations are retained when excluding misses (Figure A6). Response rates do not appear to be explanatory of these accuracy modulations as they only modulate with the stride cycle for peripheral, ipsilateral, and upwards drifting targets (Figure 3.7), only overlapping with the accuracy modulations for two conditions.

Figure 3.6

Accuracy for Motion Direction Identification Across Stride Cycle

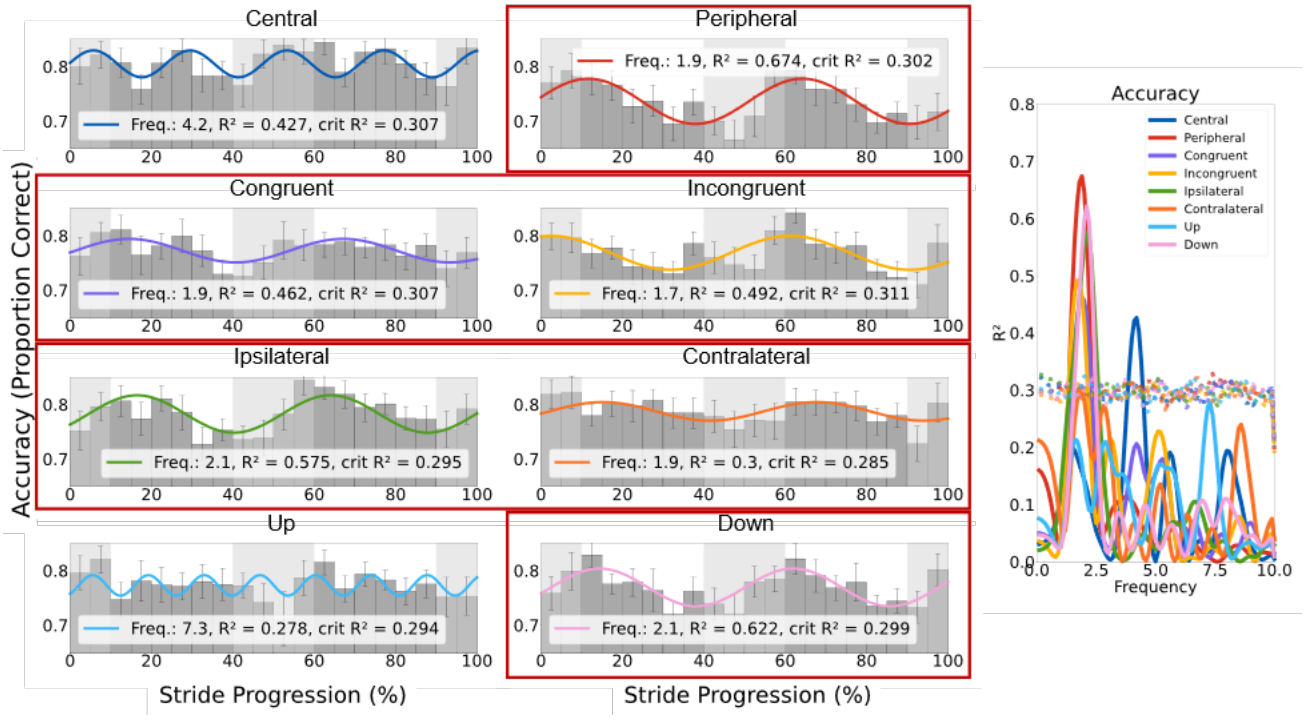

Note. Fourier fits on group-level ($N = 17$) accuracy (proportion of correct responses out of total target presentations) data from the motion identification task broken down by eight target

conditions. Significant Fourier fits in the frequency range of interest (1.5 – 2.5 cps) are outlined in red. Error bars indicate ±1 SEM. Light and dark grey columns indicate the estimated stance and swing phases of the stride cycle, respectively. Fourier models, as shown to the right, were fit at a fixed frequency between 0.1-10 cps (in steps of 0.1) on the group-level data ($N = 17$). The coloured solid lines display the goodness-of-fit (R^2) for all frequencies calculated for each target condition. Dotted lines show the upper 95th percentile of R^2 values at each fitted frequency obtained from a null distribution of group-level data shuffled in time ($n = 1000$ permutations).

Figure 3.7

Response Rate for Motion Direction Identification Across Stride Cycle

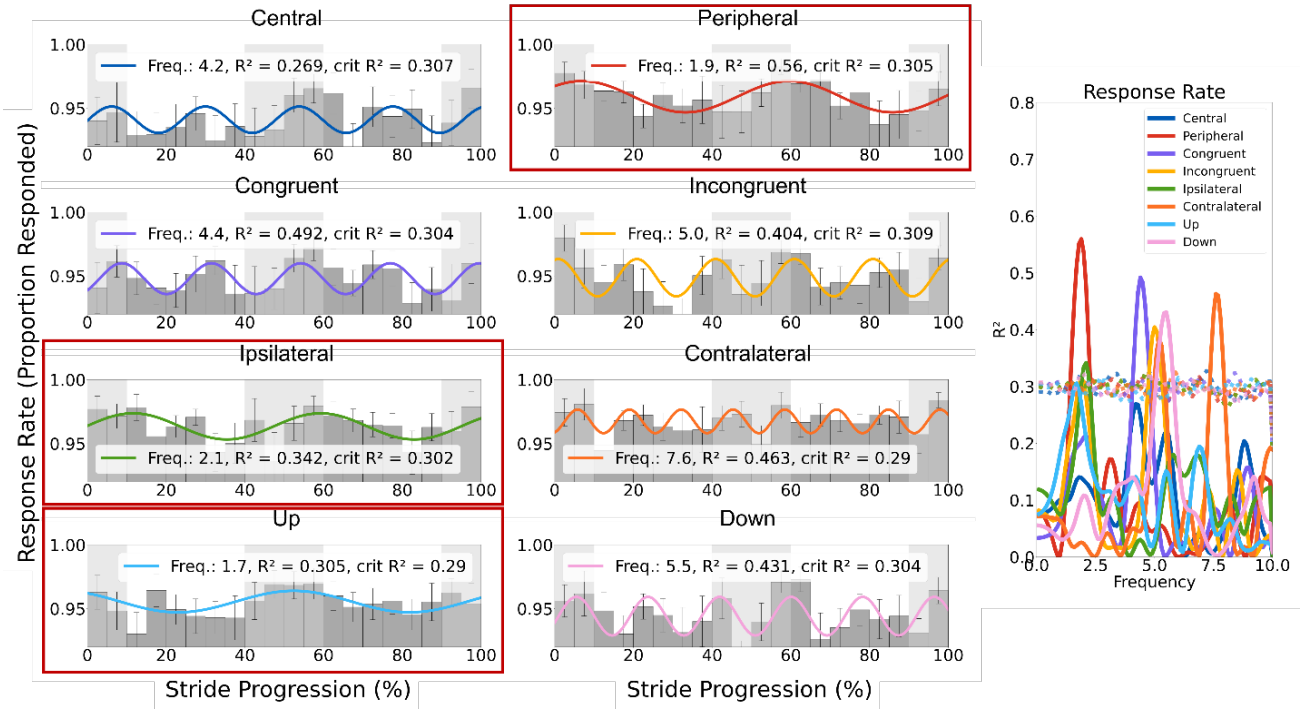

Note. Fourier fits on group-level ($N = 17$) response rate (proportion of targets responded to out of the total target presentations) data from the motion direction identification task broken down by eight target conditions. Significant Fourier fits in the frequency range of interest (1.5 – 2.5 cps) are outlined in red. Error bars indicate ±1 SEM. Light and dark grey columns indicate the

estimated stance and swing phases of the stride cycle, respectively. Fourier models, as shown to the right, were fit at a fixed frequency between 0.1-10 cps (in steps of 0.1) on the group-level data ($N = 17$). The coloured solid lines display the goodness-of-fit (R^2) for all frequencies calculated for each target condition. Dotted lines show the upper 95th percentile of R^2 values at each fitted frequency obtained from a null distribution of group-level data shuffled in time (n = 1000 permutations).

For the response time data (Figure 3.8), the only significant modulation in the frequency range of interest was for centrally presented targets. Responses were longest for centrally located targets presented during the stance phase and shortest for those presented in the swing phase. When excluding for incorrect responses (Figure A7), similar albeit noisier modulations were found for response times for contralaterally presented, upwardly and downwardly drifting targets. The ~ 3 cps modulations for congruently and incongruently oriented targets appear to be counter-phase to each other. Similarly, the modulations in response time for ipsilaterally and contralaterally presented targets are counter phase. Contrary to the differences in response time modulations across conditions, response onsets consistently modulated at ~2 cps, being greatest in the swing phase, and lowest in the stance phase (Figure A8 and A9). Hence, the response time modulations do not appear to be the result of optimizing responses to particular points of stride progression.

Figure 3.8

Response Time for Motion Direction Identification Across Stride Cycle

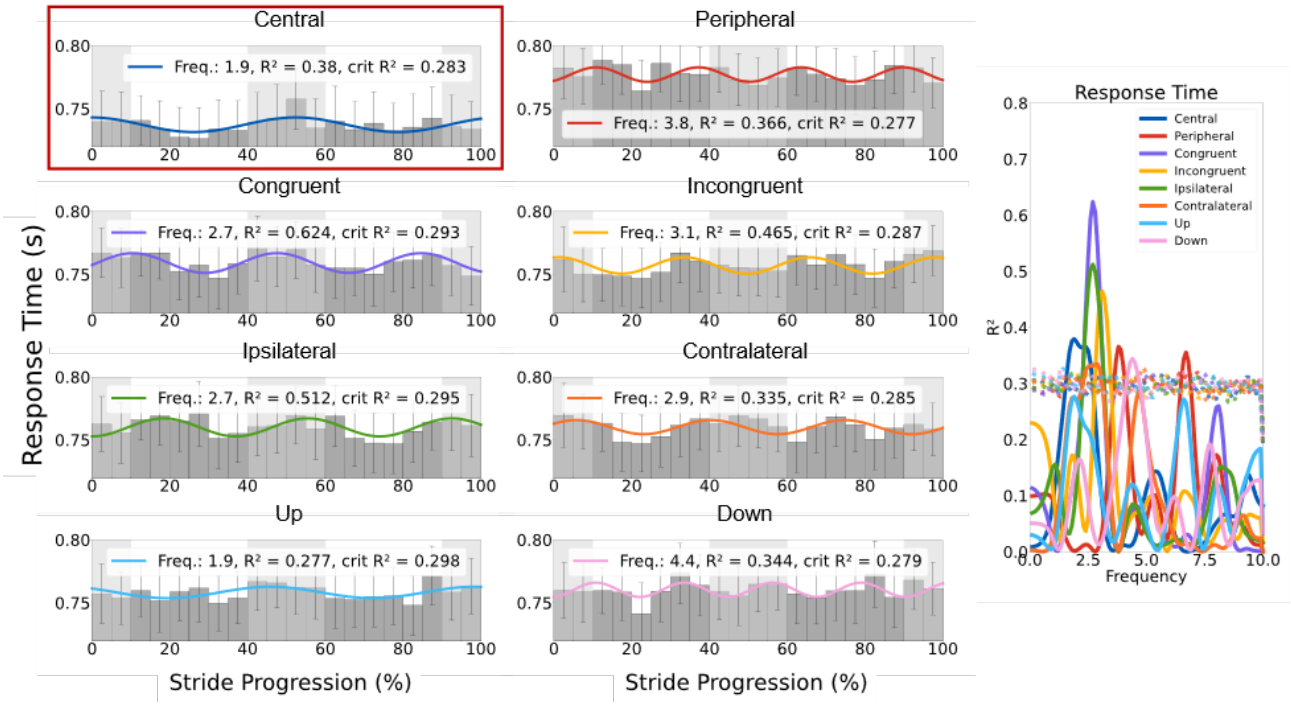

Note. Fourier fits on group-level (N = 17) response time (s) data from the motion identification task broken down by eight target conditions. Significant Fourier fits in the frequency range of interest (1.5 – 2.5 cps) are outlined in red. Error bars indicate ±1 SEM. Light and dark grey columns indicate the estimated stance and swing phases of the stride cycle, respectively. Fourier models, as shown to the right, were fit at a fixed frequency between 0.1-10 cps (in steps of 0.1) on the group-level data (N = 17). The coloured solid lines display the goodness-of-fit (R^2) calculated for each target condition. Dotted lines show the upper 95th percentile of R^2 values at each fitted frequency obtained from a null distribution of group-level data shuffled in time (n = 1000 permutations).

3.8 Discussion

Chapter 3 Experiment 2 changed the visual feature of interest from visual orientation to visual motion, increasing the complexity of the visual stimuli and the latency at which it is processed, whilst retaining the two-alternative, forced-choice response requirement. Participants made speeded button press responses on a mapped thumbpad to indicate whether a grating's motion direction was upwards or downwards.

Motion direction identification accuracy was observed to modulate with the stride cycle at ~2 cps for most conditions except for upwardly drifting stimuli and centrally located stimuli. These two exception cases did not appear to modulate at any other meaningful frequency. In comparison to the accuracy modulations in orientation identification, the ~2 cps modulations seen in Chapter 3 Experiment 2 were shifted in phase, such that accuracy peaked as individuals left the stance phase as opposed to when they entered the stance phase (i.e., the modulation was later in Chapter 3 Experiment 2). The only difference, and thus the only source of explanation, between these experiments was the visual features being identified. As a feature dependent on a spatial element changing over the course of time, motion fundamentally requires the minimum of two time point samples to be perceived, as opposed to the singular time point needed for static orientation (Del Viva & Morrone, 1998; Derrington et al., 2004). In V1, this feature tracking has been attributed to the activity of complex cells. These complex cells integrate the activity of simple cells, the orientation-selective neurons, and as a result of this hierarchical structure, have a greater latency (Hubel & Wiesel, 1962; Van Kleef et al., 2010). Beyond these early and small differences in latencies, there is an additional difference in the cortical areas involved in the perception of orientation and motion. The Middle Temporal (MT or V5) area is characterised by its involvement in motion perception (Albright & Stoner, 1995; Anstis et al., 1998; Newsome &

Pare, 1988; Zeki, 2015). V5 demonstrates much greater activity when processing a moving stimulus as opposed to the weak activity for static stimuli (Raiguel et al., 1999). As for the impetus for V5 activity, two processes have been proposed, a parallel processing account where V5 receives output from subcortical areas (Holliday et al., 1997) and the traditional hierarchical model where input originates from V1 (Maunsell & Essen, 1983). The subcortical pathway to V5 has been associated with differences in response latencies between V1 and V5 below 100 ms (Foxe & Simpson, 2002; Lamme & Roelfsema, 2000; Raiguel et al., 1989). Difference in neural response latencies that more appropriately match the differences in phase of the modulations for accuracy between Chapter 3 Experiments 1 and 2 are those attributed to the pathway between V1 and V5, specifically the feedback from V5 (Prieto et al., 2007). Therefore, if a cortical activity measure were to be incorporated, it would be probable that V5 will show a delayed oscillation than V1 during walking.

As seen in Chapter 3 Experiment 1, the response likelihood peaked during the swing phase. This repetition of phasic pattern is a strong replication but different to those seen for simple button-press responses in previous visual detection tasks. This further strengthens the possibility of the driving factor for the phase shift being the greater decision-making and motor production requirements in making a mapped alternative-choice response. The ~2 cps modulations in response time reported in our previous visual detection studies with walking participants (Davidson et al., 2024; Phan et al., 2025) were seen for centrally displayed and upwardly drifting stimuli. However, the responses to these stimuli did not demonstrate the expected ~2 cps modulation in accuracy. It would appear that individuals' response making was more entrained to the motor activity of walking for these stimuli than their perception was.

3.9 General Discussion

From both experiments, the effect of stimulus orientation on visual abilities during walking can be observed. Regardless of whether the orientation was directly relevant to the perceptual task (Chapter 3 Experiment 1) or indirectly relevant (the grating motion task in Chapter 3 Experiment 2), the alignment of the stimulus orientation to head orientation (i.e., roll) did not play a role in the modulation of task performance across the stride-cycle. The tasks used in the two experiments differ slightly. In the orientation identification task (Chapter 3 Experiment 1), stimulus orientation did not need to be further processed to determine the response. However, for the motion identification task (Chapter 3 Experiment 2), stimulus orientation eliminates two of four possible destination quadrants of the drifting grating. This leaves the participant needing to identify the orthogonal direction of the drift. Due to the drift direction being reliant on the orthogonal shift in the grating stimulus, its orientation must be involved in the process of determining the motion of the drift and cannot be ignored. While both tasks produced modulations of accuracy over the stride cycle, the difference in phase alignment between them could be attributed to this difference in processing requirement (Bair et al., 2002; Shriki et al., 2012; Turner et al., 2024). This attribution, however, ignores the accuracy modulations for different stimulus conditions. In both tasks, the accuracy modulations were similarly aligned even when dividing the targets into different visual feature categories. The similarity across visual features weakens the explanatory power of the processing difference for the difference in modulation phase between tasks. Instead, the consistency of modulation phase strengthens the argument for an overall stride-based modulation for the tasks themselves.

Focusing on the motion direction identification task in Chapter 3 Experiment 2, the asymmetry in the influence of the stride cycle on accuracy between upward and downward

drifting stimuli is unexpected. Only the identification of the direction of downwardly drifting stimuli demonstrated a stride-based modulation. The accuracy of the downward drifting stimuli peaked as individuals entered the swing phase of the stride cycle, the moments when their centre of mass and head height moved upwards. This greater accuracy could be due to a greater, more detectable motion magnitude, which would be explained by a simple vector addition between the vestibular vector and the visual targets motion vector (Fetsch et al., 2013; Hogendoorn et al., 2017). Along the same line, it was expected that the accuracy would have peaked for upwardly drifting stimuli when the individuals centre of mass and head height moved downwards. However, the absence of such an effect and its consequential stride-based modulation in accuracy for these stimuli weakens this account of vector addition. Furthermore, in a similar fashion as for stimulus orientation, the consistent observation of a similarly phase aligned modulation in pairwise comparisons for other visual features suggests a non-selective stride-based effect for vertical motion direction.

Both the experiments conducted in the current study found novel and unique effects of stride cycle on response making. Instead of the previous response preference being in the stance phase seen for simple visual detection (Davidson et al., 2024; Phan et al., 2025), both alternative-choice tasks showed response patterns that peaked during the swing phase. Furthermore, response times, previously found to peak during the stance phase, did not modulate to prioritise the phase of response making. Instead, response times between the pairwise visual feature conditions across both experiments appear to vary in counter-phase to each other. This counter-phasic pattern between each visual feature pair is suggestive of a modulation in the prioritisation of the processing. Without the respective accuracy modulations mimicking these response time

patterns, this prioritisation would appear to be in the order of processing and not necessarily affecting the visual percept the observer experiences.

Considering the previous stride-based modulations in visual detection in combination with the modulations seen in the current study, there appears to be a phasic shift effect determined by visual task complexity. Both visual detection and orientation identification is based in V1, the former is dependent on simple activation whilst the latter involves a percept-based response (Koch & Ullman, 1987; Zhang et al., 2012). Therefore, despite the cortical area involved being the same, the processing required is greater for orientation identification. Processing is greater again in the motion task as perception of visual motion requires involvement of V5, a later cortical area than V1 (Albright & Stoner, 1995; Anstis et al., 1998; Newsome & Pare, 1988; Zeki, 2015). If the stride-based modulations for performing these tasks are compared, the phase is shifted in a manner consistent with the change in task complexity. The peak of performance is in the middle of the swing phase for visual detection, the end of the swing phase for orientation identification, and the beginning of the swing phase for vertical motion identification. Due to the cyclic nature of stride, the beginning of the swing phase can be interpreted as either earlier or later dependent on whether the previous or current step is referenced. Hence, there is a need for the underlying cortical activity to be measured across the visual hierarchy to verify whether there is a stride-based modulation of visual cortical activity and, if so, whether it propagates along the hierarchy in a continuous macroscopic travelling wave manner (Muller et al., 2018).

The current study has expanded previous findings of locomotion-driven modulations in visual perception. While the original stride-modulation paper by Davidson et al. (2024) used a simple visual detection task in central vision, here we include tasks involving greater complexity

and which are presented in different visual field locations. The congruency of orientation, the lateral visual field, and the vertical direction of visual motion do not appear to undergo unique modulations during walking. However, it does appear that the general perceptual task requirements affect the phase of stride-based modulations. Orientation identification, which simply involves V1, exhibited a peak in task performance that was earlier in the stride cycle than motion direction identification, which involves the later cortical area V5. The phasic difference alongside the cortical hierarchical difference predicts that stride-based visual modulation has origins in lower cortical areas and propagate in a travelling wave nature along the cortical hierarchy. This could be tested in future research in a number of ways. One would be by employing neurophysiological measures such as electroencephalography that could reveal evidence of such propagation. Another approach would be to use higher-order stimuli such as faces and foods, both of which involve fusiform areas (Jain et al., 2023; Kanwisher & Yovel, 2006; Khosla et al., 2022), and more complex tasks such as evaluating face emotion or food categories.

3.10 Acknowledgements

Research was supported by an Australian Government Research Training Program (RTP) Scholarship (SC3227) to Cameron K. Phan, an Australian Research Council grant (DP210101691) to Professor David Alais and Professor Frans Verstraten, an Australian Research Council grant (DP250100118) to Doctor Reuben Rideaux and Professor David Alais, and a National Health and Medical Research Council Investigator grant (2026318) to Doctor Reuben Rideaux.

4

Chapter 4

Effect of different walking requirements on stride-based modulations of visual detection

Effect of different walking requirements on stride-based modulations of visual detection

Active perception focuses on the phenomenological perceptual experience of individuals during their performance of self-generated, voluntary movements. The additional dynamism and cues introduced by these movements enrich the observer's perceptual environment and have long been recognised (Gibson, 1955, 1962) although passive, laboratory-based research has been by far a more commonly used approach. Recently, however, with the advancement of wearable and virtual technologies, research in active perception has undergone a resurgence (Cao et al., 2020; Cao & Händel, 2019; Davidson et al., 2024; Hogendoorn et al., 2017; Matthis et al., 2018; Phan et al., 2025). The ability to employ experimental controls in dynamic scenarios, previously limited to passive, static and perceptually limited setups, has facilitated the conducting of experiments with verification of known phenomena, increased applicability, and increased ecological validity. However, the controls have often been limited to manipulations of the perceptual stimuli rather than the demands of the active movement.

Walking is one of the active movements most engaged in by able-bodied individuals and generates repeated patterns consistently observed that can be used to track progression. The cyclic pattern seen in walking is known as the gait cycle and is composed of two consecutive steps, which can either be focused on individually or as a pair. Each individual step has two phases, beginning with the stance phase and then entering the swing phase upon the toe-off of a foot and ending with the heel-strike of that same foot. These phases are retained even when traversing sloped surfaces such as hills and ramps, however, the energy dynamics and kinematic processes involved are modulated by the magnitude of the slope and whether the slope is an incline or a decline (Franz & Kram, 2012; Kimel-Naor et al., 2017; Lu et al., 2023; Pickle et al., 2016). Uphill, or inclined, walking requires greater muscular engagement to initiate a step and to

raise the centre of mass of the walker against gravity. On the other hand, downhill, or declined, walking involves increased muscular demand on entering the stance phase to absorb the increased energy on impact of heel strike. In either inclination scenario, as in normal flat ground walking, the primary goal of the human system when walking is the minimisation of energy consumption and the maximisation of stability. Changes in stability of the physical body are usually accompanied by changes in the sensory input experienced, this is particularly the case with walking where positional changes cascade along the postural chain – from heel to head – in what is described as a reverse pendulum fashion. A key question arising from this gait-related instability is whether it affects the perceptual system, and if so, what are its consequences for perception.

Very recent work shows that in addition to the stride cycle influencing perceptual stability, visual perception itself appears to modulate along the stride cycle. This has been shown for visual detection (Davidson et al., 2024; Phan et al., 2025) and for orientation identification and motion identification (Chapter 3), and all have been found to exhibit peak performance during the swing phase and a trough during the stance phase. Coinciding with this perceptual modulation, a modulation of motor response making has been found, where responses are more likely to be made during the stance phase (Davidson et al., 2024; Phan et al., 2025). This counterphase modulation between perception and motor response could potentially be due to an optimisation trade-off between the sensory and motor systems, where the increase in muscular recruitment during stance phase lowers the threshold for motor executions across the motor system. If this were the underlying process for the modulations previously found, changes in motor system engagement across a step should produce changes in the perceptual modulation characteristics.

The few existing studies measuring perceptual performance over the stride cycle have all been conducted in participants walking on level ground. The current study employs a treadmill mounted on a motion platform to introduce a slope to the walking surface, together with a virtual reality display to probe changes in visual perception during uphill or downhill walking. The visual perceptual ability of interest is contrast sensitivity and detection, an ability that has been recently found to modulate along the stride cycle (Davidson et al., 2024; Phan et al., 2025). Whether this modulation is altered by the motor demands specific to the walking conditions is the primary focus of this study. If a tradeoff between motor engagement and visual perception drives the modulation, the peak of visual detection ability will shift away from the initiating or terminating stance phase of a step when walking uphill or downhill, respectively (Franz & Kram, 2012; Kimel-Naor et al., 2017; Lu et al., 2023; Pickle et al., 2016).

4.1 Methods

4.2 Design

The study employed a one-way repeated-measures design, where individuals completed a single-response visual-detection task whilst they stood still, or walked on a flat, inclined, or declined surface. Walking speed was self-determined using a combination of the Optitrack-Motive motion tracking system and the large treadmill, which had its speed set in real-time to ensure the participants stayed in the middle of the length of the treadmill. The inclination for both incline and decline was 4° (approx. 7% slope) from horizontal, achieved using the Bosch Rexroth eMotion 1500 6DOF motion platform (Figure 4.1C). Participants' detection accuracy and response times were collected as measures of visual detection ability and were analysed as outlined below.

4.2.1 Participants

Twenty-one participants were recruited via physical flyers posted on bulletin boards and walls at the Universität Ulm, an online SONA advertisement, and online distribution of digital flyers through the ERASMUS student network. All participants had normal or corrected-to-normal vision (not verified) and provided written informed consent before completing the experimental sessions. Participants were paid 10 euros/hr for two one-hour sessions, totaling 20 euros. The study protocol was approved by the Universität Ulm Review Board for Research Ethics of the Faculty of Engineering, Computer Science and Psychology.

Three participants were unable to provide data due to hardware malfunctions and data loss due to corruption. The final sample of eighteen was composed of 14 males and 4 females, aged between 20 and 71 (M = 28.8, SD = 13.2), 16 were right-handed and 2 were left-handed.

4.2.2 Apparatus and Materials

An Oculus Rift CV1 head-mounted display (HMD) was used to display the virtual environment, and the right-handed Oculus Touch controller was used for collecting trigger pull responses. The HMD contained dual Pentile OLED displays (1080 x 1200 pixel resolution, 90 Hz refresh rate) with 110-degree field of view. Positions of the HMD were tracked in three-dimensional space at 100 Hz resolution, using 16 Optitrack Flex 3 cameras enclosing a rectangular space.

The virtual reality (VR) environment and experimental procedure were designed and presented within Unity (Version 2019.4.9f1), using the Oculus XR Plugin (Version 1.4.3) and Meta Quest Link App (Version 69.0.0.501.353) on a Windows 10 PC (2 × 16 GB, DDR4 2666 MHz) with a 9th Gen Intel Core i7-9800X processor (3.80 GHz), and an NVIDIA Quadro P5000 (16 GB, GDDR5X) graphics card. The motion tracking data was streamed via Motive (Version

2.0.2) and the motion platform operated via HyPCoS (Version 1.3), which was on a separate Linux PC. The VR environment consisted of a dirt pathway set in an open outdoor scene bordered by densely packed trees with a singular simulated natural overhead light source (see Figure 4.1A). The trees, ground texture, and skybox used to create the outdoor environment were all free assets available on the Unity Asset store.

All task-relevant visual stimuli were presented on a grey (RGBA 128, 128, 128, 255; 0.5, 0.5, 0.5, 1.0) rectangular screen with simulated dimensions of 10 cm × 10 cm, which was locked to the centre of the HMD at a simulated distance of 57 cm (approx. 10°). The target stimulus was a 1.7 cm (approx. 1.7°) filled circle (see Figure 4.1B). The QUEST (Watson & Pelli, 1983) adaptive staircase algorithm was implemented to adjust the contrast of the circle target to produce an overall accuracy rate of 75% for each motion condition. The initial slope (β) was set to 3.5, chance rate (γ) to .5, and lapse rate (δ) to .01 for each staircase, which had resolutions of .01 (i.e. 1%) for the range .01 to 1. As the QUEST procedure stabilised at 75% accuracy after ~40 targets, a jitter was added to each trial's contrast to enable better estimates of the slopes of the psychometric functions per target condition (see Figure 4.1D & E). This jitter was provided by the standard deviation of the prior probability density function of the staircases in real time, resulting in the contrast of the target being selected from the following array of positions: [$M - 2SD$, $M - SD$, $M - SD$, M, $M + SD$, $M + SD$, $M + 2SD$] based on the mean (M) of the distribution of QUEST-derived threshold estimates in each staircase. The positions one standard deviation from the mean were twice as likely to be sampled to provide a spread of data points along the rising portion of the psychometric function to obtain a more accurate estimate of participants' 75% detection thresholds (see Figure 4.1F).

Figure 4.1

Apparatus and Procedure

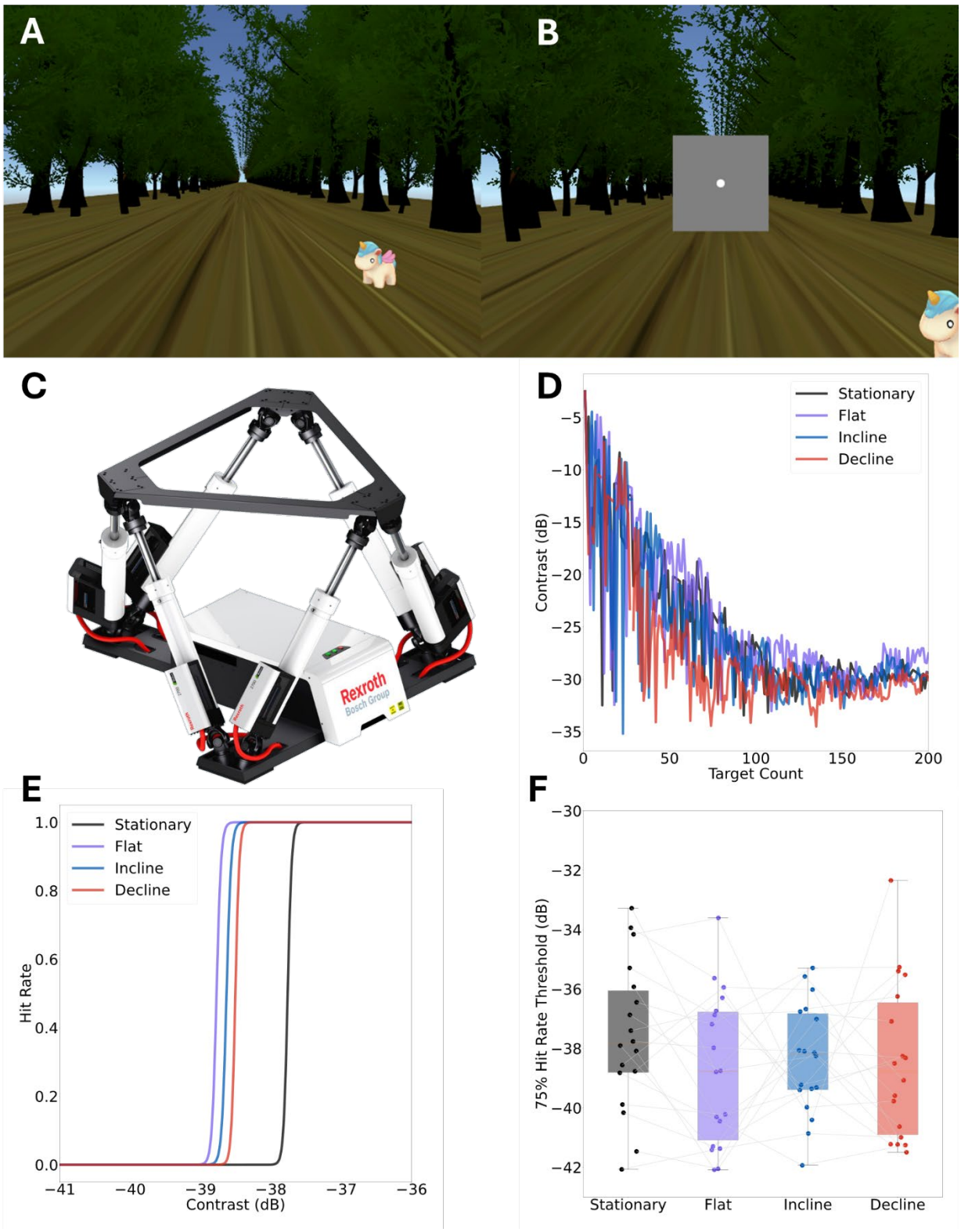

A First person-perspective of the Virtual Reality environment used in the study

B Example of the circle stimulus at suprathreshold contrast.

C Bosch Rexroth eMotion 1500 6DOF motion platform

D Example data showing the change in contrast driven by the adaptive QUEST procedure for presentation of targets when participants were stationary (black), walking on no incline (purple), walking on a 7% incline (blue) and on a 7% decline (red)

E Psychometric function with grand mean of participants' psychometric function parameters, psychometric function for targets when stationary is in black, purple for targets presented when walking on no incline, blue for when walking on 7% incline, and red for when walking on 7% decline

F The distribution of contrast thresholds for 75% hit rate across participants ($N = 18$), x-axis displays the condition in which the targets were presented; stationary, walking on flat ground, walking on a 7% incline, and walking on a 7% decline

4.2.3 Procedure

Participants were provided with a participant information statement, followed by an opportunity to ask any questions before they completed the consent form. All participants were informed that their consent and participation could be revoked at any time during the procedure if they wished not to provide their data or did not wish to complete their participation without the need to provide a reason. They were then introduced to the VR apparatus, the hand-controller, the tracked physical space, and the motion platform before being fitted with the apparatus, including being fitted into a suspension harness, and given the hand-controller.

Once the VR program was initiated, participants were told to read the task instructions displayed on the screen in the centre of the virtual environment. The instructions outlined the

trigger-response task to any detected circles (i.e., flashes) and the requirement to make speeded responses. They were then asked to describe the task they were to complete to verify their understanding. If correct in understanding, the participant was instructed to begin the first of four practice blocks whilst standing still. Otherwise, the participant was assisted in their understanding by further verbal instructions until they understood the task correctly. During this practice the targets presented were easy to detect, with a fixed supra-threshold constant in overall contrast (100%) and were not used to update any of the adaptive staircases. The remaining 3 practice blocks were for the three walking conditions (i.e., flat, incline, and decline) to allow participants to feel comfortable with the movement of the motion platform and the slope of the treadmill. Each practice block had 15 target presentations.

Participants then completed 4 blocks, one for each condition, with the order of the blocks randomized. Each block had 460 target presentations, with each target having a 10% chance of being withheld from presentation. Targets were presented in the centre of the virtual screen, which was equivalent to the centre of the HMD. Targets were presented for 22 ms and were spaced by variable intertrial intervals with a minimum of 800 ms. Targets were never presented during the first 1 s of blocks. For blocks involving walking, participants needed to reach a speed above 0.4 m/s at the beginning before an additional 5 s non-presentation period began to allow participants to be in a comfortable walk and to avoid the acceleration period when beginning walking. At any time during the block, participants could pause and upon restarting will need to reach the same speed criterion and experience the same 5 s non-presentation period.

4.2.4 Data Analyses

Each sequence provided 3D time-series data (x, y, z, coordinates) for head position. Individual steps were extracted based on changes in head height (Davidson et al., 2024; Phan et

al., 2025), which follows a roughly sinusoidal pattern during walking. Peaks and troughs in vertical head position correspond to the approximate swing and stance phases of the stride-cycle, which we identified using a peak detection algorithm. Target performance data (i.e., hits, misses, and response times) were mapped according to target onset relative to the overall time span of the step. All analyses were performed using custom Python (version 3.11.1) code, and ANOVAs were performed in JASP (version 0.18.0.0).

4.2.5 Gait Extraction

Step-onsets were extracted based on the time-series of the vertical position of head-movement data as described in Davidson et al. (2024) and Phan et al. (2025). As walking shifts the centre of mass sinusoidally, troughs on the vertical axis of motion correspond to the double support stance phase of the gait cycle. Step-lengths were normalised for analysis by resampling the time-series data to 50 points (taken as increments of 2% of progression). This deviation from previous stride-based analyses was due to the interest in the potential shift in distribution of motor requirements induced by inclination, which could potentially be averaged out with stride-based epoching.

4.2.6 Performance Relative to Stride

A rolling window of 18% was applied to all target onsets to produce 50 linearly spaced bins (from 0-100%) reflecting performance along step progression. Performance metrics analysed were hit rate, taken as the proportion of targets responded to out of total number of presented targets, and response time relative to target onset within progression (i.e., percentage).

Significant modulations were tested for each dependent variable for step at the group-level. Stepping from .1 to 10 cycles per stride (cycles per stride), in increments of .1, single component Fourier series (n=1) were fitted with the equation:

$$f(t) = a_0 + a_1 \cos(\varphi t) + b_1 \sin(\varphi t) = a_0 + A \cos(\varphi t + \phi) \quad (1)$$

where $\boldsymbol{\varphi}$ is the periodicity (cycles per stride), $\boldsymbol{t}$ is the progression of the stride (as a percentage), $\boldsymbol{a_1}$ and $\boldsymbol{b_1}$ are the coefficients of the cosine and sine components and $\boldsymbol{a_0}$ is a constant, the central value of the modulation. The resulting fits had amplitudes of $\boldsymbol{A}$ and shifts in phase of $\boldsymbol{\phi}$. The goodness of fit (R^2) at each frequency step was used as an indication of modulation strength. Fits were tested using a permutation procedure to generate a null distribution of R^2 at each frequency value. This shuffling procedure entailed randomly permuting the bin in which each target was allocated. This shuffling was repeated 1000 times and each shuffled data series was fitted at each frequency. The R^2 values for the 1000 shuffles at each fitted frequency were taken to represent the null distribution for strength of the modulations detected in the original data at the specific frequency, as the temporal intercorrelation of bins was effectively destroyed. The R^2 values from fitting the data at each frequency were compared to the 95th percentile of their respective null distributions, with those greater than this critical value taken to indicate a significant modulation.

4.2.7 Alternative Modulation Shape

In addition to the sinusoidal fitting from the Fourier fitting procedure, an additional mathematical function was fitted to the accuracy and response time performance measures across step progression. This procedure involved fitting two sinusoidal waves to the data in a piecewise manner. The point of equivalence of the two sinusoids was at their peaks, which had their amplitude provided by their respective $\boldsymbol{A}$. As the intention was to investigate the effects of slope on peak shift in performance and the lowest performance was assumed to be during stance phase, the combined period of the piecewise equation was set to be a step. The peak location, $\boldsymbol{P_t}$, along the step progression was provided by the location of the respective Fourier function. This fitting

procedure allowed for an asymmetric slope around the peak that retained the troughs at stance phase, like a sawtooth equation (see Figure 4.2):

$$P_t = 2\pi - \phi \tag{2}$$

$$\omega_0 = \frac{\pi}{P_t} \tag{3}$$

$$\omega_1 = \frac{\pi}{\phi} \tag{4}$$

$$\theta_0 = \pi \tag{5}$$

$$\theta_1 = 2\pi - \omega_1 P_t \tag{6}$$

$$f(t) = \begin{cases} a_0 + A\cos(\omega_0 t + \theta_0), & t \leq P_t \\ a_0 + A\cos(\omega_1 t + \theta_1), & t > P_t \end{cases} \tag{7}$$

Figure 4.2

Sinusoidal Functions Fitted for Performance

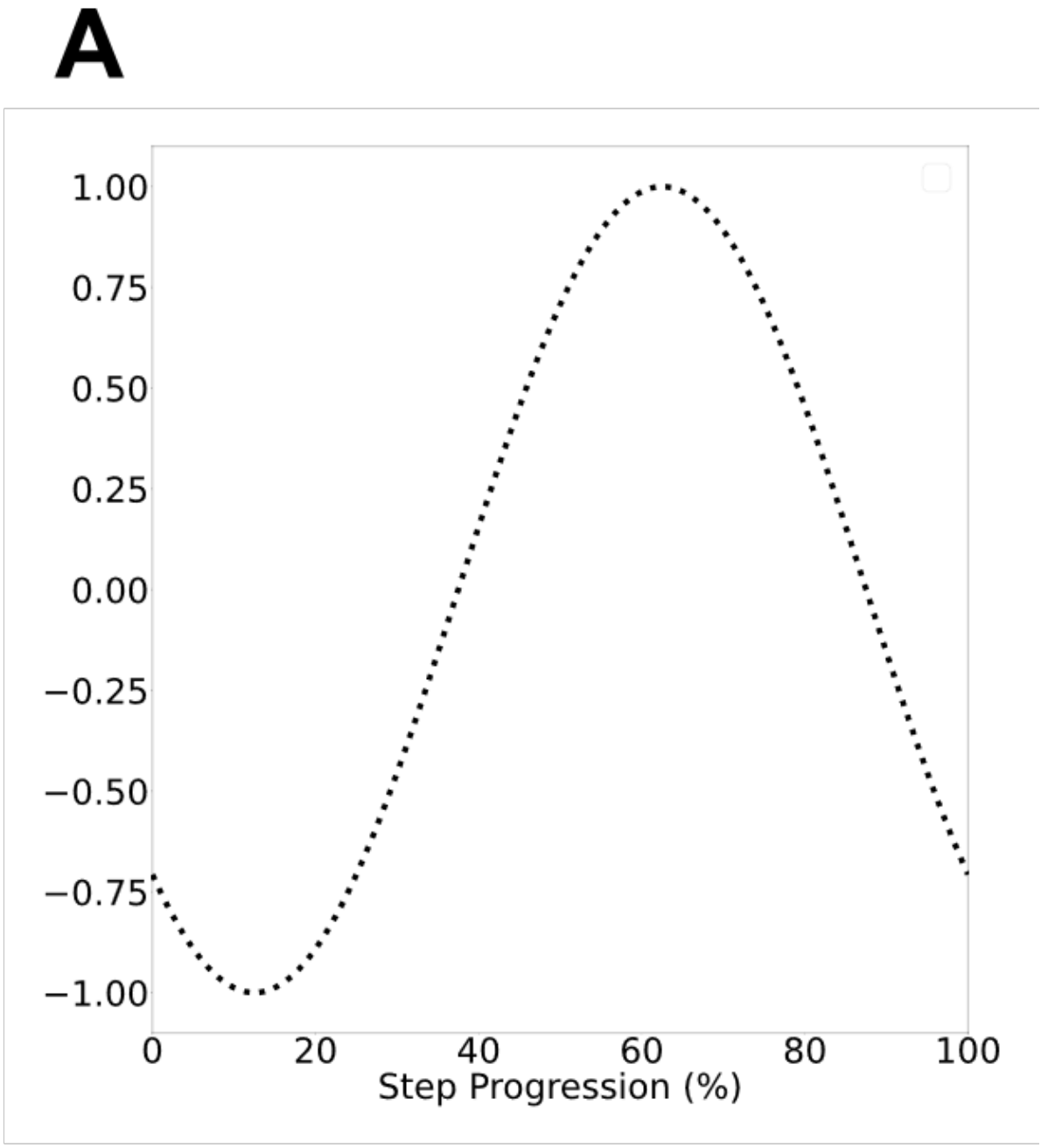

$$f(t) = a_0 + A\cos(\varphi t + \phi)$$
$$A \geq 0$$

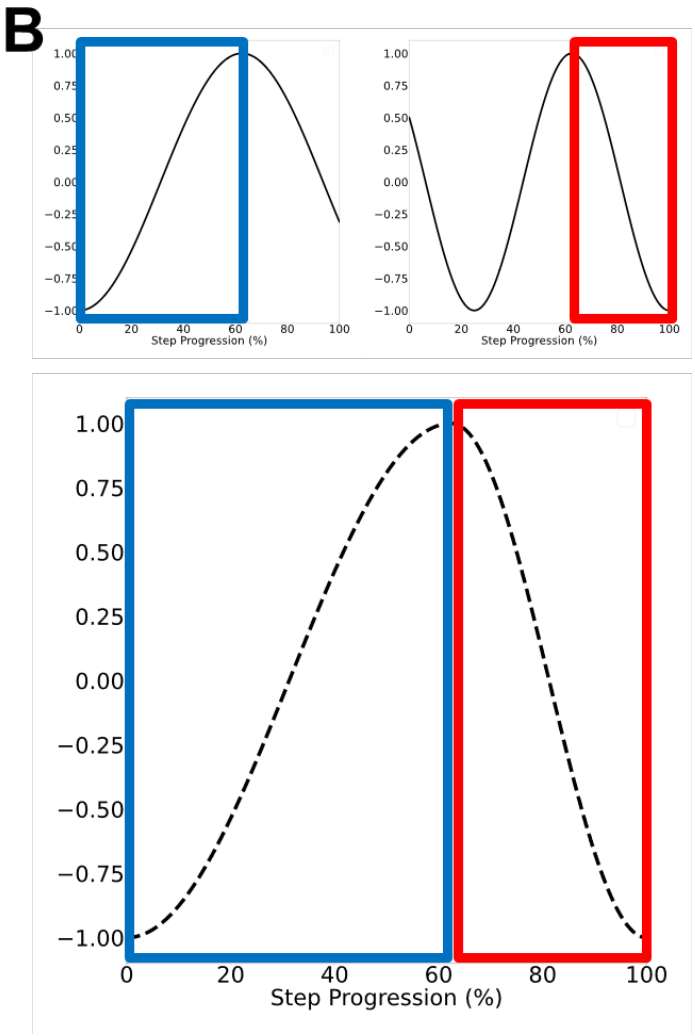

$$f(t) = \begin{cases} a_0 + A\cos(\omega_0 t + \theta_0), t \leq P_t \\ a_0 + A\cos(\omega_1 t + \theta_1), t > P_t \end{cases}$$

$$P_t = 2\pi - \phi$$

$$\omega_0 = \frac{\pi}{P_t}$$

$$\omega_1 = \frac{\pi}{\phi}$$

$$\theta_0 = \pi$$

$$\theta_1 = 2\pi - \omega_1 P_t$$

Note. To entertain peak shift without shifting the trough of performance from the stance phases, an additional piecewise function was fitted on performance data. The parameters were provided by the standard Fourier fitting procedure.

A Standard single component (n = 1) Fourier fit applied

B Piecewise two-component sinusoidal fit using parameters provided by **A**. The blue and red outlines of the sinusoidal functions are the piece components that were used for the overall fit.

4.3 Results

One-way repeated-measures ANOVAs were performed on the contrast threshold for 75% hit rate and response times across the motion levels: stationary, walking on flat ground, walking

on an incline, and walking on a decline. A main effect of motion condition was found for response times, $F(3, 51) = 4.61$, $p = .006$, $\eta^2 = 0.213$. This main effect persisted after Greenhouse-Geisser corrections for sphericity, $p = .016$. A planned contrast revealed significant differences between the response times of participants when they were stationary as opposed to walking, such that they responded faster when stationary ($M = 390$ ms, $SD = 19$ ms) than when walking ($M = 400$ ms, $SD = 16$ ms), $t(51) = -3.50$, $p < .001$. Planned contrasts between walking on no incline and walking on an incline, and between the two different inclines, revealed no significant effects, p's $> .05$. There was no significant main effect of motion condition on the contrast threshold for 75% hit rate (see Figure 4.1F), $p = .386$.

Figure 4.3

Modulations in Performance Across Step Progression

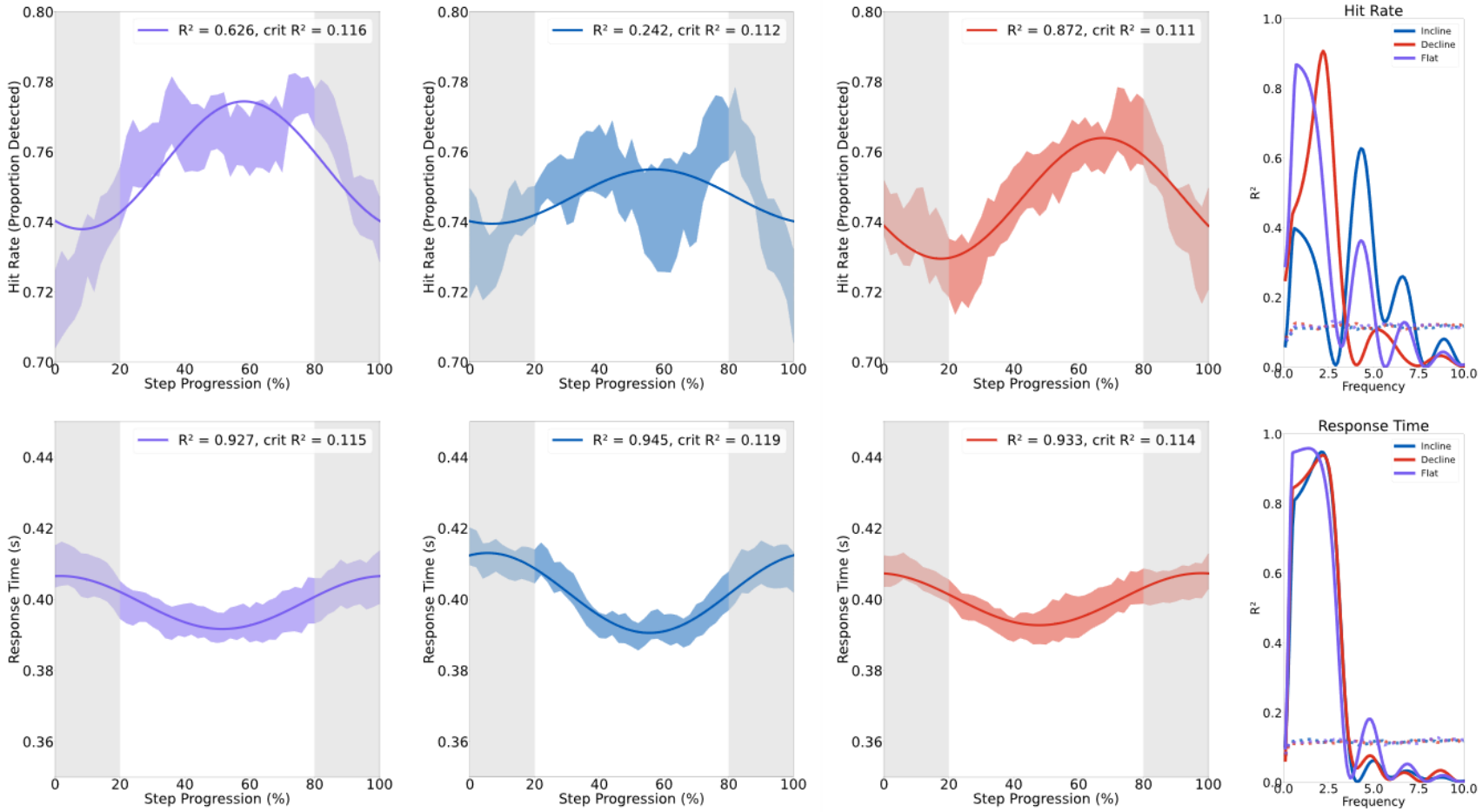

Note. Fourier models set at 2.0 cps fitted to group-level data (N=18) are displayed for walking on flat (purple), inclined (blue) and declined (red) ground. Light and dark grey regions indicate the estimated stance and swing phases of the step, respectively. Note that

the x-axis shows the progression of a single step and so the 2 cps sinusoid fitted to the data appears as a single cycle. First row displays hit rate performance across the step. Second row displays the response time across step. Fourth column displays the goodness-of-fit (R^2) calculated for each performance measure for each of the walking inclination condition. Dotted lines show the upper 95th percentile of R^2 values at each fitted frequency obtained from a null distribution of group-level data shuffled over step progression (n = 1000 permutations). Fourier models were fit at a fixed frequency between 0.1-10 cps (in steps of 0.1) on the group-level data. Shaded regions indicate ±1 SEM.

In analysing the performance data across the progression of a step, the group-level hit rate and response time demonstrated modulations at ~2 cps (see Figure 4.3). The modulations appear to be counterphase to each other. Hit rate appears to peak during the swing phase, demonstrating an increase in contrast sensitivity, and dropping to local lows in the stance phase. Instead, response times peaked for targets presented during the stance phase and were shorter for targets presented during the swing phase. None of the alternative piecewise fits constructed from two partial sinusoidal functions outperformed the one component Fourier fit for the group-level hit rate data (see Figure 4.4).

Figure 4.4

Piecewise Sinusoidal Fits on Hit Rate Across Step Progression

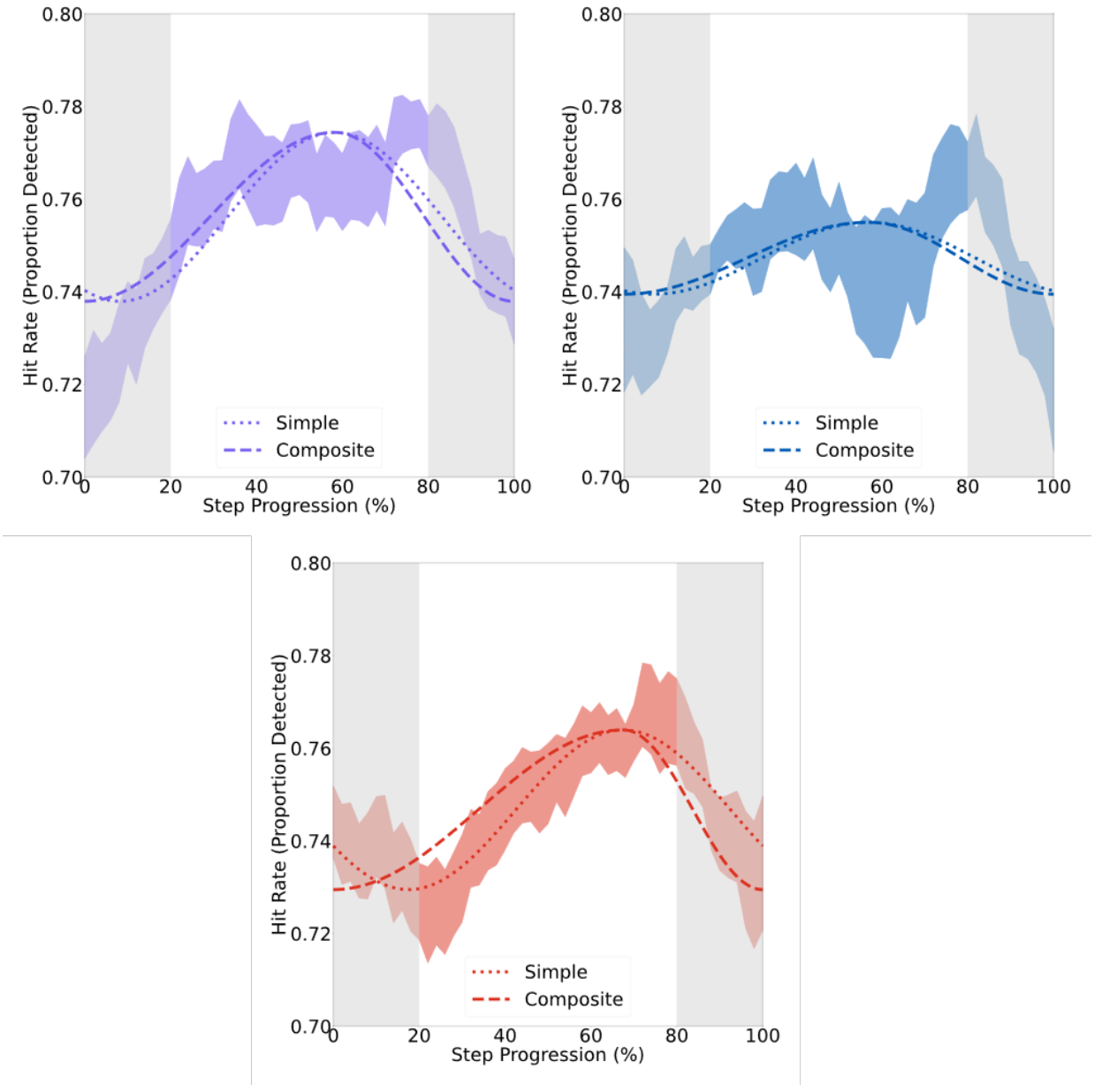

Note. Fitted equations to group-level hit rate data (N=18) are displayed for walking on flat (purple), inclined (blue) and declined (red) ground. Light and dark grey regions indicate the estimated stance and swing phases of the step, respectively. Shaded regions indicate ±1 SEM.

Dotted lines display simple one-component Fourier fits. Dashed lines display two-component composite fits (see Methods and Figure 4.4).

Additional one-way repeated-measures ANOVAs were performed on the peak and troughs of hit rate across the different walking conditions; no incline, inclined and declined ground. There was no significant main effect of walking ground inclination on the time point of peak hit rate along step progression, $p = .967$. Irrespective of whether the variable analysed was the initiating trough (defined as the lowest hit rate in the first 20% of the step) or the finishing trough (defined as the lowest hit rate in the last 20% of the step), walking ground inclination had no effect on the time point when hit rate was the lowest, p's > .05.

Figure 4.5

Four Cycles per Stride Fourier Fits for Group-Level Hit Rate

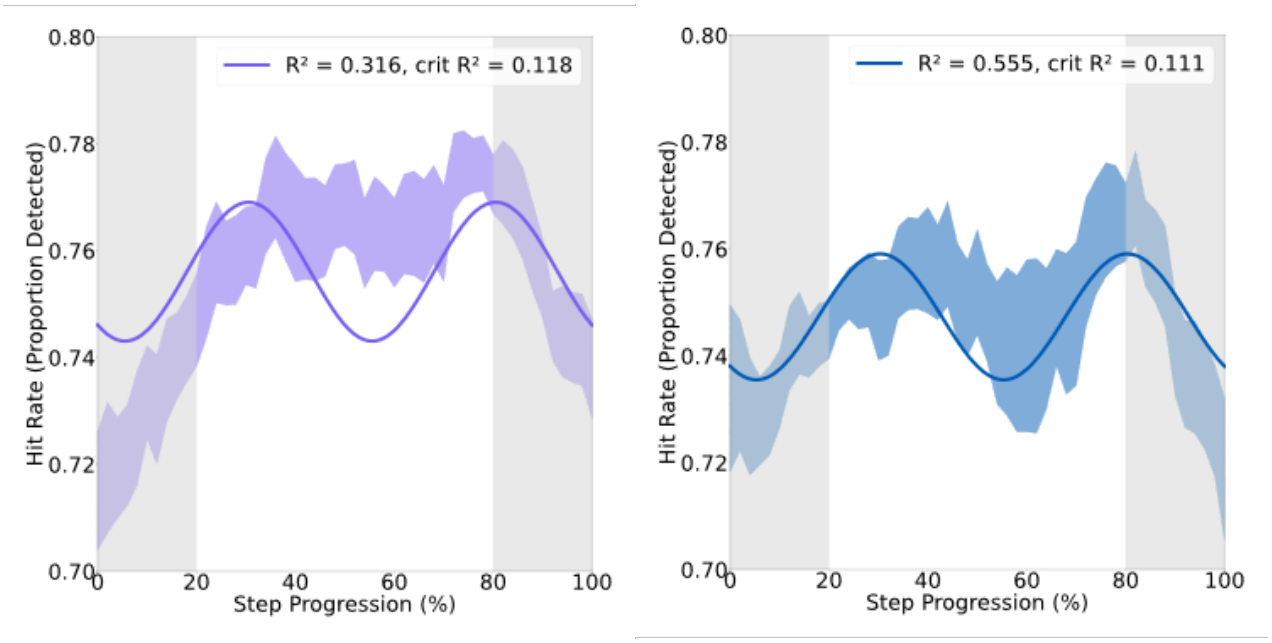

Note. Fourier models set at 4.0 cps fitted to group-level data (N=18) are displayed for walking on flat (purple), inclined (blue). Light and dark grey regions indicate the estimated stance and swing phases of the step, respectively. Both are significant when compared to the null distribution produced by permutation.

In addition to the ~2 cps region of interest, group-level hit rate showed modulations at ~4 cps for both walking on flat ground and walking on an incline (see Figure 4.5). Whilst the flat ground modulation at ~2 cps outperformed the ~4 cps Fourier fit, the higher frequency modulation was a better fit for hit rate when walking on an incline.

4.4 Discussion

The present study investigated whether changing the inclination of the surface individuals walk on would alter the modulations of visual detection across the step cycle that have been reported in recent studies (Davidson et al., 2024; Phan et al., 2025). In regard to replicating the modulations found in previous studies, the results of the current study confirm these modulations for both visual detection and response making. Visual detection hit rates peaked during the swing phase of the step and were lowest during the stance phase. Conversely, response times peaked during stance phases and were lowest in the swing phase. Despite the different motor demands of walking on flat versus inclined ground, the best and worst time points for visual detection during step progression showed no difference irrespective of the walking inclination.

An interesting finding was the ~4 cps modulation for hit rate during inclined walking. This manifested in two peaks in hit rate during step progression, one during the early swing phase and the other as the terminating stance phase began. The second peak did not differ from the late swing phase peak found for the modulation seen for walking on flat and declined ground. The first peak in visual detection performance was highly unexpected. Entering the swing phase during inclined walking has the greatest energy cost and most muscular engagement, which increases gait instability (Kimel-Naor et al., 2017; Lu et al., 2023). Despite this, visual detection performance peaked after toe off (which indicates the end of the stance phase and initiation of the swing phase). In terms of sensory input, this point of the step is particularly noisy for visual

input and would involve greater attentional resources to resolve for accurate visual perception. The visual target was always presented in the same location, and the visual environment was simple and repeated, hence, the participants did not really have to exercise much attentional control. Therefore, an increase in attentional resources or utilisation is unlikely to be the reason for the first peak in performance when walking on an inclined surface. To examine the underlying mechanism of this effect, a future study could employ an attentional measurement, such as the steady-state visual evoked potential (SSVEP) used in electroencephalographic (EEG) data (Kim et al., 2007). A systematic increase in the amplitude of the SSVEP at the initiation of the swing phase would be expected if increased directed attention were responsible for the additional peak in hit rate seen in the current study.

An alternative, more likely explanation for the first peak is that participants had a more liberal decision criterion following toe off in inclined walking. The calculation of the decision criterion requires both hit rate and false alarm, similarly both are required for the calculation of the sensitivity (d') (Stanislaw & Todorov, 1999). Whilst the hit rate can be determined from the responses in the current study, false alarms cannot be accurately determined. The single response option used in the current study makes it difficult to label responses made outside the response-time window as false alarms as they could have been highly delayed responses to the most recent target presentation. A solution for future studies would be to employ a two-alternative forced-choice task, where the participants indicate whether they did or did not detect a target and therefore can indicate a false percept of the target when it was not presented (i.e., a false alarm).

The failure of the two-component compound sinusoid functions to better explain the modulations across the step cycle is indicative of a trait of the visual detection performance modulations. The troughs of the modulation are not locked to the troughs of the head height. This

is best seen in the modulation for declined walking, where the beginning trough in hit rate was not right at the beginning of the step demarcation but close after. That is not to say the compound function is inappropriate to describe the modulation pattern in perceptual ability across the step or stride cycle. Having the ability to entertain an asymmetrical shape not available to the sinusoidal pattern of Fourier components is a key benefit to this approach and comes without the difficult interpretation of the additive series of a sawtooth function or the linear shape restrictions that are included with triangle waves. Improvements to this alternative compound function for fitting the data would be to allow the phase alignment of the troughs to be free parameters and for additional points of equivalence to allow fitting for stride-based performance windows.

Unlike previous gait-based modulations found in visual detection (Davidson et al., 2024; Phan et al., 2025), the peak in performance was not in the middle of the swing phase and was instead at the end of the swing phase. This difference can be most probably explained by the difference in mechanics involved in the treadmill walking in the current study and the free walking of previous studies. The pull of the treadmill belt whilst the individual's centre of mass is shifted forward may have created an exaggerated asymmetry between the first and second half of a step. The supporting foot would have been translating backward while the other was swinging, creating an increased angle between the legs and a more rapid height decrease in the later half of the step than for free-ground walking, resulting in a truncated descent time on each step. Unlike the in the fields of kinematics and exercise physiology, walking in the field of human perception as a tool still requires verification checks that were not prioritised or even considered, such as whether treadmill walking and free walking produce the same perceptual experience. Extensive studies have compared the muscles engaged in the two types or walking, as well as gait parameters and gross movements (Lee & Hidler, 2008; Riley et al., 2007; Semaan

et al., 2022), but have mostly dismissed the differences beyond the measure of interest. Those studies were not focused on perceptual changes within the step cycle, and the differences noted between the two types of walking and mostly ignored may yet prove to be relevant perceptually. Future active perception studies could either include tracking points or inertial measurement units (IMUs) at key points beyond the head to measure and compare the time course of a step between the two different types of walking. An alternative would be to have individuals complete the perceptual task both in free walking conditions and when walking on a treadmill, which would allow a direct comparison between perceptual modulations under the two conditions.

Overall, the current study has once more confirmed the modulatory effect of walking on visual detection. Walking on an inclined or declined slope did not shift the phase of peak visual detection, nor did it shift the lowest points of performance. Future research could investigate the differences between treadmill and free walking in their effects on perception to refine the methodology employed to study perception while walking. Additionally, this study provides the foundation for an alternative function to explain the patterns found for walking-based modulations, or more expansively, any repeated sinusoidal modulations that may produce asymmetrical patterns.

4.5 Acknowledgements

The data presented in this chapter was collected at Universität Ulm, Germany in collaboration with Professor Doctor Marc O. Ernst, Applied Cognitive Psychology.

Research was supported by an Australian Government Research Training Program (RTP) Scholarship (SC3227) and a Campbell Perry International Research Scholarship (SC0078) to Cameron K. Phan.

5

Chapter 5

General Discussion

5.1 General Discussion

The purpose of this thesis was rooted in the expansion of our understanding of active movement-based phenomena in perception. Specifically, it focused on the recently found stride-based modulations in visual detection by Davidson et al. (2024). The unknown status of the underlying mechanisms for these modulations leaves numerous opportunities for exploration. Whether the modulation in visual perceptual performance is equivalent across the visual field, whether other visual abilities demonstrate similar modulations, or if the motor system requirements of the active movement play a role in the modulations were the questions of interest of this thesis in its attempt to probe into the underlying nature of stride-based modulations. Greater understanding of how stride affects visual perception will provide a foundation for explaining other active cyclic movements, such as biking, swimming, and chewing, and a framework for all active movements in general. This chapter will summarise the findings of the empirical chapters (i.e., Chapters 2-4) and provide potential avenues of interest for future research.

5.1.1 Summary of findings

5.1.1.1 Stride-based modulation in central and peripheral visual detection

Chapter 2 had individuals indicate their detection of a visual target that appeared whilst they were walking. The target could appear in either a parafoveal or a peripheral location within their visual fields. Classical visual perception studies have shown the periphery has lower visual acuity and colour resolution but instead has better motion detection (Brindley & Lewin, 1968; Cowey & Rolls, 1974). Our interest did not lie in these classic phenomena; we were interested in whether the previously found stride-based modulations in visual detection would be replicated in the visual periphery, which they were. However, the detection modulation (i.e., hit rate) was

larger and peaked later in the stride cycle for peripheral targets than for central targets. This difference in modulatory effect for eccentricity indicates a priority, or more generally, an order effect, which prioritises the processing of central vision.

Contrast sensitivity peaked during the swing phase of stride and troughed in the stance phase for both eccentricities, as was found previously (Davidson et al., 2024). The difference in phase between modulations may indicate that stride-based modulations begin in the central visual field and propagate outward into the visual periphery (Fakche & Dugué, 2024; Sokoliuk & VanRullen, 2016). However, it should be noted that the visual detection task only involved single target presentation and therefore did not directly measure prioritisation. To account for this, only individuals with significant modulations in both eccentricities were analysed for differences in modulation amplitude. The larger modulation amplitude in peripheral vision was most probably due to the inherent lower acuity and sensitivity in the visual periphery, which may have facilitated larger deviations in detection ability.

Modulations for response time and likelihood were similarly replicated with the addition of phasic differences between visual eccentricities. The combination of the increased amplitude and earlier phase of the central response time modulations were congruent with the later peak in the central response likelihood modulation. As the difference in response time modulations were congruent with the phasic differences in response likelihood, the response time modulations can best be explained as an alignment to an optimal response phase, specifically, the stance phase, during the stride cycle. The earlier peak in response likelihood for peripheral visual targets follows along the proposed purpose of peripheral vision in action planning and response making, which would result in its prioritisation for responses. With the misalignment of response time

and hit rate modulations, it would appear that stride induces separate modulations in the sensory and motor systems.

Overall, the findings of Chapter 2 replicate the novel effects of stride in modulating visual detection and validate the need for further exploration into the parameters of these stride-based modulations.

5.1.1.2 Stride-based modulation difference between visual hierarchy level

Chapter 3 introduced more complex tasks than the visual detection task of prior research and of Chapter 2 whilst retaining enough simplicity to avoid invalidating cross-study comparisons. The use of a multiple feature stimulus instead of the singular contrast variant stimulus used previously produced a greater variety of logical pairwise comparisons, which facilitated the investigation of potential modulations of classical phenomena. However, none of these additional potential sources of modulation differences produced any effect. Instead, the difference in visual abilities being tested produced phasic differences in modulation.

Identification of the orientation of a visual grating and its direction of drift are tasks with fundamentally linked visual abilities (Del Viva & Morrone, 1998; Derrington et al., 2004). Visual perception of orientation is encoded by the cortical structure of the primary visual cortex (V1) and is dependent on the activity distribution amongst its columnar structures (Appelle, 1972; Ben-Yishai et al., 1995; Harrison et al., 2023; Hubel & Wiesel, 1962). Similarly, the percept of simple visual motion is the comparison of activity in neighbouring receptive fields over time, in short succession, and can be completed via V1 alone (Del Viva & Morrone, 1998; Derrington et al., 2004; Hubel & Wiesel, 1962; Van Kleef et al., 2010). However, the phasic shift in modulations between performance on the two tasks would indicate involvement of additional cortical areas (Maunsell & Essen, 1983; Prieto et al., 2007).

Accuracy, for both orientation and motion identification, was observed to modulate at the same two cycles per stride as hit rate did for visual detection. The difference lay in the phase of the modulations for each visual ability. The phase of orientation identification accuracy modulation was shifted in such a way that accuracy peaked at the end of the swing phase, later than the peak at mid-swing phase seen for visual detection hit rate. A further shift was seen for motion direction identification resulting in a peak in accuracy early in the swing phase. Due to the cyclical nature of stride-based modulation, this forward shift can be seen as a backward shift of magnitude equivalent to the difference between the full stride-cycle and the forward shift. As the three visual abilities follow along an axis of complexity, latency, and engagement of visual cortical hierarchy, a forward shift is the most logical and likely to be the most accurate interpretation of the findings.

Similar to the findings of Chapter 2, the phasic difference found in Chapter 3 is suggestive of a directional propagation of stride-based modulations, albeit along the visual hierarchy instead of across the spatial representation within a single visual area. However, this remains to be investigated through the measurement of neurophysiology along the cortical hierarchy.

5.1.1.3 Effect of different walking requirements on stride-based modulations of visual detection

Chapter 4 returned to the simple visual detection task employed in Chapter 2 but introduced slopes to the walking surface to change the walking requirements from the flat-ground walking conditions in Chapters 2 and 3. The focus of this experiment was the phasic alignment of the performance modulation with the progression of a step. However, neither uphill

nor downhill walking affected the highest or lowest points of visual detection performance along the time course of a step.

Once again, replication of the previous visual detection performance and response time modulations was successful (Davidson et al., 2024; Phan et al., 2025). Performance peaked for targets presented in the swing phase, with a greater hit rate and shorter response time to such targets. A lower hit rate and longer response times were observed for targets presented during the stance phase of the step. Despite the increased muscular engagement and energy costs of initiating toe off when taking a step on inclined surfaces, the peak of perceptual performance was not shifted later in step progression in comparison to flat-ground walking (Kimel-Naor et al., 2017; Pickle et al., 2016; Riley et al., 2007). Similarly, the increased energy absorption and muscular engagement at heel strike for walking on a declined surface did not shift the peak of perceptual performance to an earlier point in the step progression. Instead of the expected phasic shifts of the highest or lowest points of visual detection performance, inclined walking appeared to induce an additional peak in performance in the early swing phase, to which a 4 cps model could be fit. Across the work by Davidson et al. (2024) and Phan et al. (2025) and the experiments conducted in Chapter 3, there were instances in both participant and group-level analyses that had significant or near significant 4 cps modulations. However, in those instances, the frequency range of interest was centred at 2 cps and those infrequent 4 cps modulations were ignored. In Chapter 4, the focus on stepwise analyses and alternative model fitting allowed for a more nuanced look into the harmonics of 2 cps (e.g., 4 cps or 8 cps) without worrying of problematic phasic alignments produced by the double counting of strides. This stepwise approach should be entertained for future analyses where step-based dynamics, like the inclination driven motor engagement differences in Chapter 4, are of interest. An additional

surprising observation was a peak in performance later in the swing phase than previously found, which may be due to the difference in walking requirements of treadmill and free ground walking (Lee & Hidler, 2008; Semaan et al., 2022).

Chapter 4 emphasises the importance of the further expansion of this relatively novel and early field of active perception research, in particular, the exploration of the differences in perception across different types of walking. After all, individuals are constantly encountering various conditions, either intentionally (e.g., treadmill) or unintentionally (e.g., natural terrain), in their daily navigation and understanding perception during these scenarios is key to the development of more applicable research. Future research would also benefit from using steeper inclines than the 7% slope that was permitted for this study.

5.1.2 Limitations and future directions

The empirical chapters of this thesis have solely relied on behavioural data to probe for effects on stride-based modulations. This leaves much unanswered when trying to provide an explanatory mechanism for such modulations. The lack of neurophysiological measures to correlate with the behavioural data is a critique faced by the majority of classic psychophysical literature (Jung, 1972; Kittler et al., 2012). As a solution, electroencephalography (EEG), a noninvasive neurophysiological measurement with high temporal resolution, could be employed simultaneously with perceptual task completion. However, it should be noted that when designing for a walking experiment involving EEG, movement artefacts and mobile electrode arrays must be accounted for (Cao et al., 2015; Kilicarslan & Contreras Vidal, 2019; Shukla et al., 2023). Both issues have now been considered and can be effectively dealt with in the newer EEG apparatus and analysis techniques. With EEG, the neural correlate of the stride-based modulations seen in Chapters 2 to 4 could be investigated. This would reveal whether they occur

due to a modulation of the power of frequency bands associated with attention (i.e., alpha band) (Clayton et al., 2018), possibly due to an amplitude modulation imposed at the stride rate of 2 cps. Additionally, the proposed travelling wave nature of the stride-based modulations across the visual cortical hierarchy could be verified by observing activity across the macroscale of the brain over time (Muller et al., 2018). A caveat to the implementation of EEG is the requirement for large datasets from each individual, which introduces fatigue over the course of participation and increases participation loss through attrition. If future studies wish to implement EEG into walking studies, particularly to sample sufficiently to illustrate stride-based modulations, the development of more efficient and time-saving paradigms would be beneficial.

Future research into active movement is not limited to the addition of neurophysiology and can continue using behavioural psychophysics alone. In Chapter 2, stride-based modulations were found to have a phasic difference between parafoveal and peripheral visual detection, however, this finding was not necessarily indicative of a propagation of modulation. A paradigm involving simultaneous presentations of visual targets of different eccentricity would facilitate a direct measure of prioritisation between eccentricities (Fakche & Dugué, 2024; Sokoliuk & VanRullen, 2016). Alternatively, additional visual eccentricities could be probed for modulations and if the phase shifts correlate, it would strengthen the argument that stride-based modulations propagate. Continuation of the research in Chapter 3 would involve measuring performance in more complex visual tasks, particularly for tasks requiring the recruitment of higher visual areas of the cortex (e.g., visual working memory, visual numerosity, etc.). Research could diverge from visual perception and compare the effect of walking on other sensory modalities or for multisensory perception. If one were instead focused on the effects of walking requirement on perception, visual or otherwise, they could employ a more advanced use of a device like the

motion platform used in Chapter 4. Instead of simple inclination conditions, the walking surface could be dynamically altered in real-time to mimic more ecological terrain (Matthis et al., 2017; Matthis & Fajen, 2014), involving greater variations and interactions between multiple axes of motion. These potential directions of interest would further the understanding established in this thesis about the effect of stride, and potentially other active movements, on perception.

References

Abrams, J., Nizam, A., & Carrasco, M. (2012). Isoeccentric locations are not equivalent: The extent of the vertical meridian asymmetry. *Vision Research*, *52*(1), 70–78. https://doi.org/10.1016/j.visres.2011.10.016

Albright, T. D., & Stoner, G. R. (1995). Visual motion perception. *Proceedings of the National Academy of Sciences*, *92*(7), 2433–2440. https://doi.org/10.1073/pnas.92.7.2433

Anstis, S., Verstraten, F. A. J., & Mather, G. (1998). The motion aftereffect. *Trends in Cognitive Sciences*, *2*(3), 111–117. https://doi.org/10.1016/S1364-6613(98)01142-5

Appelle, S. (1972). Perception and discrimination as a function of stimulus orientation: The "oblique effect" in man and animals. *Psychological Bulletin*, *78*(4), 266–278. https://doi.org/10.1037/h0033117

Bair, W., Cavanaugh, J. R., Smith, M. A., & Movshon, J. A. (2002). The Timing of Response Onset and Offset in Macaque Visual Neurons. *Journal of Neuroscience*, *22*(8), 3189–3205. https://doi.org/10.1523/JNEUROSCI.22-08-03189.2002

Bardy, B. G., Warren, W. H., & Kay, B. A. (1996). Motion parallax is used to control postural sway during walking. *Experimental Brain Research*, *111*(2), 271–282. https://doi.org/10.1007/BF00227304

Barsalou, L. W. (2010). Grounded Cognition: Past, Present, and Future. *Topics in Cognitive Science*, *2*(4), 716–724. https://doi.org/10.1111/j.1756-8765.2010.01115.x

Benjamin, A. V., Wailes-Newson, K., Ma-Wyatt, A., Baker, D. H., & Wade, A. R. (2018). The Effect of Locomotion on Early Visual Contrast Processing in Humans. *Journal of Neuroscience*, *38*(12), 3050–3059. https://doi.org/10.1523/JNEUROSCI.1428-17.2017

Bent, L. R., McFadyen, B. J., & Inglis, J. T. (2005). Vestibular Contributions during Human Locomotor Tasks. *Exercise and Sport Sciences Reviews*, *33*(3), 107.

Ben-Yishai, R., Bar-Or, R. L., & Sompolinsky, H. (1995). Theory of orientation tuning in visual cortex. *Proceedings of the National Academy of Sciences*, *92*(9), 3844–3848. https://doi.org/10.1073/pnas.92.9.3844

Brindley, G. S., & Lewin, W. S. (1968). The sensations produced by electrical stimulation of the visual cortex. *The Journal of Physiology*, *196*(2), 479–493. https://doi.org/10.1113/jphysiol.1968.sp008519

Bullock, T., Elliott, J. C., Serences, J. T., & Giesbrecht, B. (2017). Acute Exercise Modulates Feature-selective Responses in Human Cortex. *Journal of Cognitive Neuroscience*, *29*(4), 605–618. https://doi.org/10.1162/jocn_a_01082

Burr, A. H. J., & Robinson, A. F. (2004). Locomotion behaviour. In *Nematode behaviour* (pp. 25–62). https://doi.org/10.1079/9780851998183.0025

Busch, N. A., & VanRullen, R. (2010). Spontaneous EEG oscillations reveal periodic sampling of visual attention. *Proceedings of the National Academy of Sciences of the United States of America*, *107*(37), 16048–16053. https://doi.org/10.1073/pnas.1004801107

Campbell, F. W., Kulikowski, J. J., & Levinson, J. (1966). The effect of orientation on the visual resolution of gratings. *The Journal of Physiology*, *187*(2), 427–436. https://doi.org/10.1113/jphysiol.1966.sp008100

Cao, K., Guo, Y., & Su, S. W. (2015). A review of motion related EEG artifact removal techniques. *2015 9th International Conference on Sensing Technology (ICST)*, 600–604. https://doi.org/10.1109/ICSensT.2015.7438469

Cao, L., Chen, X., & Haendel, B. F. (2020). Overground Walking Decreases Alpha Activity and Entrains Eye Movements in Humans. *Frontiers in Human Neuroscience*, *14*. https://www.frontiersin.org/articles/10.3389/fnhum.2020.561755

Cao, L., & Händel, B. (2019). Walking enhances peripheral visual processing in humans. *PLOS Biology*, *17*(10), e3000511. https://doi.org/10.1371/journal.pbio.3000511

Chagnaud, B. P., Simmers, J., & Straka, H. (2012). Predictability of visual perturbation during locomotion: Implications for corrective efference copy signaling. *Biological Cybernetics*, *106*(11), 669–679. https://doi.org/10.1007/s00422-012-0528-0

Chapman, C. E., Bushnell, M. C., Miron, D., Duncan, G. H., & Lund, J. P. (1987). Sensory perception during movement in man. *Experimental Brain Research*, *68*(3), 516–524. https://doi.org/10.1007/BF00249795

Chen, X., Cao, L., & Haendel, B. F. (2022a). Differential effects of walking across visual cortical processing stages. *Cortex*, *149*, 16–28. https://doi.org/10.1016/j.cortex.2022.01.007

Chen, X., Cao, L., & Haendel, B. F. (2022b). Human visual processing during walking: Dissociable pre- and post-stimulus influences. *NeuroImage*, *264*, 119757. https://doi.org/10.1016/j.neuroimage.2022.119757

Clark, A. (1999). An embodied cognitive science? *Trends in Cognitive Sciences*, *3*(9), 345–351. https://doi.org/10.1016/S1364-6613(99)01361-3

Clayton, M. S., Yeung, N., & Cohen Kadosh, R. (2018). The many characters of visual alpha oscillations. *European Journal of Neuroscience*, *48*(7), 2498–2508. https://doi.org/10.1111/ejn.13747

Corbett, J. E., & Carrasco, M. (2011). Visual Performance Fields: Frames of Reference. *PLOS ONE*, *6*(9), e24470. https://doi.org/10.1371/journal.pone.0024470

Cowey, A., & Rolls, E. T. (1974). Human cortical magnification factor and its relation to visual acuity. *Experimental Brain Research*, *21*(5), 447–454. https://doi.org/10.1007/BF00237163

Cullen, K. E. (2004). Sensory signals during active versus passive movement. *Current Opinion in Neurobiology*, *14*(6), 698–706. https://doi.org/10.1016/j.conb.2004.10.002

Curcio, C. A., & Allen, K. A. (1990). Topography of ganglion cells in human retina. *Journal of Comparative Neurology*, *300*(1), 5–25. https://doi.org/10.1002/cne.903000103

Davidson, M. (2023). *Peripersonal tracking accuracy during locomotion*. https://doi.org/10.17605/OSF.IO/JDPWC

Davidson, M. J., Keys, R. T., Szekely, B., MacNeilage, P., Verstraten, F., & Alais, D. (2023). Continuous peripersonal tracking accuracy is limited by the speed and phase of locomotion. *Scientific Reports*, *13*(1), 14864. https://doi.org/10.1038/s41598-023-40655-y

Davidson, M. J., Verstraten, F. A. J., & Alais, D. (2024). Walking modulates visual detection performance according to stride cycle phase. *Nature Communications*, *15*(1), 2027. https://doi.org/10.1038/s41467-024-45780-4

Del Viva, M. M., & Morrone, M. C. (1998). Motion analysis by feature tracking. *Vision Research*, *38*(22), 3633–3653. https://doi.org/10.1016/S0042-6989(98)00022-4

Derrington, A. M., Allen, H. A., & Delicato, L. S. (2004). Visual Mechanisms of Motion Analysis and Motion Perception. *Annual Review of Psychology*, *55*(Volume 55, 2004), 181–205. https://doi.org/10.1146/annurev.psych.55.090902.141903

Di Gregorio, F., Trajkovic, J., Roperti, C., Marcantoni, E., Di Luzio, P., Avenanti, A., Thut, G., & Romei, V. (2022). Tuning alpha rhythms to shape conscious visual perception. *Current Biology*, *32*(5), 988-998.e6. https://doi.org/10.1016/j.cub.2022.01.003

Drew, T., & Marigold, D. S. (2015). Taking the next step: Cortical contributions to the control of locomotion. *Current Opinion in Neurobiology*, *33*, 25–33. https://doi.org/10.1016/j.conb.2015.01.011

Eilam, D. (1995). Comparative Morphology of Locomotion in Vertebrates. *Journal of Motor Behavior*, *27*(1), 100–111. https://doi.org/10.1080/00222895.1995.9941703

Engel, A. K., Maye, A., Kurthen, M., & König, P. (2013). Where's the action? The pragmatic turn in cognitive science. *Trends in Cognitive Sciences*, *17*(5), 202–209. https://doi.org/10.1016/j.tics.2013.03.006

Ergenoglu, T., Demiralp, T., Bayraktaroglu, Z., Ergen, M., Beydagi, H., & Uresin, Y. (2004). Alpha rhythm of the EEG modulates visual detection performance in humans. *Cognitive Brain Research*, *20*(3), 376–383. https://doi.org/10.1016/j.cogbrainres.2004.03.009

Fakche, C., & Dugué, L. (2024). Perceptual Cycles Travel Across Retinotopic Space. *Journal of Cognitive Neuroscience*, *36*(1), 200–216. https://doi.org/10.1162/jocn_a_02075

Ferrete Ribeiro, N., & Santos, C. P. (2017). Inertial measurement units: A brief state of the art on gait analysis. *2017 IEEE 5th Portuguese Meeting on Bioengineering (ENBENG)*, 1–4. https://doi.org/10.1109/ENBENG.2017.7889458

Fetsch, C. R., DeAngelis, G. C., & Angelaki, D. E. (2013). Bridging the gap between theories of sensory cue integration and the physiology of multisensory neurons. *Nature Reviews Neuroscience*, *14*(6), 429–442. https://doi.org/10.1038/nrn3503

Fiebelkorn, I. C., Pinsk, M. A., & Kastner, S. (2018). A Dynamic Interplay within the Frontoparietal Network Underlies Rhythmic Spatial Attention. *Neuron*, *99*(4), 842-853.e8. https://doi.org/10.1016/j.neuron.2018.07.038

Fink, P. W., Foo, P. S., & Warren, W. H. (2007). Obstacle avoidance during walking in real and virtual environments. *ACM Transactions on Applied Perception*, *4*(1), 2-es. https://doi.org/10.1145/1227134.1227136

Foglia, L., & Wilson, R. A. (2013). Embodied cognition. *WIREs Cognitive Science*, *4*(3), 319–325. https://doi.org/10.1002/wcs.1226

Foxe, J. J., & Simpson, G. V. (2002). Flow of activation from V1 to frontal cortex in humans. *Experimental Brain Research*, *142*(1), 139–150. https://doi.org/10.1007/s00221-001-0906-7

Franz, J. R., & Kram, R. (2012). The Effects of Grade and Speed on Leg Muscle Activations during Walking. *Gait & Posture*, *35*(1), 143–147. https://doi.org/10.1016/j.gaitpost.2011.08.025

Fuentemilla, Ll., Marco-Pallarés, J., Münte, T. F., & Grau, C. (2008). Theta EEG oscillatory activity and auditory change detection. *Brain Research*, *1220*, 93–101. https://doi.org/10.1016/j.brainres.2007.07.079

Furmanski, C. S., & Engel, S. A. (2000). An oblique effect in human primary visual cortex. *Nature Neuroscience*, *3*(6), 535–536. https://doi.org/10.1038/75702

Gard, S. A., Miff, S. C., & Kuo, A. D. (2004). Comparison of kinematic and kinetic methods for computing the vertical motion of the body center of mass during walking. *Human Movement Science*, *22*(6), 597–610. https://doi.org/10.1016/j.humov.2003.11.002

Gibson, J. J. (1955). The Optical Expansion-Pattern in Aerial Locomotion. *The American Journal of Psychology*, *68*(3), 480–484. https://doi.org/10.2307/1418538

Gibson, J. J. (1962). Observations on active touch. *Psychological Review*, *69*(6), 477–491. https://doi.org/10.1037/h0046962

Gramann, K., Gwin, J. T., Bigdely-Shamlo, N., Ferris, D. P., & Makeig, S. (2010). Visual Evoked Responses During Standing and Walking. *Frontiers in Human Neuroscience*, *4*. https://doi.org/10.3389/fnhum.2010.00202

Harrison, W. J., Bays, P. M., & Rideaux, R. (2023). Neural tuning instantiates prior expectations in the human visual system. *Nature Communications*, *14*(1), 5320. https://doi.org/10.1038/s41467-023-41027-w

Hausdorff, J. M., Purdon, P. L., Peng, C. K., Ladin, Z., Wei, J. Y., & Goldberger, A. L. (1996). Fractal dynamics of human gait: Stability of long-range correlations in stride interval fluctuations. *Journal of Applied Physiology*, *80*(5), 1448–1457. https://doi.org/10.1152/jappl.1996.80.5.1448

Heeley, D. W., & Timney, B. (1988). Meridional anisotropies of orientation discrimination for sine wave gratings. *Vision Research*, *28*(2), 337–344. https://doi.org/10.1016/0042-6989(88)90162-9

Himmelberg, M. M., Winawer, J., & Carrasco, M. (2023). Polar angle asymmetries in visual perception and neural architecture. *Trends in Neurosciences*, *46*(6), 445–458. https://doi.org/10.1016/j.tins.2023.03.006

Hirasaki, E., Moore, S. T., Raphan, T., & Cohen, B. (1999). Effects of walking velocity on vertical head and body movements during locomotion. *Experimental Brain Research*, *127*(2), 117–130. https://doi.org/10.1007/s002210050781

Ho, H. T., Leung, J., Burr, D. C., Alais, D., & Morrone, M. C. (2017). Auditory Sensitivity and Decision Criteria Oscillate at Different Frequencies Separately for the Two Ears. *Current Biology: CB*, *27*(23), 3643-3649.e3. https://doi.org/10.1016/j.cub.2017.10.017

Hogendoorn, H., Verstraten, F. A. J., MacDougall, H., & Alais, D. (2017). Vestibular signals of self-motion modulate global motion perception. *Vision Research*, *130*, 22–30. https://doi.org/10.1016/j.visres.2016.11.002

Holliday, I. E., Anderson, S. J., & Harding, G. F. A. (1997). Magnetoencephalographic evidence for non-geniculostriate visual input to human cortical area V5. *Neuropsychologia*, *35*(8), 1139–1146. https://doi.org/10.1016/S0028-3932(97)00033-X

Hubel, D. H., & Wiesel, T. N. (1962). Receptive fields, binocular interaction and functional architecture in the cat's visual cortex. *The Journal of Physiology*, *160*(1), 106–154. https://doi.org/10.1113/jphysiol.1962.sp006837

Hwang, T.-H., & Effenberg, A. O. (2021). Head Trajectory Diagrams for Gait Symmetry Analysis Using a Single Head-Worn IMU. *Sensors*, *21*(19), Article 19. https://doi.org/10.3390/s21196621

Jain, N., Wang, A., Henderson, M. M., Lin, R., Prince, J. S., Tarr, M. J., & Wehbe, L. (2023). Selectivity for food in human ventral visual cortex. *Communications Biology*, *6*(1), 175. https://doi.org/10.1038/s42003-023-04546-2

Jung, R. (1972). Neurophysiological and Psychophysical Correlates in Vision Research. In A. G. Karczmar & J. C. Eccles (Eds.), *Brain and Human Behavior* (pp. 209–258). Springer. https://doi.org/10.1007/978-3-642-95201-2_14

Kanwisher, N., & Yovel, G. (2006). The fusiform face area: A cortical region specialized for the perception of faces. *Philosophical Transactions of the Royal Society B: Biological Sciences*, *361*(1476), 2109–2128. https://doi.org/10.1098/rstb.2006.1934

Kharb, A., Saini, V., Jain, Y., Dhiman, S., Tech, M., & Scholar. (2011). A review of gait cycle and its parameters. *IJCEM Int J Comput Eng Manag*, *13*.

Khosla, M., Murty, N. A. R., & Kanwisher, N. (2022). A highly selective response to food in human visual cortex revealed by hypothesis-free voxel decomposition. *Current Biology*, *32*(19), 4159-4171.e9. https://doi.org/10.1016/j.cub.2022.08.009

Kilicarslan, A., & Contreras Vidal, J. L. (2019). Characterization and real-time removal of motion artifacts from EEG signals. *Journal of Neural Engineering*, *16*(5), 056027. https://doi.org/10.1088/1741-2552/ab2b61

Kim, Y. J., Grabowecky, M., Paller, K. A., Muthu, K., & Suzuki, S. (2007). Attention induces synchronization-based response gain in steady-state visual evoked potentials. *Nature Neuroscience*, *10*(1), 117–125. https://doi.org/10.1038/nn1821

Kimel-Naor, S., Gottlieb, A., & Plotnik, M. (2017). The effect of uphill and downhill walking on gait parameters: A self-paced treadmill study. *Journal of Biomechanics*, *60*, 142–149. https://doi.org/10.1016/j.jbiomech.2017.06.030

Kittler, R., Kocifaj, M., & Darula, S. (2012). The Neurophysiology and Psychophysics of Visual Perception. In R. Kittler, M. Kocifaj, & S. Darula (Eds.), *Daylight Science and Daylighting Technology* (pp. 285–309). Springer. https://doi.org/10.1007/978-1-4419-8816-4_11

Koch, C., & Ullman, S. (1987). Shifts in Selective Visual Attention: Towards the Underlying Neural Circuitry. In L. M. Vaina (Ed.), *Matters of Intelligence: Conceptual Structures in*

Cognitive Neuroscience (pp. 115–141). Springer Netherlands. https://doi.org/10.1007/978-94-009-3833-5_5

Köhler, M. H. A., Demarchi, G., & Weisz, N. (2021). Cochlear activity in silent cue-target intervals shows a theta-rhythmic pattern and is correlated to attentional alpha and theta modulations. *BMC Biology*, *19*(1), 48. https://doi.org/10.1186/s12915-021-00992-8

Lacquaniti, F., Grasso, R., & Zago, M. (1999). Motor Patterns in Walking. *Physiology*, *14*(4), 168–174. https://doi.org/10.1152/physiologyonline.1999.14.4.168

Lamme, V. A. F., & Roelfsema, P. R. (2000). The distinct modes of vision offered by feedforward and recurrent processing. *Trends in Neurosciences*, *23*(11), 571–579. https://doi.org/10.1016/S0166-2236(00)01657-X

Landau, A. N., & Fries, P. (2012). Attention samples stimuli rhythmically. *Current Biology*, *22*(11), 1000–1004.

Lee, S. J., & Hidler, J. (2008). Biomechanics of overground vs. Treadmill walking in healthy individuals. *Journal of Applied Physiology*, *104*(3), 747–755. https://doi.org/10.1152/japplphysiol.01380.2006

Lewis, P., Rosén, R., Unsbo, P., & Gustafsson, J. (2011). Resolution of static and dynamic stimuli in the peripheral visual field. *Vision Research*, *51*(16), 1829–1834. https://doi.org/10.1016/j.visres.2011.06.011

Lozano-Soldevilla, D., & VanRullen, R. (2019). The Hidden Spatial Dimension of Alpha: 10-Hz Perceptual Echoes Propagate as Periodic Traveling Waves in the Human Brain. *Cell Reports*, *26*(2), 374-380.e4. https://doi.org/10.1016/j.celrep.2018.12.058

Lu, C., Al-Juaid, R., & Al-Amri, M. (2023). Gait Stability Characteristics in Able-Bodied Individuals During Self-paced Inclined Treadmill Walking: Within-Subject Repeated-Measures Study. *JMIR Formative Research*, *7*, e42769. https://doi.org/10.2196/42769

Lum, H. C., Elliott, L. J., Aqlan, F., & Zhao, R. (2020). Virtual Reality: History, Applications, and Challenges for Human Factors Research. *Proceedings of the Human Factors and Ergonomics Society Annual Meeting*, *64*(1), 1263–1268. https://doi.org/10.1177/1071181320641300

MacDougall, H. G., & Moore, S. T. (2005). Marching to the beat of the same drummer: The spontaneous tempo of human locomotion. *Journal of Applied Physiology*, *99*(3), 1164–1173. https://doi.org/10.1152/japplphysiol.00138.2005

MacNeilage, P. R. (2020). *Characterization of natural head movements in animals and humans*.

MacNeilage, P. R., & Glasauer, S. (2017). Quantification of Head Movement Predictability and Implications for Suppression of Vestibular Input during Locomotion. *Frontiers in Computational Neuroscience*, *11*. https://www.frontiersin.org/articles/10.3389/fncom.2017.00047

Malpica, S., Serrano, A., Allue, M., Bedia, M. G., & Masia, B. (2020). Crossmodal perception in virtual reality. *Multimedia Tools and Applications*, *79*(5), 3311–3331. https://doi.org/10.1007/s11042-019-7331-z

Matthis, J. S., Barton, S. L., & Fajen, B. R. (2017). The critical phase for visual control of human walking over complex terrain. *Proceedings of the National Academy of Sciences*, *114*(32). https://doi.org/10.1073/pnas.1611699114

Matthis, J. S., & Fajen, B. R. (2014). Visual control of foot placement when walking over complex terrain. *Journal of Experimental Psychology: Human Perception and Performance*, *40*(1), 106–115. https://doi.org/10.1037/a0033101

Matthis, J. S., Yates, J. L., & Hayhoe, M. M. (2018). Gaze and the control of foot placement when walking in natural terrain. *Current Biology*, *28*(8), 1224–1233.

Maunsell, J. H., & Essen, D. van. (1983). The connections of the middle temporal visual area (MT) and their relationship to a cortical hierarchy in the macaque monkey. *Journal of Neuroscience*, *3*(12), 2563–2586. https://doi.org/10.1523/JNEUROSCI.03-12-02563.1983

MOORE, S. T., HIRASAKI, E., RAPHAN, T., & COHEN, B. (2001). The Human Vestibulo-Ocular Reflex during Linear Locomotion. *Annals of the New York Academy of Sciences*, *942*(1), 139–147. https://doi.org/10.1111/j.1749-6632.2001.tb03741.x

Mulavara, A. P., & Bloomberg, J. J. (2002). Identifying head-trunk and lower limb contributions to gaze stabilization during locomotion. *Journal of Vestibular Research: Equilibrium & Orientation*, *12*(5–6), 255–269.

Muller, L., Chavane, F., Reynolds, J., & Sejnowski, T. J. (2018). Cortical travelling waves: Mechanisms and computational principles. *Nature Reviews Neuroscience*, *19*(5), 255–268. https://doi.org/10.1038/nrn.2018.20

Nasr, S., & Tootell, R. B. H. (2018). Visual field biases for near and far stimuli in disparity selective columns in human visual cortex. *NeuroImage*, *168*, 358–365. https://doi.org/10.1016/j.neuroimage.2016.09.012

Newsome, W. T., & Pare, E. B. (1988). A selective impairment of motion perception following lesions of the middle temporal visual area (MT). *Journal of Neuroscience*, *8*(6), 2201–2211. https://doi.org/10.1523/JNEUROSCI.08-06-02201.1988

O'Regan, J. K., & Noë, A. (2001). A sensorimotor account of vision and visual consciousness. *Behavioral and Brain Sciences*, *24*(5), 939–973. https://doi.org/10.1017/S0140525X01000115

Paradiso, M. A., & Carney, T. (1988). Orientation discrimination as a function of stimulus eccentricity and size: Nasal/temporal retinal asymmetry. *Vision Research*, *28*(8), 867–874. https://doi.org/10.1016/0042-6989(88)90096-X

Parker, P. R. L., Brown, M. A., Smear, M. C., & Niell, C. M. (2020). Movement-Related Signals in Sensory Areas: Roles in Natural Behavior. *Trends in Neurosciences*, *43*(8), 581–595. https://doi.org/10.1016/j.tins.2020.05.005

Pecher, D., & Zwaan, R. A. (2005). *Grounding Cognition: The Role of Perception and Action in Memory, Language, and Thinking*. Cambridge University Press.

Phan, C. K., Davidson, M. J., & Alais, D. (2024). *Walking entrains unique oscillations for central and peripheral visual detection* (p. 2024.07.04.602020). bioRxiv. https://doi.org/10.1101/2024.07.04.602020

Phan, C. K., Davidson, M. J., & Alais, D. (2025). Optimal phase for central and peripheral visual detection differs within the stride cycle. *PNAS Nexus*, *4*(9), pgaf270. https://doi.org/10.1093/pnasnexus/pgaf270

Pickle, N. T., Grabowski, A. M., Auyang, A. G., & Silverman, A. K. (2016). The functional roles of muscles during sloped walking. *Journal of Biomechanics*, *49*(14), 3244–3251. https://doi.org/10.1016/j.jbiomech.2016.08.004

Pozzo, T., Berthoz, A., & Lefort, L. (1990). Head stabilization during various locomotor tasks in humans. *Experimental Brain Research*, *82*(1), 97–106. https://doi.org/10.1007/BF00230842

Prechtl, J. C., Bullock, T. H., & Kleinfeld, D. (2000). Direct evidence for local oscillatory current sources and intracortical phase gradients in turtle visual cortex. *Proceedings of the National Academy of Sciences*, *97*(2), 877–882. https://doi.org/10.1073/pnas.97.2.877

Prieto, E. A., Barnikol, U. B., Soler, E. P., Dolan, K., Hesselmann, G., Mohlberg, H., Amunts, K., Zilles, K., Niedeggen, M., & Tass, P. A. (2007). Timing of V1/V2 and V5+ activations during coherent motion of dots: An MEG study. *NeuroImage*, *37*(4), 1384–1395. https://doi.org/10.1016/j.neuroimage.2007.03.080

Rafal, R., Henik, A., & Smith, J. (1991). Extrageniculate Contributions to Reflex Visual Orienting in Normal Humans: A Temporal Hemifield Advantage. *Journal of Cognitive Neuroscience*, *3*(4), 322–328. https://doi.org/10.1162/jocn.1991.3.4.322

Raiguel, S. E., Lagae, L., Gulyàs, B., & Orban, G. A. (1989). Response latencies of visual cells in macaque areas V1, V2 and V5. *Brain Research*, *493*(1), 155–159. https://doi.org/10.1016/0006-8993(89)91010-X

Raiguel, S. E., Xiao, D.-K., Marcar, V. L., & Orban, G. A. (1999). Response Latency of Macaque Area MT/V5 Neurons and Its Relationship to Stimulus Parameters. *Journal of Neurophysiology*, *82*(4), 1944–1956. https://doi.org/10.1152/jn.1999.82.4.1944

Rakovac, M. (2021). On Evolution and Development of Human Gait. In V. Medved (Ed.), *Measurement and Analysis of Human Locomotion* (pp. 39–59). Springer International Publishing. https://doi.org/10.1007/978-3-030-79685-3_3

Re, D., Inbar, M., Richter, C. G., & Landau, A. N. (2019). Feature-Based Attention Samples Stimuli Rhythmically. *Current Biology*, *29*(4), 693-699.e4. https://doi.org/10.1016/j.cub.2019.01.010

Richards, J., Chohan, A., & Erande, R. (2013). Chapter 15—Biomechanics. In S. B. Porter (Ed.), *Tidy's Physiotherapy (Fifteenth Edition)* (pp. 331–368). Churchill Livingstone. https://doi.org/10.1016/B978-0-7020-4344-4.00015-8

Riley, P. O., Paolini, G., Della Croce, U., Paylo, K. W., & Kerrigan, D. C. (2007). A kinematic and kinetic comparison of overground and treadmill walking in healthy subjects. *Gait & Posture*, *26*(1), 17–24. https://doi.org/10.1016/j.gaitpost.2006.07.003

Rovamo, J., & Virsu, V. (1979). An estimation and application of the human cortical magnification factor. *Experimental Brain Research*, *37*(3), 495–510. https://doi.org/10.1007/BF00236819

Selinger, J. C., O'Connor, S. M., Wong, J. D., & Donelan, J. M. (2015). Humans Can Continuously Optimize Energetic Cost during Walking. *Current Biology*, *25*(18), 2452–2456. https://doi.org/10.1016/j.cub.2015.08.016

Semaan, M. B., Wallard, L., Ruiz, V., Gillet, C., Leteneur, S., & Simoneau-Buessinger, E. (2022). Is treadmill walking biomechanically comparable to overground walking? A systematic review. *Gait & Posture*, *92*, 249–257. https://doi.org/10.1016/j.gaitpost.2021.11.009

Shriki, O., Kohn, A., & Shamir, M. (2012). Fast Coding of Orientation in Primary Visual Cortex. *PLOS Computational Biology*, *8*(6), e1002536. https://doi.org/10.1371/journal.pcbi.1002536

Shukla, P. K., Roy, V., Shukla, P. K., Chaturvedi, A. K., Saxena, A. K., Maheshwari, M., & Pal, P. R. (2023). An Advanced EEG Motion Artifacts Eradication Algorithm. *The Computer Journal*, *66*(2), 429–440. https://doi.org/10.1093/comjnl/bxab170

Smit, A. C., Van Gisbergen, J. A., & Cools, A. R. (1987). A parametric analysis of human saccades in different experimental paradigms. *Vision Research*, *27*(10), 1745–1762. https://doi.org/10.1016/0042-6989(87)90104-0

Sokoliuk, R., & VanRullen, R. (2016). Global and local oscillatory entrainment of visual behavior across retinotopic space. *Scientific Reports*, *6*(1), 25132. https://doi.org/10.1038/srep25132

Stanislaw, H., & Todorov, N. (1999). Calculation of signal detection theory measures. *Behavior Research Methods, Instruments, & Computers*, *31*(1), 137–149. https://doi.org/10.3758/BF03207704

Szekely, B., Keys, R., MacNeilage, P., & Alais, D. (2024). Short communication: Binocular rivalry dynamics during locomotion. *PLOS ONE*, *19*(4), e0300222. https://doi.org/10.1371/journal.pone.0300222

THOMSON, K. S., & SIMANEK, D. E. (1977). Body Form and Locomotion in Sharks. *American Zoologist*, *17*(2), 343–354. https://doi.org/10.1093/icb/17.2.343

Turner, W., Sexton, C., & Hogendoorn, H. (2024). Neural mechanisms of visual motion extrapolation. *Neuroscience and Biobehavioral Reviews*, *156*, 105484. https://doi.org/10.1016/j.neubiorev.2023.105484

Van Kleef, J. P., Cloherty, S. L., & Ibbotson, M. R. (2010). Complex cell receptive fields: Evidence for a hierarchical mechanism. *The Journal of Physiology*, *588*(18), 3457–3470. https://doi.org/10.1113/jphysiol.2010.191452

Virsu, V., & Rovamo, J. (1979). Visual resolution, contrast sensitivity, and the cortical magnification factor. *Experimental Brain Research*, *37*(3). https://doi.org/10.1007/BF00236818

W. Sakowitz, O., Schürmann, M., & Başar, E. (2000). Oscillatory frontal theta responses are increased upon bisensory stimulation. *Clinical Neurophysiology*, *111*(5), 884–893. https://doi.org/10.1016/S1388-2457(99)00315-6

Warren, W. H., & Hannon, D. J. (1988). Direction of self-motion is perceived from optical flow. *Nature*, *336*(6195), 162–163. https://doi.org/10.1038/336162a0

Watson, A. B., & Pelli, D. G. (1983). Quest: A Bayesian adaptive psychometric method. *Perception & Psychophysics*, *33*(2), 113–120. https://doi.org/10.3758/BF03202828

WEBB, P. W. (1984). Body Form, Locomotion and Foraging in Aquatic Vertebrates1. *American Zoologist*, *24*(1), 107–120. https://doi.org/10.1093/icb/24.1.107

Weisz, N., Hartmann, T., Müller, N., & Obleser, J. (2011). Alpha Rhythms in Audition: Cognitive and Clinical Perspectives. *Frontiers in Psychology*, *2*. https://doi.org/10.3389/fpsyg.2011.00073

Wilson, C. J., & Soranzo, A. (2015). The Use of Virtual Reality in Psychology: A Case Study in Visual Perception. *Computational and Mathematical Methods in Medicine*, *2015*(1), 151702. https://doi.org/10.1155/2015/151702

Wilson, M. (2002). Six views of embodied cognition. *Psychonomic Bulletin & Review*, *9*(4), 625–636. https://doi.org/10.3758/BF03196322

Windau, J., & Itti, L. (2016). Walking compass with head-mounted IMU sensor. *2016 IEEE International Conference on Robotics and Automation (ICRA)*, 5542–5547. https://doi.org/10.1109/ICRA.2016.7487770

Winter, D. A. (1983). Biomechanical Motor Patterns in Normal Walking. *Journal of Motor Behavior*, *15*(4), 302–330. https://doi.org/10.1080/00222895.1983.10735302

Witte, K., Bürger, D., & Pastel, S. (2025). Sports training in virtual reality with a focus on visual perception: A systematic review. *Frontiers in Sports and Active Living*, *7*. https://doi.org/10.3389/fspor.2025.1530948

Wolpert, D. M., & Flanagan, J. R. (2001). Motor prediction. *Current Biology: CB*, *11*(18), R729-732. https://doi.org/10.1016/s0960-9822(01)00432-8

Zeki, S. (2015). Area V5—A microcosm of the visual brain. *Frontiers in Integrative Neuroscience*, *9*, 21. https://doi.org/10.3389/fnint.2015.00021

Zhang, H., Morrone, M. C., & Alais, D. (2019). Behavioural oscillations in visual orientation discrimination reveal distinct modulation rates for both sensitivity and response bias. *Scientific Reports*, *9*(1), 1115. https://doi.org/10.1038/s41598-018-37918-4

Zhang, X., Zhaoping, L., Zhou, T., & Fang, F. (2012). Neural Activities in V1 Create a Bottom-Up Saliency Map. *Neuron*, *73*(1), 183–192. https://doi.org/10.1016/j.neuron.2011.10.035

Zoefel, B., & VanRullen, R. (2017). Oscillatory Mechanisms of Stimulus Processing and Selection in the Visual and Auditory Systems: State-of-the-Art, Speculations and Suggestions. *Frontiers in Neuroscience*, *11*. https://doi.org/10.3389/fnins.2017.00296

Appendix

Supplementary Figures

Figure A1

One second reference frame: No modulations in performance

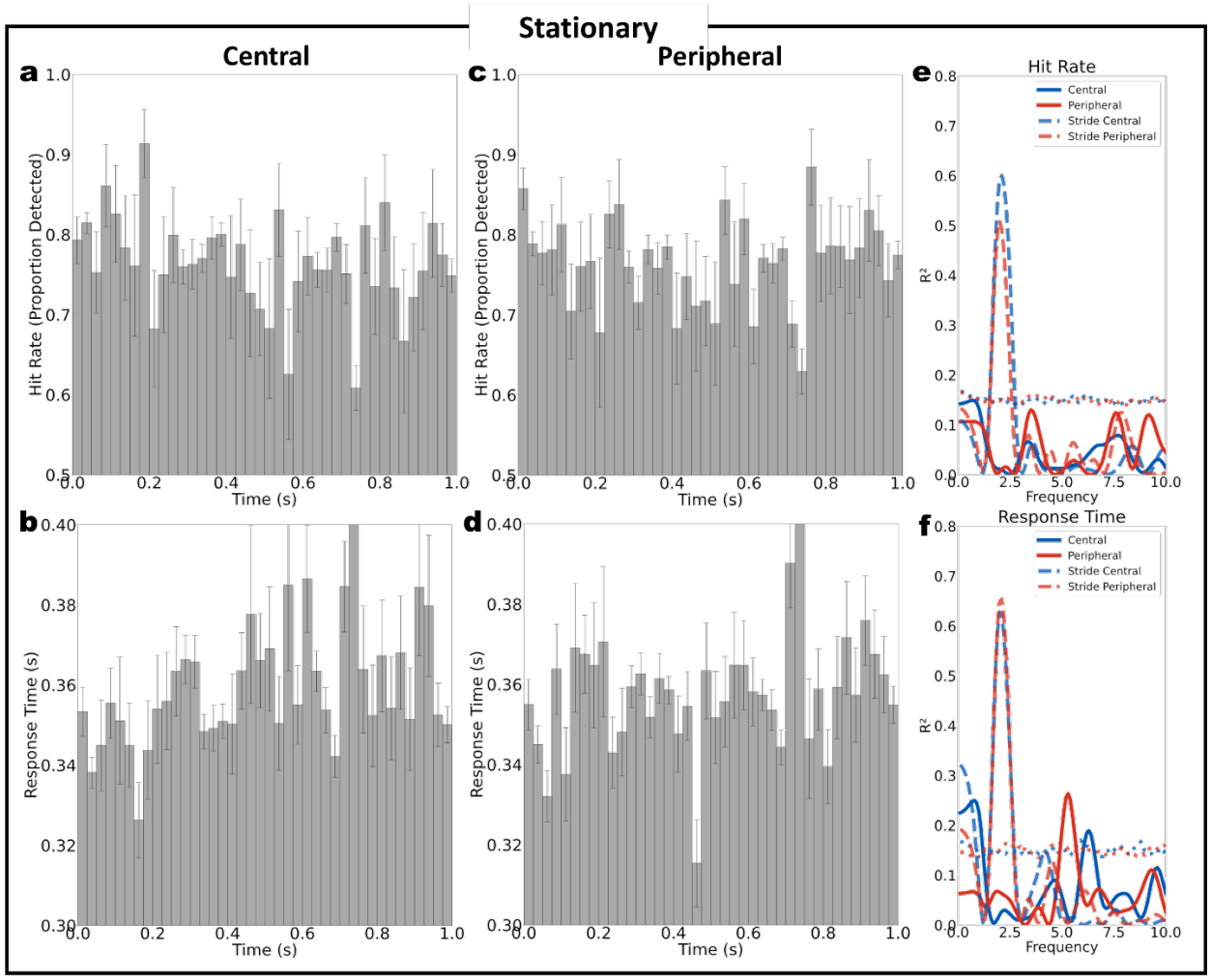

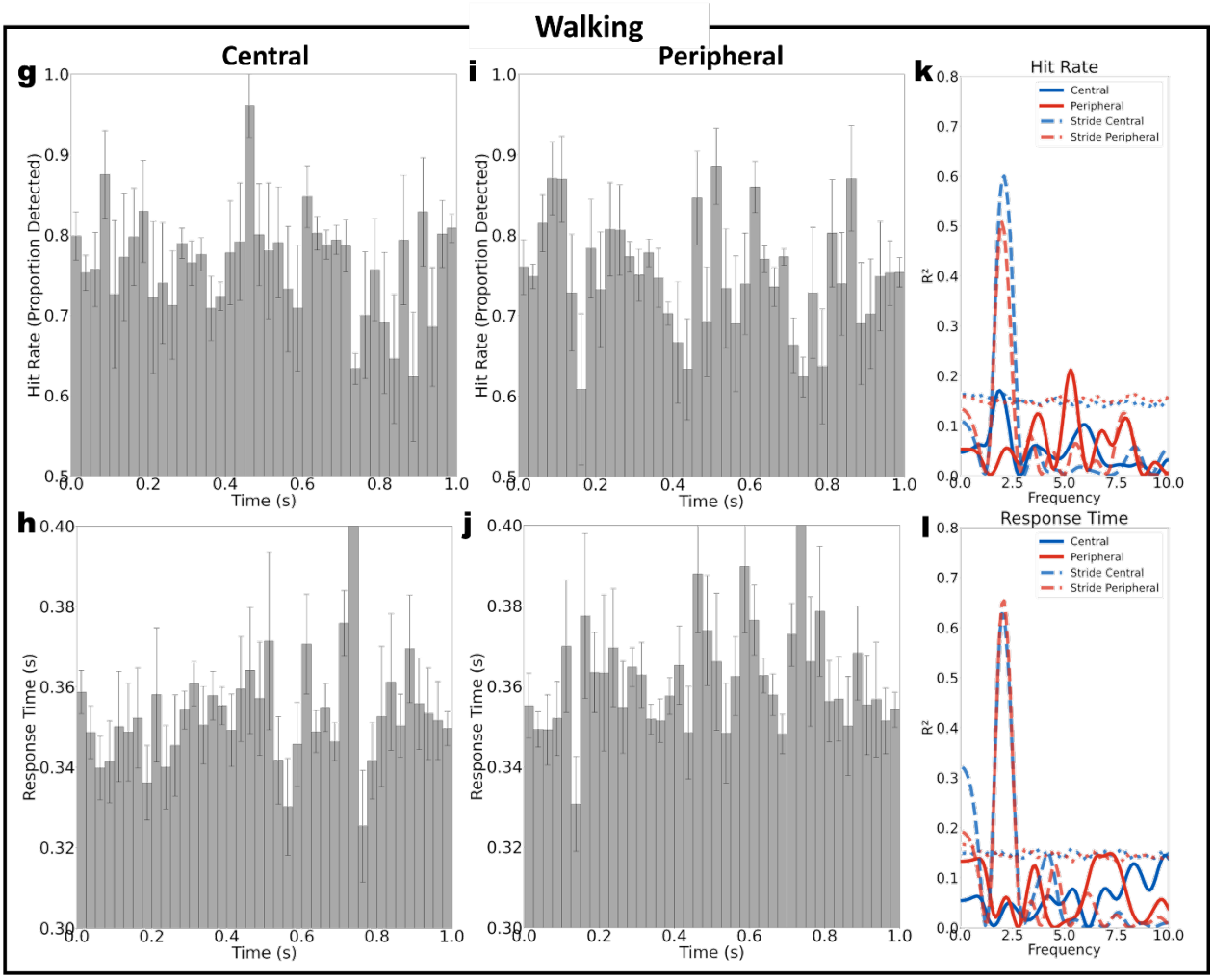

a, c Group-level ($N = 34$) hit rate data for centrally and peripherally presented targets whilst participants were stationary, respectively.

b, d Group-level reaction time data for centrally and peripherally presented targets whilst participants were stationary, respectively.

g, i Group-level hit rate data for centrally and peripherally presented targets whilst participants were walking, respectively.

h, j Group-level reaction time data for centrally and peripherally presented targets whilst participants were walking, respectively.

e, f, k, l Fourier models were fit at a fixed frequency between 0.1-10 Hz (in steps of 0.1) on the group-level data ($N = 34$). The solid blue and red lines display the goodness-of-fit (R^2) calculated for each performance measure at central and peripheral target locations, respectively. Dotted lines show the upper 95th percentile of R^2 values at each fitted frequency obtained from a null distribution of group-level data shuffled in time ($n = 1000$ permutations). Dashed lines represent the R^2 values at each fitted frequency (in cps) for the performance measures when the data was framed in the stride cycle instead of seconds.

Figure A2

Accuracy for Orientation Identification Across Stride Cycle Excluding Non-responses

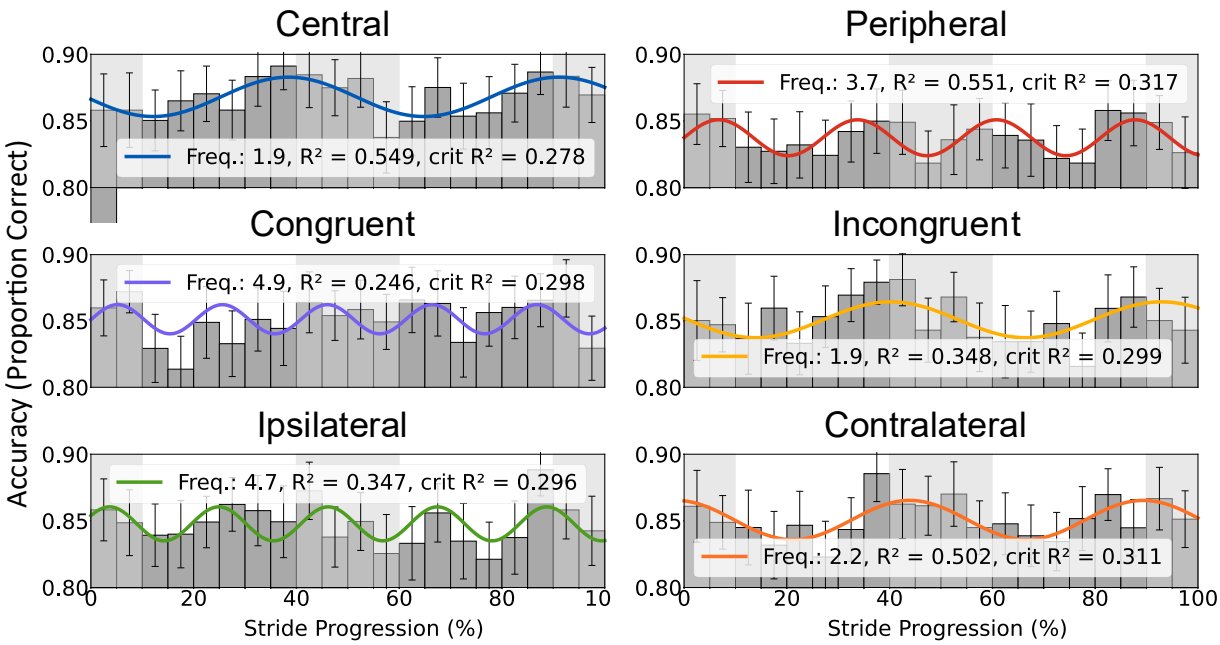

Note. Fourier fits on group-level ($N = 28$) accuracy (proportion of correct responses out of total responses) data from the orientation identification task broken down by six target conditions. Error bars indicate ±1 SEM. Light and dark grey columns indicate the estimated stance and swing phases of the stride cycle, respectively.

Figure A3

Correct Response Time for Orientation Identification Across Stride Cycle

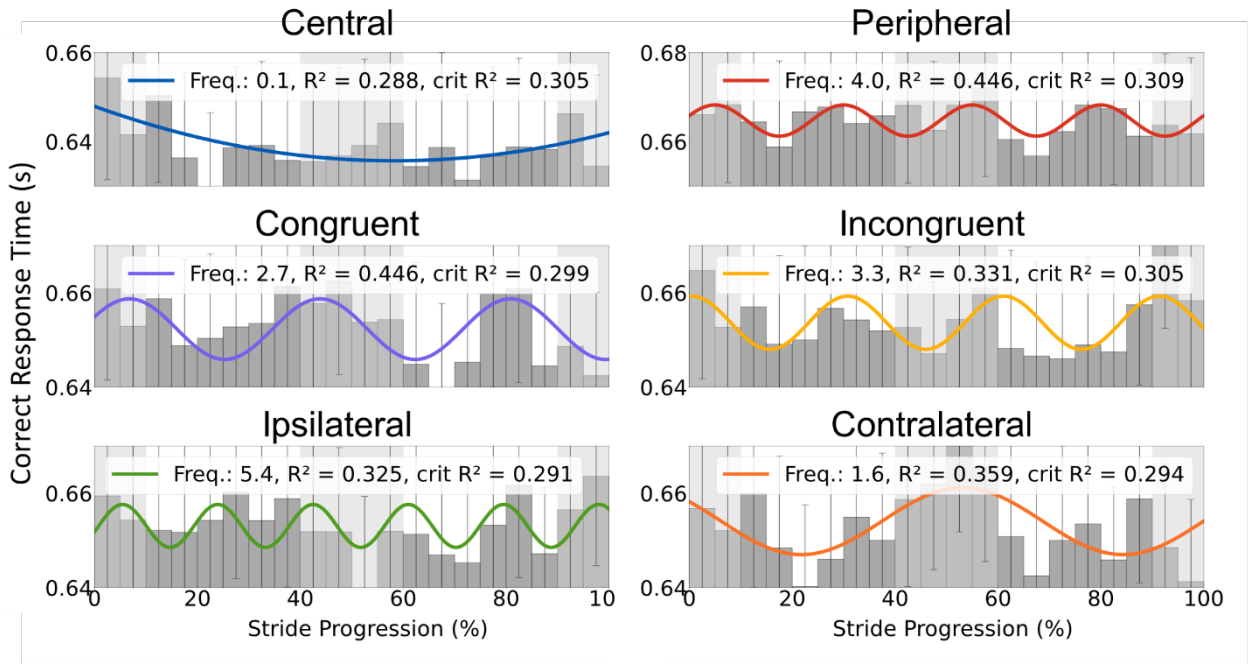

Note. Fourier fits on group-level ($N = 28$) response time (s) data from the orientation identification task for only correct responses broken down by six target conditions. Error bars indicate ±1 SEM. Light and dark grey columns indicate the estimated stance and swing phases of the stride cycle, respectively.

Figure A4

Response Likelihood for Orientation Identification Across Stride Cycle

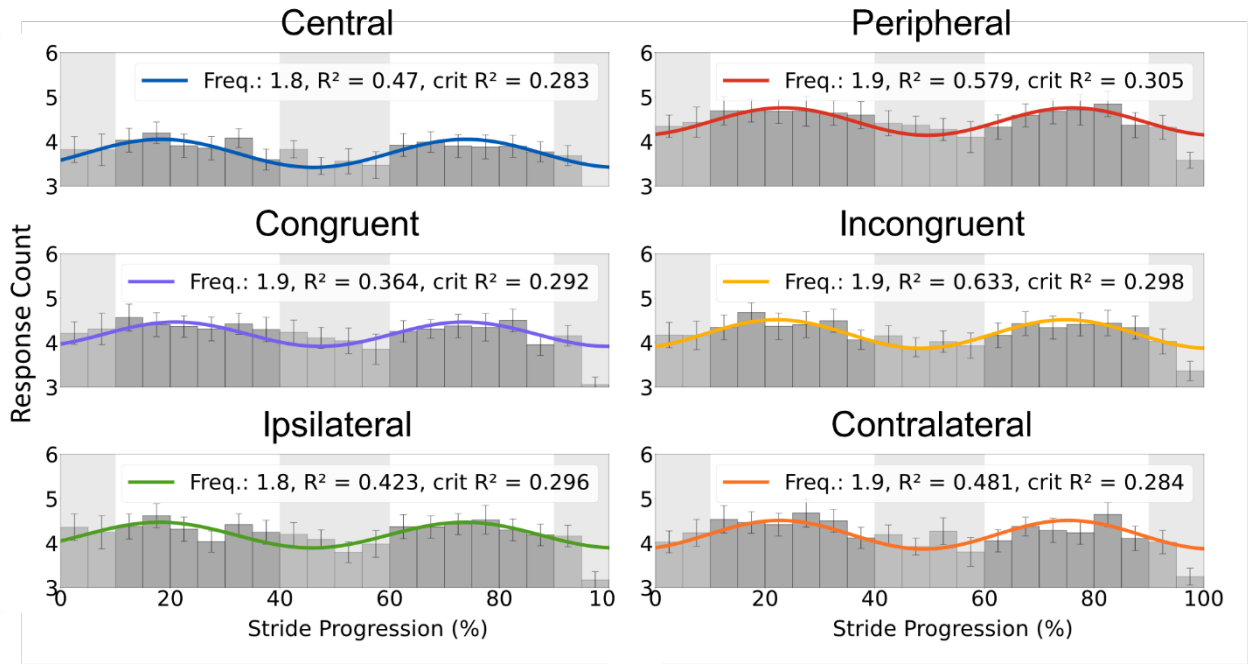

Note. Fourier fits on group-level ($N = 28$) response count data from the orientation identification task broken down by six target conditions. Error bars indicate ±1 SEM. Light and dark grey columns indicate the estimated stance and swing phases of the stride cycle, respectively.

Figure A5

Correct Response Likelihood for Orientation Identification Across Stride Cycle

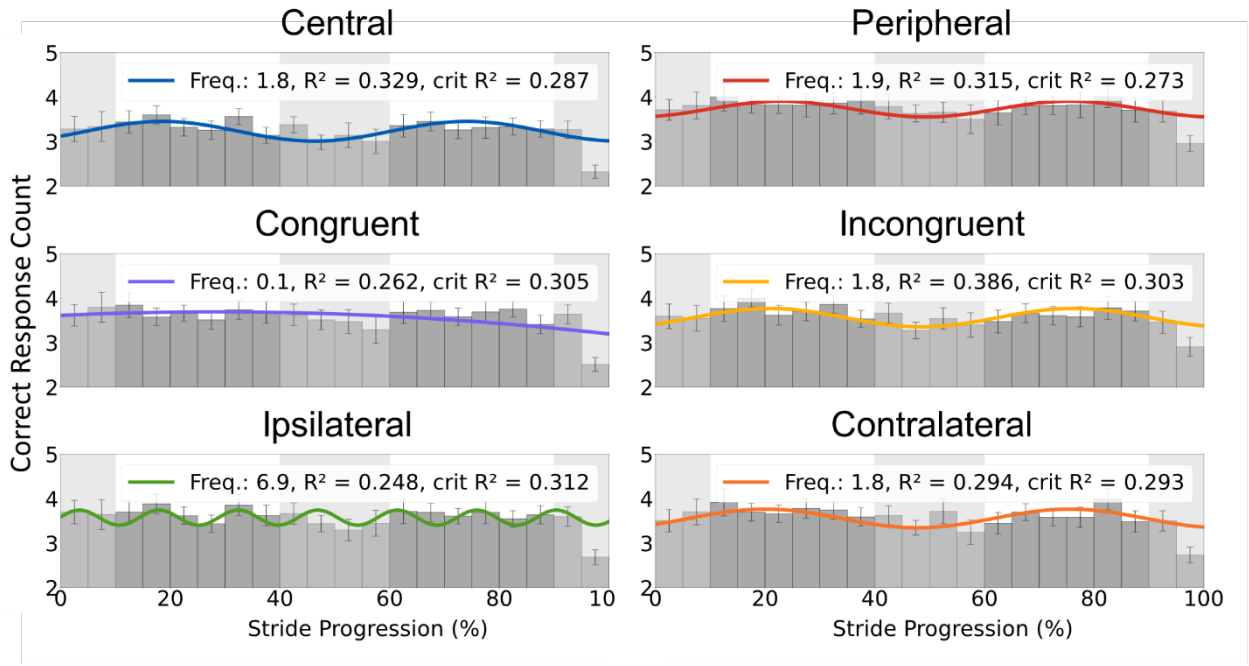

Note. Fourier fits on group-level ($N = 28$) response count data from the orientation identification task for only correct responses broken down by six target conditions. Error bars indicate ±1 SEM. Light and dark grey columns indicate the estimated stance and swing phases of the stride cycle, respectively.

Figure A6

Accuracy for Motion Direction Identification Across Stride Cycle Excluding Non-responses

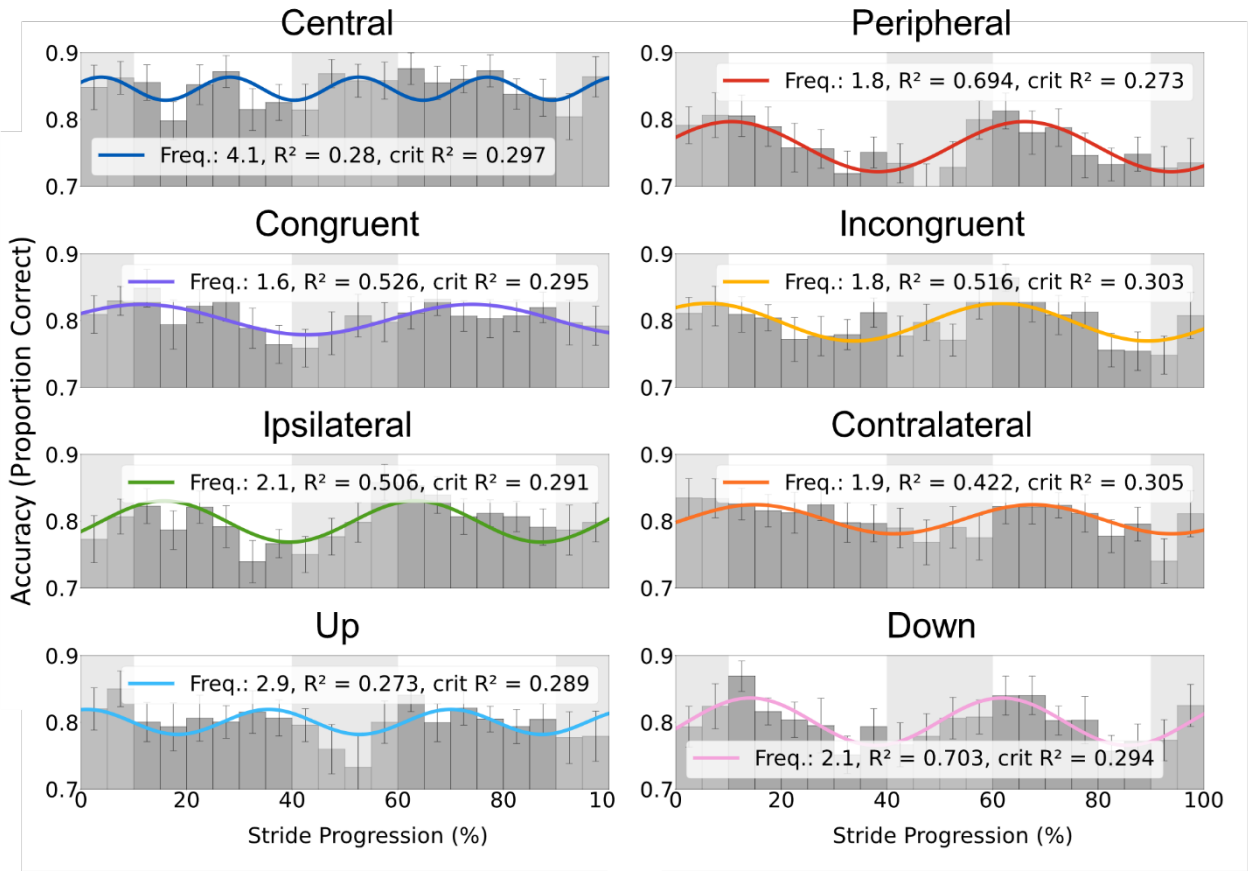

Note. Fourier fits on group-level ($N = 17$) accuracy (proportion of correct responses out of total responses) data from the motion identification task broken down by eight target conditions. Error bars indicate ±1 SEM. Light and dark grey columns indicate the estimated stance and swing phases of the stride cycle, respectively.

Figure A7

Correct Response Time for Motion Direction Identification Across Stride Cycle

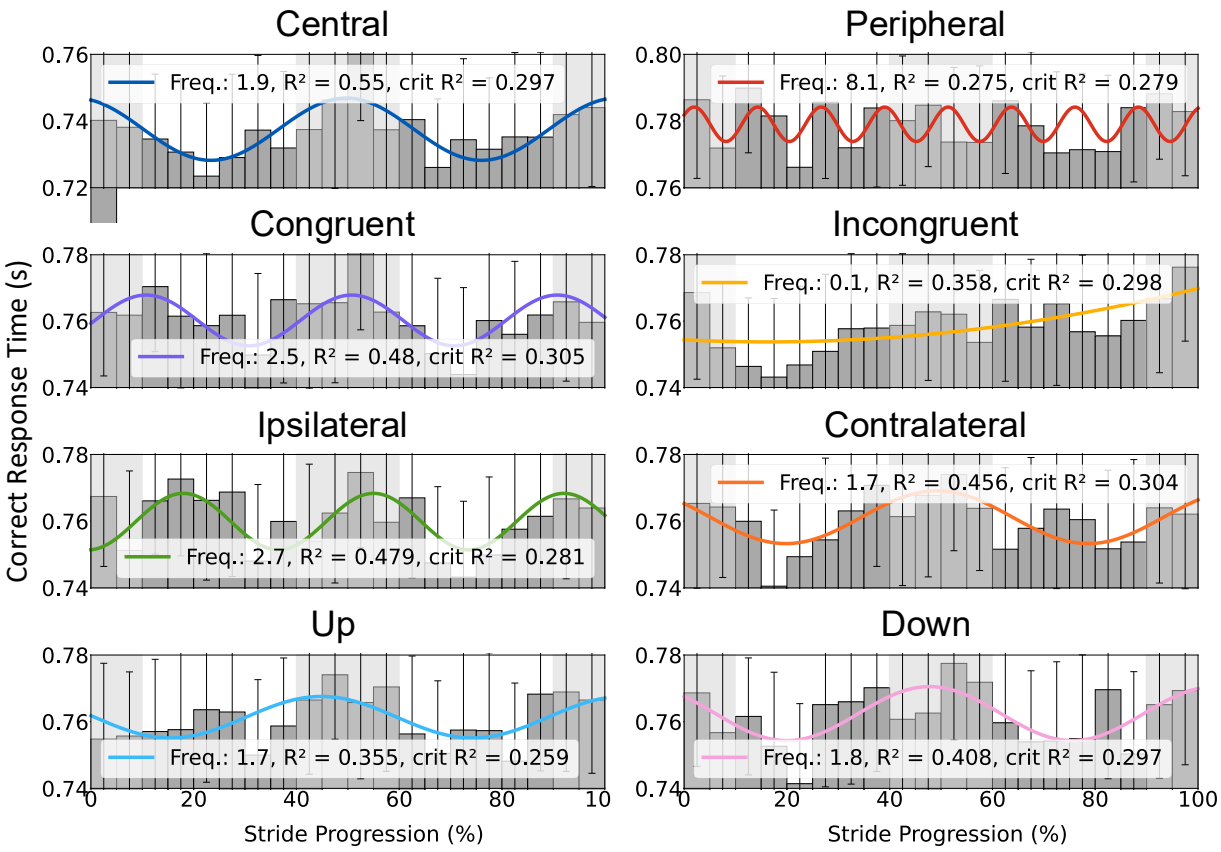

Note. Fourier fits on group-level ($N = 17$) response time (s) data from the motion identification task for only correct responses broken down by eight target conditions. Error bars indicate ±1 SEM. Light and dark grey columns indicate the estimated stance and swing phases of the stride cycle, respectively.

Figure A8

Response Likelihood for Motion Direction Identification Across Stride Cycle

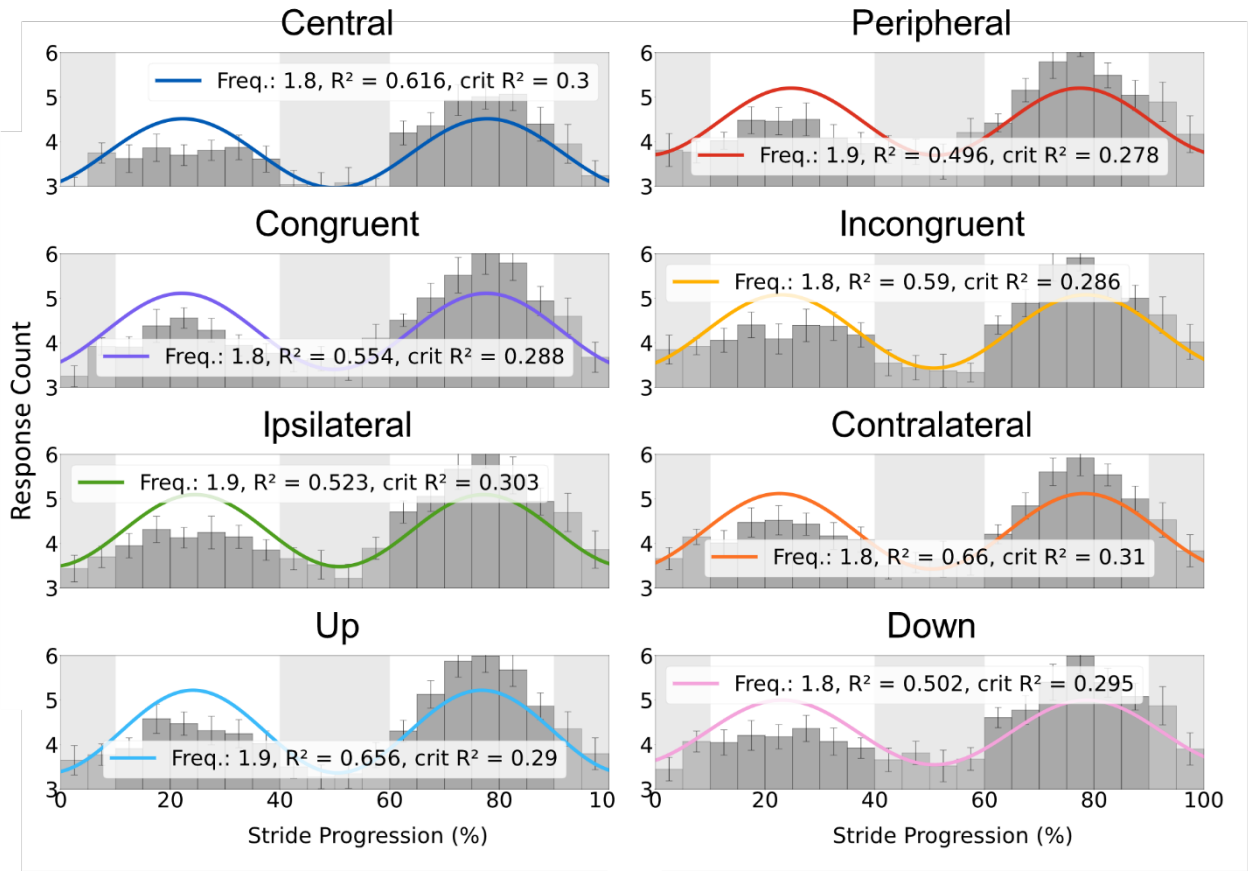

Note. Fourier fits on group-level ($N = 17$) response count data from the motion identification task broken down by eight target conditions. Error bars indicate ±1 SEM. Light and dark grey columns indicate the estimated stance and swing phases of the stride cycle, respectively.

Figure A9

Correct Response Likelihood for Motion Direction Identification Across Stride Cycle

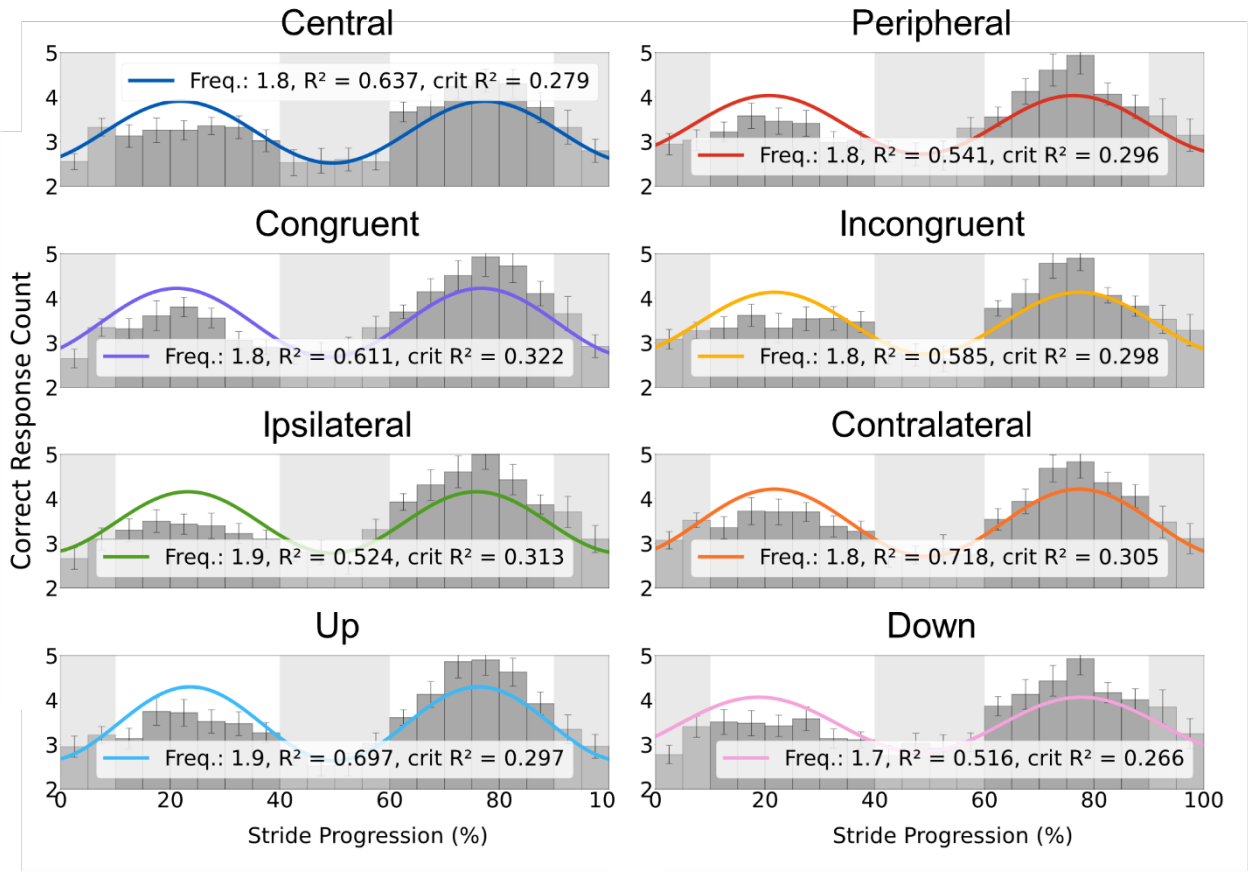

Note. Fourier fits on group-level ($N = 17$) response count data from the motion identification task for only correct responses broken down by eight target conditions. Error bars indicate ±1 SEM. Light and dark grey columns indicate the estimated stance and swing phases of the stride cycle, respectively.